DISSERTATION

MECHANISM OF NEURONAL CELL DEATH IN CANINE GLAUCOMA

Submitted by

Khaleel I. Alyahya

Department of Biomedical Sciences

In partial fulfillment of the requirements

For the Degree of Doctor of Philosophy

Colorado State University

Fort Collins, Colorado

Spring 2009

COLORADO STATE UNIVERSITY

January 9, 2009

WE HEREBY RECOMMEND THAT THE DISSERTATION PREPARED UNDER OUR SUPERVISION BY KHALEEL ALYAHYA ENTITLED [MECHANISM OF NEURONAL CELL DEATH IN CANINE GLAUCOMA] BE ACCEPTED AS FULFILLING IN PART REQUIREMENTS FOR THE DEGREE OF DOCTOR OF PHILOSOPHY.

Committee on Graduate work

John P. Walrond 1-9-09
John P. Walrond

Anna D. Fails 1/9/09
Anna D. Fails

Julie Gionfriddo 1/9/09
Julie Gionfriddo

James E. Madl 1/8/09
Advisor (James E. Madl)

Barbara M. Sanborn 1/10/09
Department Head/Director/Chair (Barbara M. Sanborn)

ABSTRACT OF DISSERTATION

MECHANISM OF NEURONAL CELL DEATH IN CANINE GLAUCOMA

Glaucoma is one of the most important causes of blindness in human and dogs. Glaucoma is characterized by a progressive loss of retinal ganglion cells that is often associated with increased intraocular pressure and decreased retinal blood flow. In previous investigations, we found that changes in glutamate distribution occur selectively in damaged areas of retinas of dogs with primary glaucoma. This glutamate redistribution is consistent with high levels of extracellular glutamate (↑GluE) contributing to excitotoxic damage to neurons. In this dissertation, we used immunohistochemical methods to test three mechanisms by which this glutamate redistribution may occur in retinas from clinical cases of canine glaucoma. First, we tested if ischemia due to microvessel loss causes the changes in glutamate distribution. We found significantly lower microvessel density in damaged regions, consistent with ischemia occurring in canine glaucoma. Second, we tested if loss of glutamine synthetase induces the glutamate redistribution. We have found significantly decreased amounts of glutamine synthetase in areas with neuronal damage and glutamate redistribution, consistence with decreased glutamate synthetase contributing to glutamate redistribution. Third, leakage of glutamate from blood vessels from inflamed areas may lead to glutamate redistribution. We found that there is albumin leakage from blood vessels in damaged regions with other inflammatory indicators in those areas. The smaller size of glutamate suggests that it should also diffuse out of blood into the extracellular fluid of the retina even more readily than albumin. Increase leakiness of blood vessels in canine glaucoma is consistent with glutamate leakage contributing to glutamate

redistribution. In conclusion, our results are consistent with all three mechanisms contributing to glutamate redistribution in canine glaucoma. The dissertation includes further discussion of more refined hypotheses of the mechanisms by which glutamate redistribution and neuronal damage may occur.

Khaleel I Alyahya
Department of Biomedical Sciences
Colorado State University
Fort Collins, CO 80523
Spring 2009

ACKNOWLEDGEMENTS

TO MY FAMILY, MY WIFE, MY COMMITTEE, AND DR. MADL

THANK YOU FROM MY DEEP HEART FOR ALL YOUR SUPPORT AND ENCOURGMENT. YOUR BELIVE ON ME MAKE A HUGE DIFFERENCE IN COMPLETEING THIS DEGREE AND KEEPING THE HOPE ALWAYS HIGH.

ALLAH BLESS YOU

CONTENTS

LIST OF FIGURES

Chapter One:

Chapter Two:

Fig. 2.5 Staining of microvessels in paraffin sections with lectin and antibodies to laminin. A. A section of control retina immunohistochemically stained for laminin shows labeling of microvessels, three of which are indicated by arrows. B. A section from a PG retina stained with lectin shows labeling of microvessels, two of which are indicated by arrows. C. A section of control retina stained with hematoxylin and eosin illustrates the appearance of typical microvessels (arrows). All images are shown with the same orientation and magnification. Bars = x μm.

Fig. 2.6 Microvessel densities were reduced in the retinas of dogs with PG when either lectin staining or laminin immunohistochemistry was used to identify vessels. The number of microvessels in 500 μm fields of paraffin sections was counted in the peripheral retina (starting 1 mm from the ora ciliaris) and central retina in sagittal sections of eyes stained with either lectin or antibodies to laminin. Three fields were counted from each region of each retina. * $p < 0.05$ by Tukey's multiple comparison test.

Fig. 2.7 A. Microvessel densities were decreased in regions with increased severity of damage when either lectin staining or laminin immunohistochemistry were used to identify blood vessels. Microvessels were counted in 250 μm regions of retina with different severities of damage in the INL. Bars = SEM. * $p < 0.05$ for both lectin and laminin compared to control (Tukey's multiple comparison test). B. Control retina showing lack of damage to the INL. C. Moderately damaged retina showing damaged INL cells (arrows). D. Severely damaged retina with reduced INL thickness.

Fig. 2.8 Larger vessels showed signs of inflammation and damage in PG retinas. A. Immunohistochemical staining for CD3 revealed vascular cuffing with T lymphocytes around some vessels (arrowheads) of PG retinas. BV indicates a blood vessel. B. Larger vessel walls were often thickened in PG. Arrowheads indicates the thickened wall of a blood vessel. Plastic section stained with toluidine blue. C. Albumin was often found outside the lumen of blood vessels in PG. Immunohistochemical staining for albumin was especially prominent in the walls of blood vessels (arrowheads).

Chapter Three:

Fig. 3.1 Immunogold localization of glutamate and GS in plastic sections of control and PG retinas. A-D Immunostaining for glutamate in 0.5 μm sections of regions with different severities of damage. E-F. Immunostaining for GS in sections adjacent to A-D. A. Control glutamate staining. Note the low levels of glutamate in Müller cells and their processes (m). High levels of glutamate were found in many neurons (N) of the INL. Nerve fiber bundles (NF) also contained high levels of glutamate. B. A region with mild damage and high glutamate levels. Müller cells contained low levels of glutamate.

Fig. 3.2 GS and neuronal glutamate immunostaining densities were dependent on the severity of damage. GS staining densities in Müller cells and average glutamate staining densities in the INL (primarily neurons) were measured in regions with different severities of damage. In mildly damaged regions, staining densities were measured in areas with high levels of glutamate immunostaining (Mild, High Glu) and areas with low levels of glutamate immunstaining (Mild, Low Glu).

Fig. 3.3 GS immunostaining density was highly correlated with glutamate immunostaining densities in neurons and Müller cells. A. The average immunostaining densities for glutamate in the INL were plotted against GS immunostaining densities (data from Fig. 3.2). There was a strong correlation (R^2 = 0.88) between decreases in GS immunoreactivity and decreases in glutamate immunoreactivity in INL regions. The decreases in the average INL levels of glutamate reflect primarily the glutamate loss that occurs in neurons in PG.

Fig. 3.4 Immunostaining for GS in paraffin sections of archived eyes was similar to plastic sections. A. Avidin-biotin peroxidase immunostaining of control sections revealed strong GS immunoreactivity in Müller cells and astrocytes homogeneously distributed throughout the length of the retinas. B. Some acute ($\leq$ 5 days from clinical detection) PG retinas had focal regions with reduced immunostaining for GS. The edge of a region of reduced staining is indicated by arrowheads.

Fig. 3.5 In paraffin sections, GS immunostaining was reduced in chronic PG retinas and in small regions of some acute retinas. A. GS immunostaining densities (Gray scale) were reduced in the central regions of chronic PG retinas. B. In focal regions of some acute retinas, decreases in GS immunostaining densities were observed. Bars = SEM. N $\geq$ 12 for each column.

Fig. 3.6 GFAP may be induced in reactive Müller cells in PG. A. Paraffin section of control retina showing lack of GFAP immunostaining in Müller cell processes in the ONL. Note the immunostaining of putative astrocytes in the inner layers of the retina. B. Paraffin section of an acute PG retina showing GFAP immunostaining of Müller cell processes (arrowheads). Such regions with GFAP immunostaining in the ONL were infrequent seen. C. Paraffin section of a chronic PG retina showing strong GFAP immunostaining in many regions of the retina.

Chapter Four:

Fig. 4.1 The retinal pigment epithelium (RPE) was abnormal in glaucomatous eyes. (a) Control RPE (H&E stain). (b) Hypertrophied and disrupted RPE (arrowheads) with a rounded appearance in primary glaucoma (PG) retina (H&E stain). (c) Putative RPE cells (arrow) displaced into the neuroretina in PG (H&E stain).

Fig. 4.2 Putative macrophage/microglia and pigment granules accumulate in the neuroretina of glaucomatous eyes. (a) Putative macrophages (arrowheads) containing pigment granules and free

pigment granules (arrows) in the neuroretina in primary glaucoma (PG) (H&E stain). (b) Lectin-labeled macrophages (arrowheads) in the neuroretina in PG (GSL stain).

Fig. 4.3 Pigmented cells and pigment granules accumulated in the vitreous body of glaucomatous eyes. (a) Pigment-containing cells with the typical appearance of macrophages (arrowheads) and free pigment granules (arrow) found in the vitreous body of an eye with primary glaucoma (PG) (H&E stain). (b) Lectin-positive cells (arrowheads) in the vitreous consistent with macrophages (GSL stain).

Fig. 4.4 Regions of neuroretina with pigment accumulations were more severely damaged than other regions. (a) Tapetal region showing no thinning or abnormal pigmentation (H&E stain). (b) Nontapetal region without pigmentary changes (H&E stain). (c) Loss of the inner nuclear layer (INL) and attenuation of the outer nuclear layer (ONL) in a region with an accumulation of pigmented cells and pigment granules (H&E stain). ILM, internal limiting membrane; RPE, retinal pigment epithelium.

Fig. 4.5 Adjacent regions of nonswollen and swollen regions exhibiting neutrophilic inflammation in acute PG. (a) Nonswollen region (H&E stain). (b) Neutrophilic inflammation in the inner layers of the retina (H&E stain). (c) Neutrophils in the neuroretina (H&E stain).

Fig. 4.6 Perivascular inflammation in the neuroretinas of glaucomatous eyes. (a) Perivascular inflammatory cells in the neuroretina in PG (H&E stain). (b) CD3 positive cells (arrowhead) associated with a retinal blood vessel in PG (Immunohistochemical CD3 stain). (c) Presumptive amacrine cells with cross-reactivity to CD3 in the inner retina of a control eye (Immunohistochemical CD3 stain). (d) A negative control showing absence of staining when the primary antibody is not applied (Immunohistochemical CD3 stain).

Fig. 4.7 Albumin leakage from retinal blood vessels. (a) Control retina showing albumin within the blood vessel lumen (arrow) (Immunohistochemical albumin stain). (b) Albumin leakage (arrows) from a vessel in the outer layers of the retina in primary glaucoma (immunohistochemical albumin stain).

Chapter Five:

Fig. 5.1 Initial hypothesized mechanisms of neuronal damage in canine PG. We have found changes in glutamate (Glu) distribution in damaged regions of PG retinas. We hypothesized three mechanisms which may induce an increase in extracellular glutamate (↑GluE). In A, microvessel obliteration may lead to focal ischemia that releases Glu from cells. In B, reactive glia may reduce their levels of glutamine synthetase, leading to decreased glial metabolism of Glu, decreased levels of Glu in neurons, and perhaps decreased clearance of Glu from the extracellular fluid. In C, inflammation increases leakage of Glu from blood vessels.

Fig. 5.2 Revised hypothesized mechanisms of neuronal damage in canine PG. We have found changes in glutamate distribution in damaged regions of PG retinas. We revised the mechanisms

of the original three hypotheses (Fig. 5.1) to a new mechanism, which may induce an increase in extracellular glutamate (↑GluE). In A, inflammation may lead to oxidative stress (OS) that decreases glutamine synthetase (↓GS). In B, ischemia may play a role in decreasing glutamine synthetase through oxidative stress leading to Glu redistribution and neuronal damage.

CHAPTER 1:
INTRODUCTION

1.1 DEFINITION

Glaucoma is one of the most important causes of blindness in human (Coleman and Greenland, 1995) and dogs (VPL Survey, 2000). Clinically, glaucoma is defined as neuropathy of the optic nerve head where ganglion cells are lost (Haefliger et al, 2003). Glaucoma is characterized by a progressive loss of retinal ganglion cells that is often associated with increased intraocular pressure (Gelatt and Brooks, 1999; Miller, 1995) and decreased retinal blood flow (Cheng et al, 2001; Cioffi et al, 2001; Chung et al, 1999). Primary glaucoma (PG) in dogs is a neurodegenerative disease that can involve all layers of the neuroretinal and not just the retinal ganglion cells (McIlnay et al, 2004; Whiteman et al, 2002).

1.2 BACKGROUND

1.2.1 Importance

Glaucoma is characterized by visual field defects (Kitazawa and Yamamoto, 1997) that may be the result nonuniform loss of ganglion cells and their axons (Low et al, 2006). Glaucoma is the second leading cause of blindness in humans worldwide. Estimates indicate that 60.5 million people will be affected by glaucoma by 2010, and bilateral blindness will be present in 4.5 million people with open-angle glaucoma and 3.9 million people with angle-closure glaucoma (Coleman and Greenland, 1995).

Two decades ago, it was generally accepted that glaucomatous degeneration of the optic nerve and retina were linked to the development of elevated intraocular pressure (Nickells,

2007). There is now evidence that in humans and in animal models of experimental glaucoma that high intraocular pressure (IOP) is not required to induce ganglion cell loss.

In dogs, glaucoma involves more than the ganglion cell layer and it affects all retinal layers and cell types. Studies found that in canine glaucoma, neurons of the inner nuclear layer (INL) and outer nuclear layer (ONL) in addition to the retinal ganglion cells die (Whiteman et al, 2002). This cell death leads to thinning of ONL (Madl et al, 2006) and INL (McIlnay et al, 2004). According to a recent survey of veterinary ophthalmologists, approximately more than 12,000 canine new cases of glaucoma occur each year in the United States (VPL Survey, 2000) and these dogs are at risk of going blind if treatment is delayed.

1.1.2 Species Differences in Severity

Human glaucoma

Glaucoma is a common disease making approximately 67 million people worldwide at risk of blindness (Quigley, 1996). In human glaucoma, the primary cells affected in the retina appear to be the ganglion cells and their process that form the optic nerve. It is a selective loss of retinal ganglion cells (Nickells, 2007). In addition to being selective for ganglion cells, glaucoma tends to be extremely slow in human, while in dogs severe damage may occur within days of clinical onset (Whiteman et al, 2002; McIlnay et al, 2004).

Canine glaucoma

Primary angle-closure glaucoma (PACG) is characterized by a sudden substantial increase in IOP and is the most common form of spontaneous primary glaucoma in dogs (Whitman et al, 2002). In most cases of canine glaucoma, all the layers of the retina are damaged. (Whitman et al, 2002).

The exact time course of retinal degeneration in acute PACG remains unclear (Whitman et al, 2002) due to our lack of certainty of when the disease begins. By the time signs are noticed in PACG, severe retinal damage may already be present. Sight is not always maintained or regained in dogs presented during the acute stage of onset of glaucoma despite a rapid lowering of IOP (Smedes and Dubielzig, 1994; Harris et al, 2001). Changes in the neural retinal layers include coagulation (Smedes and Dubielzig, 1994), necrosis, polymorphonuclear cell infiltrates, macrophage infiltrates, and disorganization of retinal layers. Inner and outer nuclear layers were not always affected to the same degree.

In addition to clinical cases in dogs, there is a hereditary dog model for glaucoma in beagles. This model has been classified as canine primary open angle glaucoma (POAG) (Gelatt and Brooks, 1999). However, the clinical course of hereditary POAG in dogs is very different form the common clinical form, PACG, in that the increase in IOP is more extreme and more abrupt in onset in PACG and PACG may involve many more cell types and layers of the retina.

DBA/2J mice

The DBA/2J (D2) inbred strain of mice develops a form of progressive glaucoma with increasing age. The retinas of D2 mice are characterized by a reduction in retinal thickness cause by loss of RGCs and their axons (Johns et al, 1998). More recent studies suggest that a thinning of the inner nuclear layer may also occur, with a loss of some types of amacrine cells (Jung Moon, 2005). The D2 mouse model may reproduce certain aspects of the pathogenetic mechanism of human glaucoma (Schuettauf et al, 2004). The glaucoma in D2 mice is perhaps the best laboratory animal model for canine PACG where most of the cells and layers are

affected. However, the progressive glaucoma in the D2 mice requires a longer period of time to develop than canine PACG.

1.2.3 Types of Glaucoma

Primary versus Secondary glaucoma

Glaucoma can be classified in many different ways. One clinical classification is primary versus secondary glaucoma. Primary glaucoma (PG) is a neurodegenerative disease that cannot be attributed to another disease process. In contrast, secondary glaucoma is a neurodegeneration due to other diseases processes such as trauma, infection, and tumors.

This system of classification is difficult to apply. As previously mentioned, the D2 mouse is a model of glaucoma. Some investigators classify this disease as glaucoma secondary to genetic defects, but we consider this type of glaucoma to be a primary glaucoma. Similarly, in dogs many cases of glaucoma are related to pigment dispersion. We consider these to be primary glaucoma.

High intraocular pressure versus normal tension

In recent years, researchers have found that many people suffering from glaucoma do not have an increased intraocular pressure. These cases have been classified as normal tension glaucoma. However, in other cases high intraocular pressure is still associated with glaucoma high intraocular pressure is still considered a risk factor for developing glaucoma.

In dogs, primary glaucoma is usually associated with high intraocular pressure. However, there are several studies of a hereditary POAG in beagle dogs that may be classified as normal tension glaucoma. The dogs studied in this dissertation are all considered to have primary glaucoma and are expected to have high intraocular pressure. (Described in section 1.3.3).

Pigmentary Glaucoma

Pigment dispersion is very common in humans. Some studies claimed it may occur with a frequency of 4% in different populations (Ritch, 1998; Ritch et al, 1993). Studies have reported that about 15-50% of people with pigment dispersion will develop glaucoma over an extended period of time (Farrar and Shields, 1989; Migliazzo et al, 1986). The mechanism(s) by which pigment dispersion leads to ganglion cell damage are not fully understood.

A lab animal model of pigment dispersion/PG has been described, the D2 mouse. In addition, many dogs with PACG have been reported to have pigment dispersion (Reilly et al, 2005). Recent studies suggested that glutamate redistribution occurs in both of these models of PG (Low et al, 2006; Madl, 2005 et al, McIlnay et al, 2004), perhaps leading to increased extracellular glutamate and excitotoxicity to retinal neurons. Previous studies of D2 mice and PG in dogs indicate that damage to blood vessels (Schuettauf et al, 2004; Smedes and Dubielzig, 1994), inflammation (Reilly et al, 2005) and reactive glia (Low et al, 2006, Schuettauf et al, 2004) occur in these of PG.

Glaucoma in other Species

Glaucoma is clinically important in many other species including cats (Blocker and Van Der, 2001; Glaze and Gelatt, 1999; Wilcock et al, 1990) and horses (Miller et al, 1995; Pickett and Ryan, 1993; Wilcock et al, 1991; Cullen and Grahn, 2000), but in these species the disease in often secondary to other ocular diseases. Laboratory lab animal models of glaucoma include several models that increase the intraocular pressure of the eye. However, pigment dispersion maybe an important factor in inducing glaucoma in dogs (Reilly et al, 2005; Chapter 4). Pigment dispersion and inflammation in the anterior segment have been reported in a form of canine

primary angle-closure glaucoma (PACG) and in the DBA/2J murine model of pigmentary glaucoma (Anderson et al, 2002; Jeohn et al, 1998; Zhou et al, 2005).

1.3 PATHOPHYSIOLOGY

1.3.1 Decreased Blood Flow in Glaucoma

The eye is very sensitive to any disruption of its blood supply. Disruption may become very common when people get older. In humans, disruptions of the blood supply may be caused by atherosclerosis where cholesterol deposits and other changes in the tunica intima block the blood flow in arteries. In dogs, atherosclerosis does not occur but inflammation, infection, vessel attenuation or perhaps other forms of damage to blood vessels may be possible causes of disruption of blood flow to the eye. Retinal damage, including neuronal damage, may be the result of a blood flow disruption. Although increased intraocular pressure is considered the major risk factor in glaucoma, there is strong evidence that the pathogenesis of glaucoma is also linked to altered ocular blood flow (Stewart et al, 2007). Inadequate blood supply to the retina is known to lead to death of ganglion cell neurons through the release of glutamate (Adachi et al, 1998).

Several studies suggest there may be alteration in blood flow and damage to blood vessels in the canine retinas with glaucoma. Altered ocular blood flow occurs before intraocular pressure is elevated in Beagles with POAG. (Gelatt et al, 2003). The altered blood flow and vascular damage in canine glaucoma might cause ischemia that lead to retinal damage in canine PG (Alyahya et al, 2007; Savagian et al, 2008). Retinal damage in canine PG is consistent with focal ischemia in the following ways: (1) It is often focal, and may involve multiple layers (McIlnay et al, 2004; Whiteman et al, 2002) and (2) Loss of neuronal cells is greater in the inner retina than in any other retinal layers (McIlnay et al, 2004).

Although decreased blood flow occurs in at least in some types of glaucoma, it remains unknown if the decrease is severe enough to cause damage.

1.3.2 Ischemia

Ischemia is a severely decreased or complete absense of blood flow to the retina. This may be due to a blockage of the blood vessels to that area. According to Siegel et al (1994), ischemia or inadequate cerebral blood supply can cause hypoxia with inadequate oxygen delivery. Focal retinal ischemia is a common feature of diabetic retinopathy (Bresnick et al, 1983). Global ischemia results in the interruption of blood supply to the entire brain, while in focal ischemia, the interruption is restricted in a particular region. Blood vessel distribution plays an important role in the location and extension of focal ischemia (Siegel et al, 1994). Focal retinal ischemia might be expected to lead to focal differences in the degree of retinal damage, with more severely damaged regions next to less damaged. In chapter 3, we have reported that there are different levels of damage in different regions of the retina in canine PG and also focal decreases in the number of microvessels.

In chapter 3, we tested the hypothesis that vascular damage may lead to microvessel obliteration and focal ischemia. We compared the microvessel densities of retinal regions with differing degrees of damage and glutamate redistribution to determine if microvessel loss may contribute to glutamate redistribution and retinal damage in PG. We have found that the densities of microvessels in PG eyes were significantly reduced compared to control retinas. This finding was consistent in all three of the different methods of identifying blood vessels. However, the densities of larger vessels in both the central and the peripheral regions of PG retinas were not significantly reduced. This suggests that a selective loss of microvessels occurs as PG

progresses. This loss could be similar to diseases such as microscopic polyangitis, in which small vessels, but not larger vessels, develop vasculitis. The result of the study supported the idea that decreases in microvessel numbers are dependent on the severity of INL damage, which suggests that the loss of microvessels may increase as retinal damage progresses.

1.3.3 Intraocular pressure

Glaucoma is associated with increased intraocular pressure (Källberg et al, 2007) and decreased blood flow. Intraocular pressure (IOP) elevation is one of the characteristics of PACG which is the most common form of primary canine glaucoma (Whiteman et al, 2002). Increased intraocular pressure has often been suggested to lead to vision loss due to a progressive retinal and optic nerve degeneration (Bentley et al, 1999), but the mechanisms leading to this loss are poorly understood. Nickless (2007) has reported that high IOP could cause ganglion cell loss. Källberg also claimed in her paper that there is a risk of glaucomatous damage at every level of IOP, and the risk become high with the elevation of IOP. However, (Whiteman et al, 2002) claimed in her studies that the mechanism of cell death in inner and outer nuclear layers in acute canine PACG has not been well studied. Intraocular pressure may develop some morphological changes in retinal layers determined by alterations in layers, ganglion cell loss, and retinal attenuation.

1.3.4 How decreased blood flow and high intraocular pressure may affect primary glaucoma in dogs.

Decreased blood flow and ischemia have not been directly shown to occur in primary glaucoma in dogs. However, ischemia will lead to severe retinal damage that resembles that seen in primary glaucoma in dogs (McIlnay et al, 2004). Increased intraocular pressure occurs in dogs with primary glaucoma, but increased IOP does not occur in all cases in all species. Therefore,

we hypothesized in our study that it is not a high intraocular pressure which causes damage in canine glaucoma; but rather it is the loss of blood flow that lead to damage.

1.3.5 Vascular Damage in Glaucoma

In some studies, vascular abnormalities have been reported in canine glaucoma, including PG (Semedes and Dubielzig, 1994). In Chapter 2, we tested the hypothesis that vascular damage may lead to microvessel obliteration and focal ischemia. In Chapter 4, we also tested if vascular damage might include breakdown of the blood retinal barrier that occurs when tight junctions between retinal vascular endothelial cells. This could lead to leakage of glutamate from blood to the extracellular space of the retina.

In Chapter 4, we also looked at whether inflammation, a specific type of pathophysiological change, may contribute to vascular damage as well damage to neurons and glia. Inflammation of the retina and surrounding vascular tracts is referred to as uveitis. Inflammation was clearly present in these eyes. This was shown by the accumulation of inflammatory cells and other markers of inflammation.

1.4 MECHANISM OF CELL DAMAGE AND DEATH

1.4.1 Glutamate – mediated cell death

Glutamate (Glu) is the most common excitatory neurotransmitter in the mammalian nervous system. It is a nonessential amino acid which does not cross the blood-retinal barrier, and it is synthesized from glutamine and other precursors. Glu is present in a very high concentration in CNS. It is has an excitatory effect on neurons, and it is released in a Ca^{+2}-dependent manner at synapses (Siegel et al, 1994). The synthesis and metabolism of Glu is

dependent on the interaction between nerve terminals and glial cells. In healthy retina, the level of glutamate is normally high in neurons and low in glial cells. Muller cells, the radial glia of the retina, have glutamate transporters on their surface, primarily of the GLAST type. These transporters rapidly take up any glutamate released at synapses. Once glutamate is transported into Muller cells, it is converted to glutamine by glutamine synthetase, and then sends back to neurons to make more glutamate. Glutamate released from neurons at synapses interacts with multiple receptors types, such as NMDA and AMPA receptors on postsynaptic neurons to mediate cellular responses. Increased amount of glutamate in extracellular space during ischemia can cause neuronal injury by over activation of those receptors. NMDA antagonists have been used to block the neuronal damage in glaucoma, suggesting overactivation of these receptors may mediate much of the neuronal damage that occurs in glaucoma (Scheutauff et al, 2004; Hare et al, 2001).

During retinal disease, the exposure of neurons to glutamate can cause acute neuronal swelling due to the influx of Na^+, Cl^-, and H_2O. However, the importance of this process remains unclear in retinal disease. In the case of overstimulation of other glutamate receptors, such as NMDA receptors, a massive Ca^{2+} influx will activate lipases, protein kinases, and proteases that lead to cellular death through apoptosis. In DBA/2J mice, retinal damage has been decreased by treatment with memantine suggesting that the neuronal death may be due to NMDA receptor stimulation (Scheutauff et al, 2004). In rats, glutamate release as a result of ischemia has been found with loss of glutamate from neuronal cell bodies and dendrites.

1.4.2 Normal Glutamate/Glutamine Synthetase cycle

Glutamate is the main excitatory neurotransmitter in the retina but it is neurotoxic when present in excessive amounts in the extracellular fluid. Thus, an appropriate clearance of synaptic glutamate is required for the normal function of retinal excitatory synapses and for prevention of neurotoxicity. Glial cells, mainly astrocytes and Muller cells surround gluamatergic synapses and express glutamate transporters and the glutamate-metabolizing enzyme glutamine synthetase. Glutamate is transported into glial cells and amidated by glutamine synthetase to the nontoxic amino acid glutamine. Glutamine is then released by the glial cells and taken up by neurons, where it is drolyzed by glutaminase to form glutamate again, completing the retinal glutamate/glutamine cycle. In this way, the neurotransmitter pool is replenished and glutamate neurotoxicity is prevented.

1.4.3 Müller Cells

Müller cells are radial glial cells that span all the depth of neuronal retina (Uga and Smelser, 1973; Reichenbach et al, 1989) extending from the internal to the external limiting membranes of the retina (Junqueira and Carneiro, 2003). In addition to their critical functions of maintaining appropriate glutamate levels in extracellular fluid and within different cell types through the actions of glutamine synthetase, Müller cells also provide other types of support, nourishment, and insulation of retinal neurons and fibers.

1.4.4 How decreases GS may lead to increase Glu outside cells.

Glutamine synthetase activity may be decreased in hypoxia/ischemia (Krajnk et al, 1996; Moreno et al, 2005), and loss of glutamine synthetase immunoreactivity has also been reported after ischemia in the retina (Nishiyama et al, 2000). Decreased glutamine synthetase activity may

lead to a high level of glutamate in glial cells and in the extracellular fluid that may lead to neuronal damage. Models of glutamate transport by GLAST, the main glutamate transporter in the retina (Rauen et al, 1998), suggest an increase in the intracellular level of glutamate in glial cells may lead to a proportionate increase in the extracellular level of glutamate (Attwell et al, 1993; Bouvier et al, 1992)

1.4.5 Glia Reactivity

Reactive Müller cells are induced in several different types of retinal diseases, including some types of glaucoma (Schuettauf et al, 2004 and Low et al, 2006). The reactive glial cells alter their cytoskeleton, thus allowing their detection by immunohistochemical staining for glial fibrillary acidic protein (GFAP) and other cytoskeletal components. Other changes that occur in reactive glia include altered expression of enzymes. Thus one possible mechanism leading to decreased levels of GS may be decreased expression of GS in reactive glial cells.

GFAP immunoreactivity is often used as a marker for reactive glia (Lewis and Fisher, 2003; Davidson et al, 1990). Müller cells do not normally express GFAP (Davidson et al, 1990). In many regions of chronic PG retinas, some putative Müller cells contained substantial amounts of GFAP immunoreactivity, indicating that these glias are reactive. However, it should be noted that astrocytes normally contain GFAP and the increased GFAP in thinned retinas may be at least partially due to retention of astrocytes in these severely damaged regions. In contrast to chronic PG, fewer GFAP-containing Müller cells were seen in acute PG. In those regions of acute PG retinas where GFAP immunoreactivity was substantial, severe damage was generally seen in the INL. This suggests that Müller cells show signs of classic reactive glia in the later stages of the pathogenesis of glaucoma after many of the INL neurons have been lost.

1.4.6 Oxidative Stress

Although our initial hypothesis doesn't include the concept that oxidative stress induces the disease, the result of our studies suggests that oxidative stress may be involved. Therefore, we include some background in the introduction to help understand the discussion.

Oxidative stress can be defined as increased free radical reactions or antioxidant depletion (Katz et al, 2004; Katz et al, 1998; Traystman et al, 1991). Free radicals directly damage neuronal membranes during reperfusion from cerebral ischemia, resulting in lipid peroxidation (Komara et al, 1986). Lipid peroxidation, a representation of oxidative stress in the brain, can be quantified by measuring malondialdehyde (MDA); the product of free radical mediated neuronal membrane damage (Yang et al, 1998).

The free radicals formed as partially reduced metabolites of molecular oxygen (O_2) are referred to as reactive oxygen species (ROS) due to their higher reactivities relative to molecular O_2. ROS are generated intracellularly through a variety of processes, for example, as by-products of normal aerobic metabolism and as second messengers in various signal transduction path-ways. ROS can also be derived from exogenous sources, either being taken up directly by cells from the extracellular milieu, or produced as a consequence of the cell's exposure to some environmental insult (Tezel et al, 2005). Similarly, free radicals formed by metabolites of nitrate may be referred to as reactive nitrogen species (RNS).

1.5 HYPOTHESIS

Based on our understanding of glaucoma as described above, we developed three hypotheses. These hypotheses are based in part on previous findings of the laboratory showing

that glutamate redistribution is associated with neuronal death in canine PACG. (Madl et al, 2005; McIlnay et al, 2004).

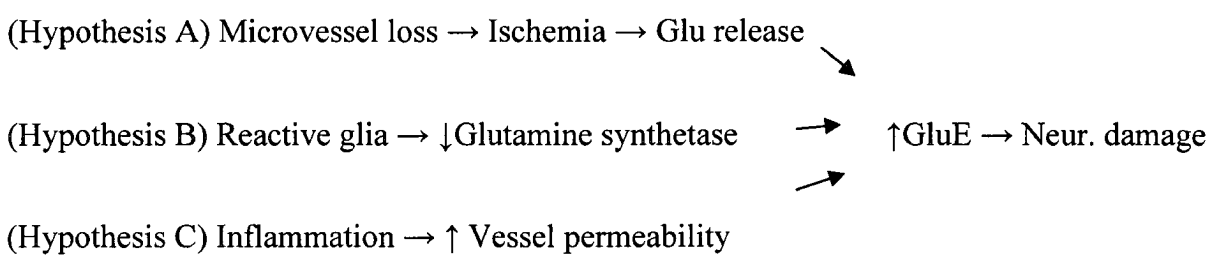

Fig. 1.5: Hypotheses:

We hypothesize three mechanisms by which glutamate may kill neurons in canine primary glaucoma mediated by an increase in extracellular glutamate (↑GluE). To test these hypotheses, we perform immunohistochemical studies on archived eyes as described in details in the following three chapters. We have found changes in glutamate distribution in damaged regions of PG retinas. In A, micrvessel obliteration may lead to focal ischemia that releases glutamate (Glu) from cells. In B, reactive glia may reduce their levels of glutamine synthetase (GS) leading to decreased glial metabolism of glutamate (Glu), decreased levels of Glu in neurons, and perhaps decreased clearance of Glu from the extracellular fluid. In C, inflammation increases leakage of glutamate (Glu) from blood vessels.

1.6 THE STRUCTURE OF THE EYE AND RETINA

The eye is a complex photosensitive organ that analyzes light intensity and color reflection from objects. It is specialized to collect the light and the processes of the original visual information. The eyes are located in protective bony structure of the skull called orbits (Kelley, 1998). Each eye contains a tough fibrous globe to maintain its shape, a lens system to focus the image, a layer of photosensitive cells, and a group of cells and nerves to function as collecting, processing, and transmitting the visual information to the brain (Junqueira & Carneiro, 2003; Kelley, 1998).

The retina is a thin delicate layer that is located in inner surface of the eye posteriorly. The retina has two components, neuronal retina that contains light sensitive receptors and complex neuronal networks, and retinal pigment epithelium that is consists of simple cuboidal melanin containing cells (Ross et al, 1995). The neural retina composed of the photoreceptors and other associated neurons of the eye (Kelley, 1998). The neural retina is specialized for sensing the light and processing the resulting information (Tortora & Derrickson, 2005).

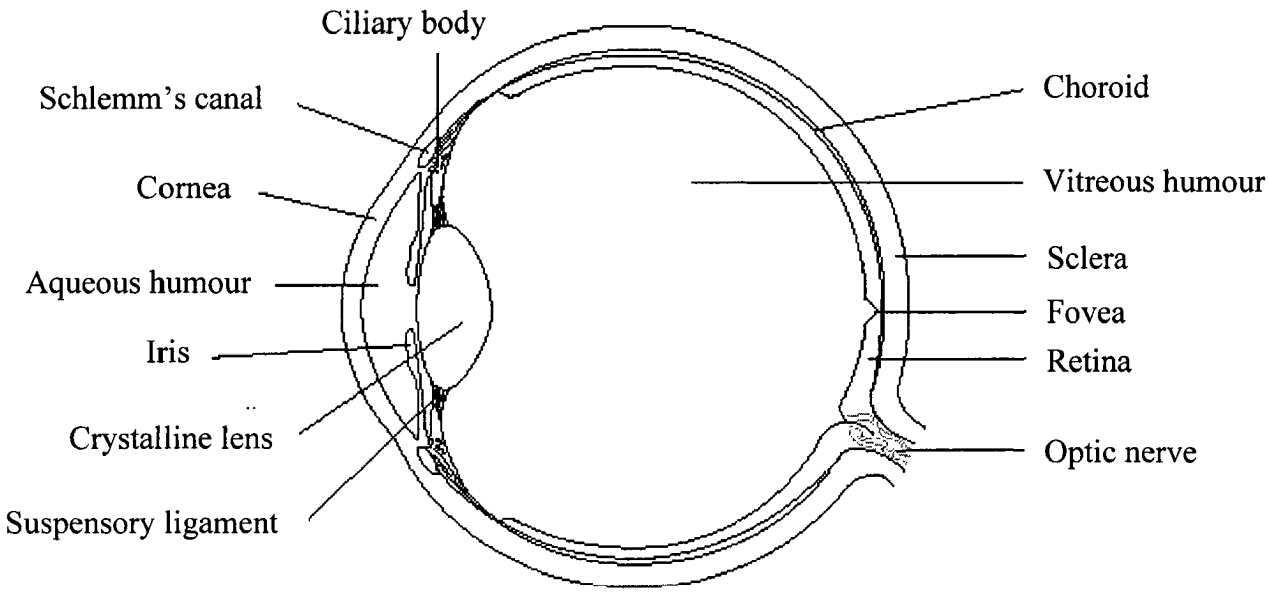

1.6.1 Layers of retina

There are several characteristic layers of the retina. These layers are, from outer to inner, Retinal Pigment Epithelium, Outer Nuclear Layer, Outer Plexiform Layer, Inner Nuclear Layer, Inner Plexiform Layer, Ganglion Cell Layer, and The Nerve Fiber Layer. The ganglion cell layer, the inner nuclear layer and the photoreceptor layer are the most layers affected by canine glaucoma. Each layer has certain retinal cells with specific functions. Following this section we are going to describe normal retina cells to allow better interpretation to understanding what this damage mean.

1.6.2 Neuronal cells of retina

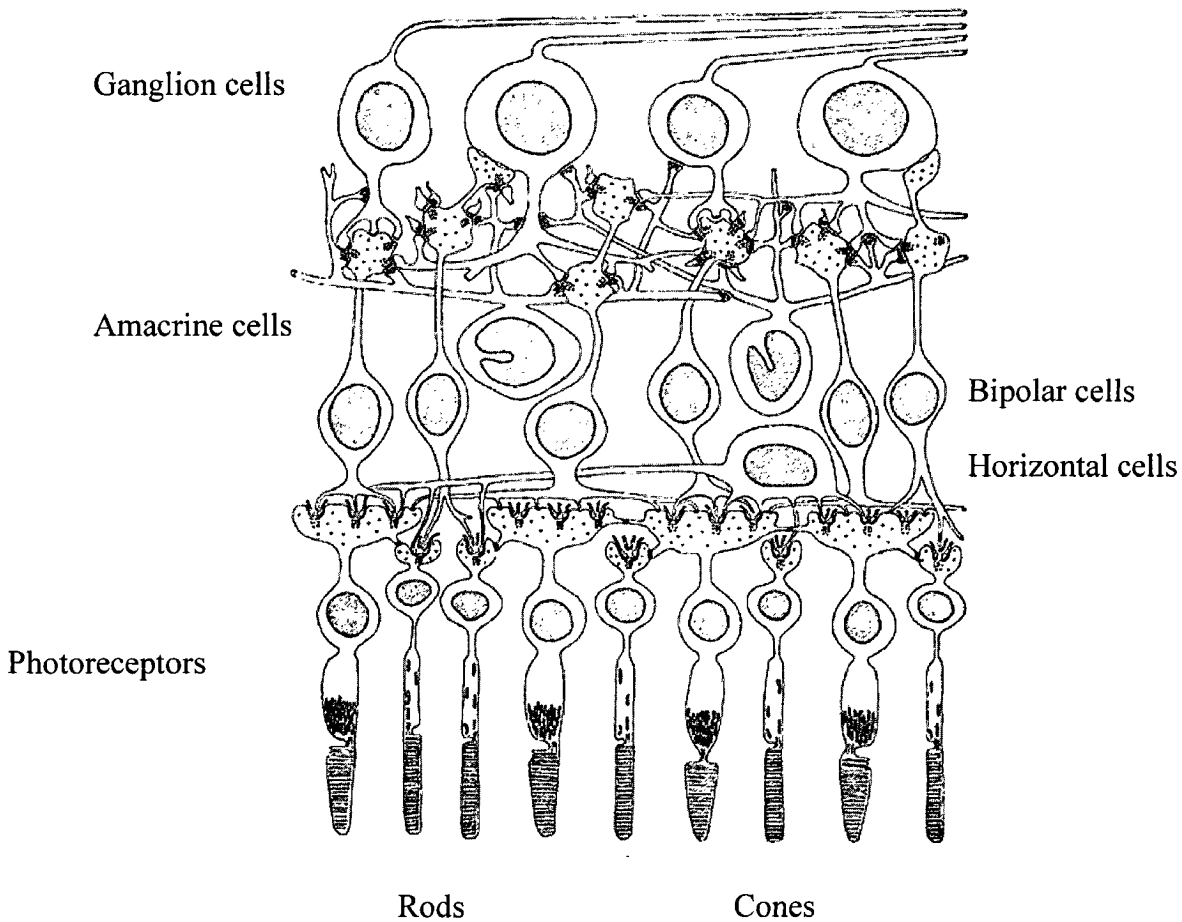

Photoreceptors Cells

The photoreceptor cells are composed of a cell body, an outer and inner segment, and inner fibers. Photoreceptors are very specialized cells that function to convert the light into nerve signals by a process called phototransduction. The distal part of photoreceptors is modified to capture the light, where the proximal part is modified to transmit it. Rod and cone are considered the two main types of photoreceptors in retina.

Horizontal Cells

Horizontal cells have very long processes that arborize completely in the outer plexiform layer. The narrow single axon of horizontal cells does not transmit any electrical signal, and the telodentric part of the cells is thus electrically insulated from the dendritic part.

Bipolar Cells

Bipolar cells carry the signal from photoreceptor cells to ganglion cells or amacrine cells. Cone and Rod bipolar cells are the first visual cells to display the center-surround receptive field organization. Both rod and cone bipolar cells of the invaginating type send their axons into inner plexiform layer, where the dendrites of ON ganglion cells end.

Amacrine Cells

Most amacrine cell neurons are located in the proximal part of the inner nuclear layer, where some may be found in the ganglion cell layer, but rarely in the inner plexiform layer. Amacrine cells function to adjust signals in the inner plexiform layer and are diverse in both their morphology and neurochemistry. Amacrine cells have no axons, in which it reflects their name. Most amacrine cells have Glycine or GABA.

Glial Cells

There are several types of glial cells found in the retina such as Muller cells, which are the most numerous; the astrocytes, the microglial cells, and oligodendrocyte cells.

Muller Cells

They are the main glial cells of the retina that extend through the whole thickness of the neural retina, and they issue many processes which cover most surfaces of the neuron cell bodies in the nuclear layers. In the plexiform layer, Muller cell processes cover the dendritic processes of the neurons to the synaptic clefts, insulating them both electrically and chemically. They also cover most ganglion axons in the nerve fiber layer. Moreover, Muller cells cover the blood vessels within the retina. Distally, Muller cells form a series of junctional complexes with themselves and with photoreceptor cells. These junction complexes composed mainly of zonulae adherens.

Muller cells extend beyond the outer limiting membrane into the subretianl space, forming microvilli. Their surface is increased so that they can more easily handle metabolites and ions in the subretianl space. In addition to the structural support, Muller cells offer neurons, and remove glutamate from the extracellular space by active uptake. Specific ion channels and transport system are located in the specific parts of the Muller cells. Moreover, Muller cells are believed to perform many of the functions provided in the brain by oligodendroglia and astrocytes, which are absent or spare in mammalian retinas.

Ganglion Cells

Ganglion cells are neuronal cells that collect all visual information processed in the retina and send it to the brain via optic nerve. The perikarya are located mainly in the ganglion cell layer and their dendrites form synapses with bipolar and amacrine cells in the inner plexiform layer. The axons of the ganglion cells form the optic nerve, and they terminate in the later geniculate body. Like many long axon cells in the CNS, the ganglion cells use glutamate for their neurotransmission, but some of these cells also contain substance P. Midget ganglion cells are one type of ganglion cells and they become more important and prominent. These are small cells that send a single dendritic process to the inner plexiform layer. Ganglion cells are responsible for carrying and sending visual information from a single cone. They probably carry information regarding form and color perception.

CHAPTER TWO:
MICROVESSELS LOSS, VASCULAR DAMAGE AND GLUTAMATE REDISTRIBUTION IN THE RETINAS OF DOGS WITH PRIMARY GLAUCOMA

Khaleel I. Alyahya, Chu-Te Chen, Brendan G. Mangan, Juliet R. Gionfriddo, Marie E. Legare, Richard R. Dubielzig, and James E. Mad

Acknowledgment

My roles in the study described in chapter 2 were helping conducting the immunohistochemical studies in under the supervision and direction of Dr. James Madl. Also, I was involved in interpreting the results of the studies and I was primary author in writing the manuscript describing this study. The manuscript describing this study has been published in Veterinary Ophthalmology volume 10, 2007.

This study was to test the hypothesis that vascular damage may lead to microvessel obliteration and focal ischemia. The microvessel densities of retinal regions were compared with differing degrees of damage and glutamate redistribution to determine if microvessel loss may contribute to glutamate redistribution and retinal damage in PG.

2.1 Abstract

Objective: Vascular damage and ischemia-like changes in glutamate distribution occur in primary glaucoma (PG) in dogs. We measured the microvessel density in PG retinas to determine if microvessel loss may induce ischemia and glutamate redistribution. Animals studied. Sections from 12 control and 33 glaucomatous dog retinas. *Procedures:* Vessels in retinas were identified by staining with *Griffonia simplicifolia* isolectin B4 or immunohistochemical staining for laminin or glutamate. Damage to regions of the inner nuclear

layer (INL) was classified as mild (< 10% damaged neurons), moderate (≥ 10% damaged neurons, INL ≥ 2 cells thick) or severe (INL < 2 cells thick). *Results:* Glutamate redistribution was found in some mildly damage regions and increased as damage increased. Regions with increased glutamate redistribution and increased damage had lower densities of microvessels in plastic sections. However, neuronal damage and glutamate redistribution were seen even in areas adjacent to the remaining microvessels. Microvessel loss in damaged regions was confirmed in paraffin sections with lectin staining and immunohistochemical localization of laminin. The density of larger vessels was not decreased in PG, but larger vessels often had thickened walls, cuffing with leukocytes, and leakage of albumin. *Conclusions:* Microvessel loss may occur in regions of glutamate redistribution and neuronal damage in PG retinas. Larger vessels were often damaged. The redistribution of glutamate is associated with a loss of microvessels even in mildly damaged regions. However, neuronal damage and glutamate redistribution may occur close to remaining microvessels, suggesting microvessel loss was not the sole factor inducing these changes.

2.2 Introduction

Glaucoma is characterized by a progressive loss of retinal ganglion cells that is often associated with increased intraocular pressure (Gelatt et al, 1999; Miller et al, 1995) and decreased retinal blood flow (Cheng et al, 2001; Cioffi et al, 2001; Chung et al, 1999). Progressive damage to other types of retinal cells also occurs in primary glaucoma (PG) in dogs, including cells of the inner nuclear layer (INL) and outer nuclear layer (ONL) (Whiteman et al, 2002). Cell loss with focal thinning of these layers eventually occurs in PG in dogs (McIlnay et al, 2004; Whiteman et al, 2002).

Several studies suggest there may be altered blood flow and damage to blood vessels in the retinas of dogs with glaucoma. Damage to retinal blood vessels occurs in dogs with PG (Smedes and Dubielzig, 1994). These damaged vessels have thickened walls containing deposits that are labeled by periodic acid-Schiff stain. Beagles with open-angle glaucoma also have structural abnormalities in the endothelium of capillaries of the lamina cribrosa (Brooks et al, 1989). Gelatt and coworkers have reported that altered ocular blood flow occurs before intraocular pressure is elevated in Beagles with open-angle glaucoma (Gelatt et al, 2003).

The altered blood flow and vascular damage reported in canine glaucoma might lead to ischemia and contribute to retinal damage in canine PG. PG-induced damage is often focal, and may involve all neuroretinal layers (McIlnay et al, 2004; Whiteman et al, 2002). Neuronal loss is greatest in the inner retina, which is consistent with ischemic damage (McIlnay et al, 2004). A redistribution of glutamate (Madl et al, 2005; McIlnay et al, 2004) and taurine glutamate (Madl et al, 2005) also consistent with ischemia, is greater in the more severely damaged regions. The redistribution consists of a loss of glutamate from neurons and an accumulation of glutamate in glial cells. We hypothesized that this focal pattern of changes may be due to ischemia which is induced by microvessel losses such as those that occur in diabetic retinopathy (Ishida et al, 2003) retinopathy of prematurity (Joussen et al, 2003), and some retinal degenerative diseases (Padnick-Silver et al, 2006; Blanks et al, 1986).

2.3 Methods

Acquisition and processing of eyes

Retinal samples were of two types: 1) plastic-embedded retinas which were acquired for immunohistochemical studies of glutamate distribution and 2) archived, paraffin-embedded

retinas (acquired by RRD) which were used for identification of blood vessels using lectin staining and immunohistochemical localization of laminin. The retinas that were plastic-embedded were from dogs with PG undergoing enucleation as part of treatment. Control plastic-embedded retinas were obtained from dogs euthanized at a local Humane Society. A complete ophthalmic examination (slit-lamp biomicroscopy, binocular indirect ophthalmoscopy, and applanation tonometry) was performed prior to euthanasia and found to be normal in each control dog. Eyes were obtained with adherence to the Association for Research in Vision and Ophthalmology Statement for the Use of Animals in Ophthalmic and Vision Research with approval from the Animal Care and Use Committee of Colorado State University.

The 10 plastic-embedded glaucomatous retinas were acquired from several veterinary ophthalmologists and from the Colorado State University Veterinary Medical Center. In the plastic-embedded eyes, no more than two globes were obtained from any single breed. 23 The paraffin embedded glaucomatous samples were obtained from 19 Cocker Spaniels, 3 Basset Hounds, and 1 Dachshund. The duration between presentation of the dogs to ophthalmologists for clinical signs and subsequent enucleation was known for the archived specimens. Retinas acquired $\leq$ 5days after onset of clinical signs were considered acute, while retinas acquired > 5 days after onset of signs were considered chronic.

Fixation and sectioning

Plastic embedded specimens were fixed as previously described (McIlnay et al, 2004). Eyes were rapidly dissected and the dorsotemporal quadrant of the globe was then placed in 0.3 % glutaraldehyde-4% paraformaldehyde in phosphate buffered saline (0.05 M phosphate). Quarters were then processed and embedded in Epon as previously described (Madl et al, 2005).

Paraffin embedded retinas were fixed by immersion in either 4% buffered formalin or Bouin's fixative/ethanol, without penetration of the globe. The samples were embedded in paraffin and sagittally sectioned at 5 μm thickness.

Staining of paraffin sections

Microvessel counts: Paraffin sections from PG and control dog eyes were stained by two methods to determine microvessel numbers per unit length of retina. Sections from each eye were immunohistochemically stained for laminin using an avidin-biotin method. In brief, sections were dewaxed in xylene and graded ethanol. Sections underwent antigen retrieval by autoclaving for 15 min in a 0.1 M citrate buffer, pH 6.0. After endogenous peroxidase was inactivated in 3% peroxide for 15 min, sections were incubated in primary rabbit antisera to laminin (1:100 in phosphate buffered saline) from Dako (Dako Cytomation) overnight. A Vectastain elite kit for rabbit antisera (Vector Laboratories, Burlingame, CA) was then used to visualize the primary antibody using peroxidase with diaminobenzidine as chromogen. Other sections were stained with biotinylated Griffonia simplicafolia isolectin B4 (Vector Laboratories). Sections were processed as described for laminin immunhistochemistry with biotinylated lectin diluted 1:100 substituting for the primary antibody. The biotinylated lectin was visualized with the ABC component of the Vectastain kit with metal-enhanced diaminobenzidine (Sigma-Aldrich) as chromogen. All slides were dehydrated through graded ethanol, cleared in xylene, and coverslipped.

Albumin and CD3 immunohistochemistry: Sections from each eye were processed essentially as described above for laminin immunohistochemistry using rabbit primary antibodies

to albumin or rabbit primary antibodies to CD3 (Dako) and diluted 1:400 in PBS for albumin or 1:50 in PBS for CD3.

Staining of plastic-embedded eyes

Post-embedment immunogold and toluidine blue staining were performed on adjacent, 0.5 μm sections using the same methods we have previously employed. Serial semi-thin sections (0.5μm) of retinas embedded in Epon were made using a Reichert-Jung Ultracut E ultramicrotome. Some sections were stained for 20 min at 60° C with 1% toluidine blue in 1% sodium borate buffer. Other, near-adjacent sections were etched and immunogold stained for glutamate using the method for silver-intensified immunogold labeling suggested by Chemicon International, (Temecula, CA) for their antisera to amino acids. Sections mounted on gel coated slides were etched with sodium ethoxide diluted 1:5 in ethanol for 20 min, rinsed in ethanol and water, and blocked with 5% normal goat serum diluted in 0.05 M, PBS. Sections were rinsed in PBS and incubated overnight in 1:400 dilutions of rabbit antisera to glutamate (Sigma/Aldrich) in PBS. After rinsing in PBS, sections were incubated for 4 h in secondary gold-labeled (ultrasmall particles) anti-rabbit or anti-mouse antisera (Electron Microscopy Sciences, Hatfield, PA) diluted in PBS (1:20). Sections were rinsed for 30 min in PBS and then two rapid changes of water. Staining was silver enhanced for 6 min, rinsed in water, and the slides coverslipped for image capture. Digital images were captured using a Zeis Axioplan 2 microscope with Axiovision 3.1 software. For measurements of staining density, images were analyzed using ImageJ 1.34 (National Institutes of Health). Controls for specificity included omission of the primary antibody and inhibition of staining by preincubation of antisera with glutamate conjugated to bovine serum albumin (absorption controls).

Assessment of damage

Regions of INL in glaucomatous retinas were classified as mildly damaged, moderately damaged or severely damaged by the estimated percentage of damaged cells and the thickness of the INL in the region in both paraffin and plastic sections. Plastic sections were stained with toluidine blue and paraffin sections were stained with hematoxylin and eosin to evaluate damage. Mildly damaged regions contained $\leq$ 10% damaged INL cells and an INL thickness of $\geq$ 2 cells. Moderately damaged regions contained > 10% damaged cells and an INL thickness of $\geq$ 2 cells. Severely damaged regions showed thinning of the INL to < 2 cells in thickness. Damaged INL cells were defined as those with a dark, condensed nucleus and/or swollen, pale cytoplasm. Regions with highly variable thickness of INL or variable percentages of damaged cells were not included in the study unless at least 70% of the region fit one of the categories.

Statistical analysis

Quantitative data on microvessel density and quantitative immunohistochemical staining densities obtained from plastic sections were analyzed for statistical significance using ANOVA followed by Tukey's multiple comparison tests using GraphPad Instat 3 software.

2.4 Results

Glutamate redistribution in PG

In plastic sections the densities of glutamate immunostaining of cells and INL regions were measured in a semi-quantitative manner using an immunogold technique. Control retinas showed high levels of glutamate immunoreactivity in putative neurons of the INL with much lower levels in putative Muller cells (Fig. 2.1A & E).

Regions with different degrees of damage were evaluated for glutamate redistribution in plastic sections. Damage to INL cells in PG may progress from mild damage, where a normal number of cells are still present but some have clumping of chromatin and pale, swollen cytoplasm, to more severe damage where the loss of cells results in thinning of the INL (McIlnay et al, 2004). To determine the stage of damage at which microvessels are lost, damage to INL regions was classified as mild, moderate or severe. Cells were classified as damaged if they had dark nuclei with condensed chromatin or pale, swollen cytoplasm.

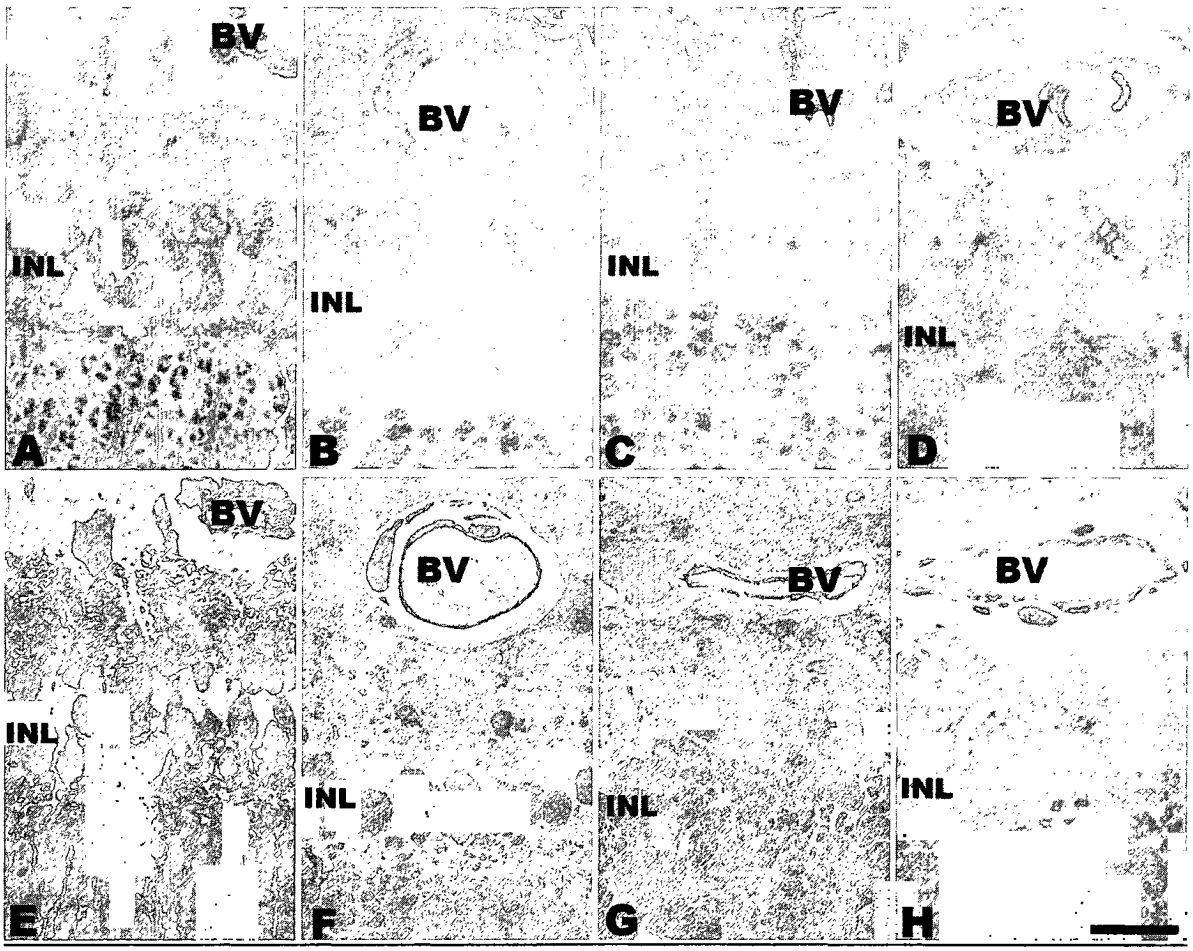

Fig. 2.1 Glutamate redistribution occurred in regions with different severities of damage in PG. A-D. Morphologic appearances of the INL in regions with different severities of damage are shown in toluidine blue stained sections. E-H. Glutamate immunostaining of adjacent 0.5 □m sections from the same regions shown in A-D. A. Control section. Typical undamaged neurons of the INL are indicated by asterisks. A typical Muller cell is indicated by m, and a microvessel

is indicated by BV. B. A region with mild damage and high glutamate levels. C. A region with mild damage and low glutamate levels. Almost all neurons appear undamaged (asterisks). D. A region with severe damage. Note thinning of the INL (between arrowheads). E. Glutamate immunostaining of the same region of control retina as A. Note the high levels of glutamate immunoreactivity in the INL neurons (asterisks) also labeled in A and a low level of glutamate in the Muller cell (m) also labeled in A. F. Glutamate immunostaining of the same region as B with mild damage and high levels of glutamate. Note the large number of neurons with high levels of glutamate immunoreactivity. G. Glutamate immunostaining of an adjacent section of the same region as C with mild damage and low levels of glutamate. Note the low levels of glutamate in some undamaged neurons (asterisks). H. Glutamate immunostaining of the same region as D with severe damage. Note the low levels of glutamate immunoreactivity in the thinned INL. All images are shown with the same orientation and magnification. Bar = 15 □m.

The densities of glutamate immunostaining in putative neurons of the INL were decreased in damaged regions (Fig. 2.2). The average level of glutamate immunoreactivity was measured in 50 μm long areas of INL in regions with different degrees of damage. The average density of INL glutamate immunostaining decreased as the severity of damage increased (Fig. 2.2A). In contrast to neurons, the average level of glutamate immunostaining was increased in putative Muller cell bodies of the INL and in Muller cell processes of the nerve fiber layer (Fig. 2.2B) in a similar manner to the glutamate redistribution we have previously described. Within mildly damaged regions of the INL, 50 μm areas were seen that had either near-normal levels of glutamate (Fig. 2A; Mild, High Glu) or significantly decreased levels of glutamate (Fig. 2.2A; Mild, Low Glu). When control retinas were examined for similar focal regions of glutamate loss from the INL, none were seen except in regions with obvious sectioning or staining artifacts. Quantitative measures of staining density for glutamate in control retinas confirmed that regions with the lowest levels of glutamate staining on visual inspection were not significantly different from adjacent regions with higher levels of glutamate staining ($p > 0.4$; data not shown).

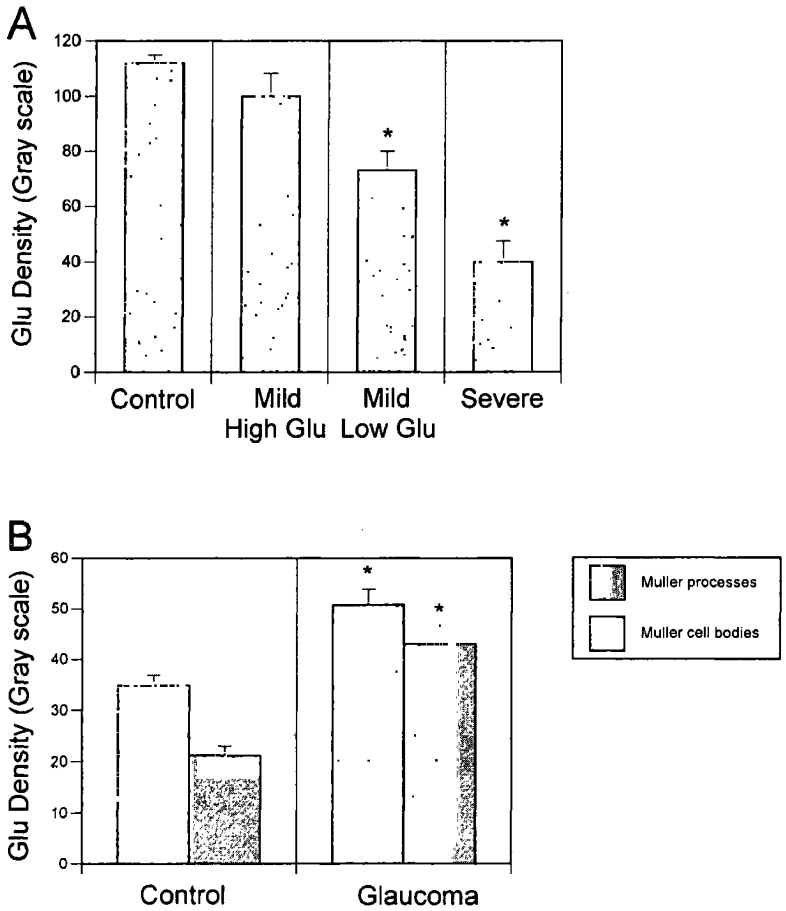

Fig. 2.2 Glutamate redistribution was dependent on the severity of damage in PG. A. The average glutamate immunostaining density in 50 μm regions of the INL was reduced as the severity of damage increased. Within mildly damaged regions, smaller areas ≥ 50 μm in length were seen that had either near-normal levels of glutamate (Mild, High Glu) or decreased levels of glutamate (Mild, Low Glu). B. The glutamate immunostaining density in Muller cell process of the nerve fiber layer and putative Muller cell bodies of the INL was increased in PG. Bars = SEM. * $p < 0.05$ by Tukey's multiple comparison test.

Microvessel densities were decreased in regions with glutamate redistribution and neuronal damage

Microvessel densities in plastic sections were measured using glutamate immunoreactivity as a marker for endothelial cells. As shown in Figure 3, endothelial cells of the

vessels maintained substantial levels of glutamate at all severities of damage, allowing glutamate immunostaining to be used as a marker to identify microvessels.

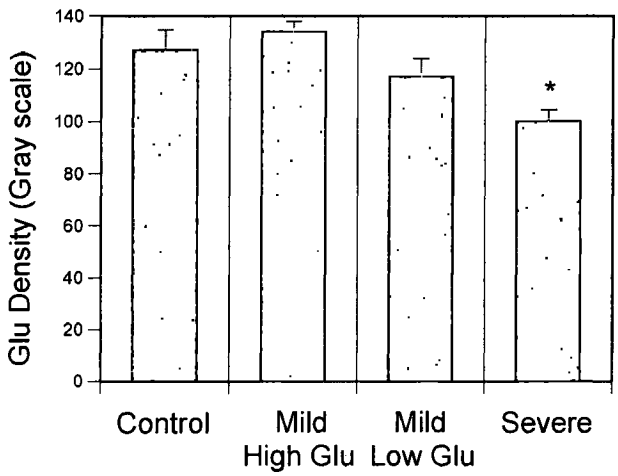

Fig. 2.3 Glutamate immunoreactivity was maintained at high levels in the endothelium of blood vessels in PG. Replicate sections from control and PG eyes were immunogold stained at the same time and images captured under the same conditions. Bars indicate SEM. * $p < 0.05$ by Tukey's multiple comparison test compared to control.

The densities of microvessels in PG retinas were significantly decreased in regions with increased severity of damage (Fig. 2.4A) and lowered neuronal glutamate staining densities (Fig. 2.4B). Microvessels were identified by the high levels of glutamate immunoreactivity maintained in endothelial cells even in severely damaged regions (Figs. 2.1 & 2.3).

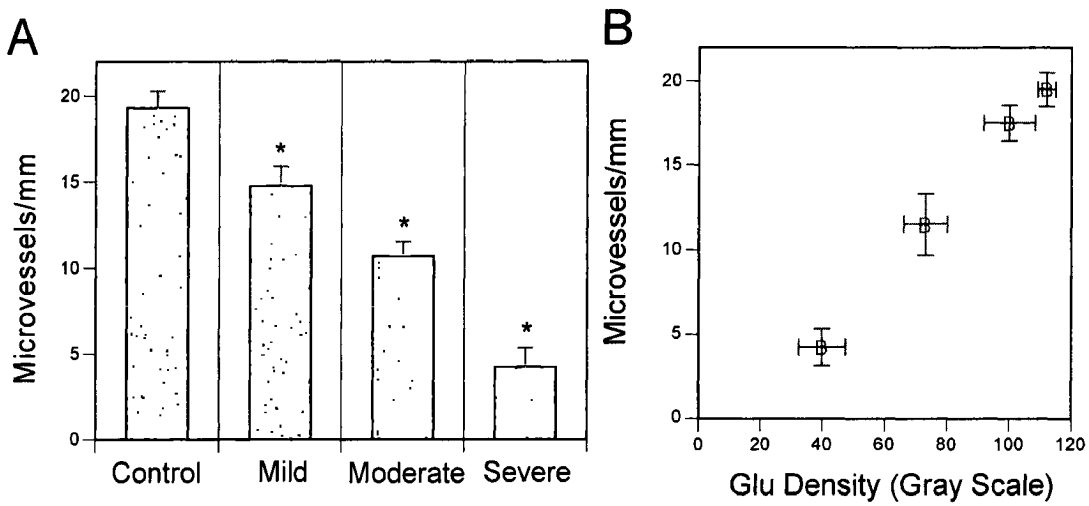

Fig. 2.4 Microvessels were lost in regions with increased glutamate redistribution and increased severity of damage. A. Microvessels were counted in 200 μm regions of retina with different severities of damage in the INL. Microvessels were identified by the high levels of glutamate retained in endothelial cells. * $p < 0.05$ by Tukey's multiple comparison test compared to control. B. Microvessel densities from regions with different severities of damage were plotted against the average glutamate staining density in the INL of the same regions. Glu densities are those from Figure 2A. Bars = SEM.

Microvessel obliteration was confirmed using other markers for blood vessels.

To confirm that a microvessel loss occurred in PG, other methods of labeling vessels were used. Staining with *Griffonia simplicafolia* isolectin B4 or antibodies to laminin have often been used to identify blood vessels.

Sagittal sections from paraffin-embedded retinas of dogs with PG and control dogs were stained with lectin or immunohistochemically stained for laminin to measure microvessel densities. We were unable to use either lectin staining or immunohistochemical staining for laminin successfully on plastic sections. Leukocytes and macrophages are also labeled with the lectin. To ensure that leukocytes outside of blood vessels were not counted as microvessels in

lectin-stained retina, labeled structures needed to have an identifiable lumen to be considered a microvessel. No significant differences were found between the numbers of microvessels in sections stained with lectin or antibodies to laminin in controls ($P > 0.6$; data not shown). Typical staining of microvessels with lectin and antibodies to laminin are illustrated in Fig. 2.5.

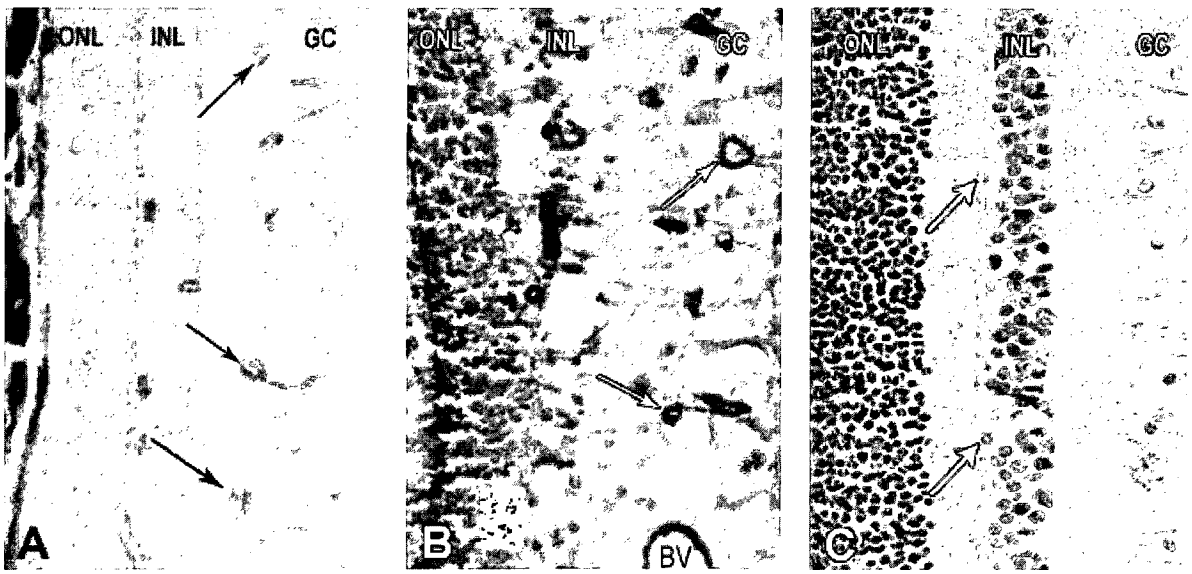

Fig. 2.5 Staining of microvessels in paraffin sections with lectin and antibodies to laminin. A. A section of control retina immunohistochemically stained for laminin shows labeling of microvessels, three of which are indicated by arrows. B. A section from a PG retina stained with lectin shows labeling of microvessels, two of which are indicated by arrows. C. A section of control retina stained with hematoxylin and eosin illustrates the appearance of typical microvessels (arrows). All images are shown with the same orientation and magnification. Bars = x μm.

Microvessel densities in both the peripheral and central regions of retinas were reduced in PG retinas (Fig. 2.6). The number of microvessels in 500 μm fields of sections of control and PG retinas stained with lectin and antibodies to laminin were counted. Significant decreases in microvessel densities were seen in both central and peripheral regions of PG eyes.

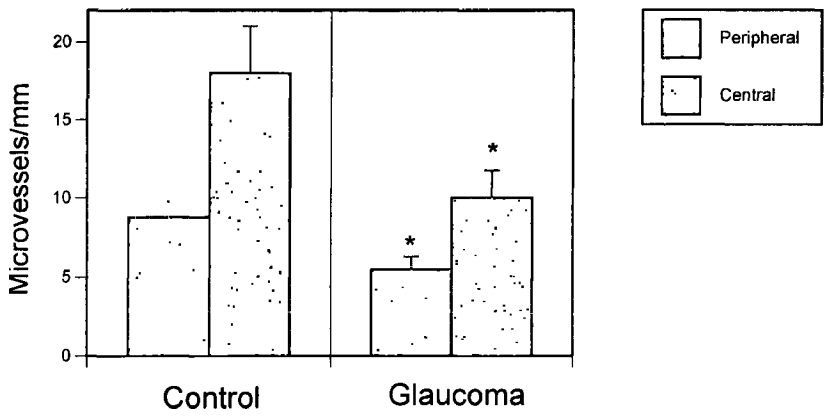

Fig. 2.6 Microvessel densities were reduced in the retinas of dogs with PG when either lectin staining or laminin immunohistochemistry was used to identify vessels. The number of microvessels in 500 μm fields of paraffin sections was counted in the peripheral retina (starting 1 mm from the ora ciliaris) and central retina in sagittal sections of eyes stained with either lectin or antibodies to laminin. Three fields were counted from each region of each retina. * $p < 0.05$ by Tukey's multiple comparison test.

The densities of microvessels in regions with different degrees of damage were quantified using lectin staining and laminin immunohistochemistry to identify blood vessels (Fig. 2.7). The density of microvessels was reduced as the severity of damage increased in a manner similar to that seen when glutamate was used as a marker for endothelial cells in plastic sections (Fig. 2.4B).

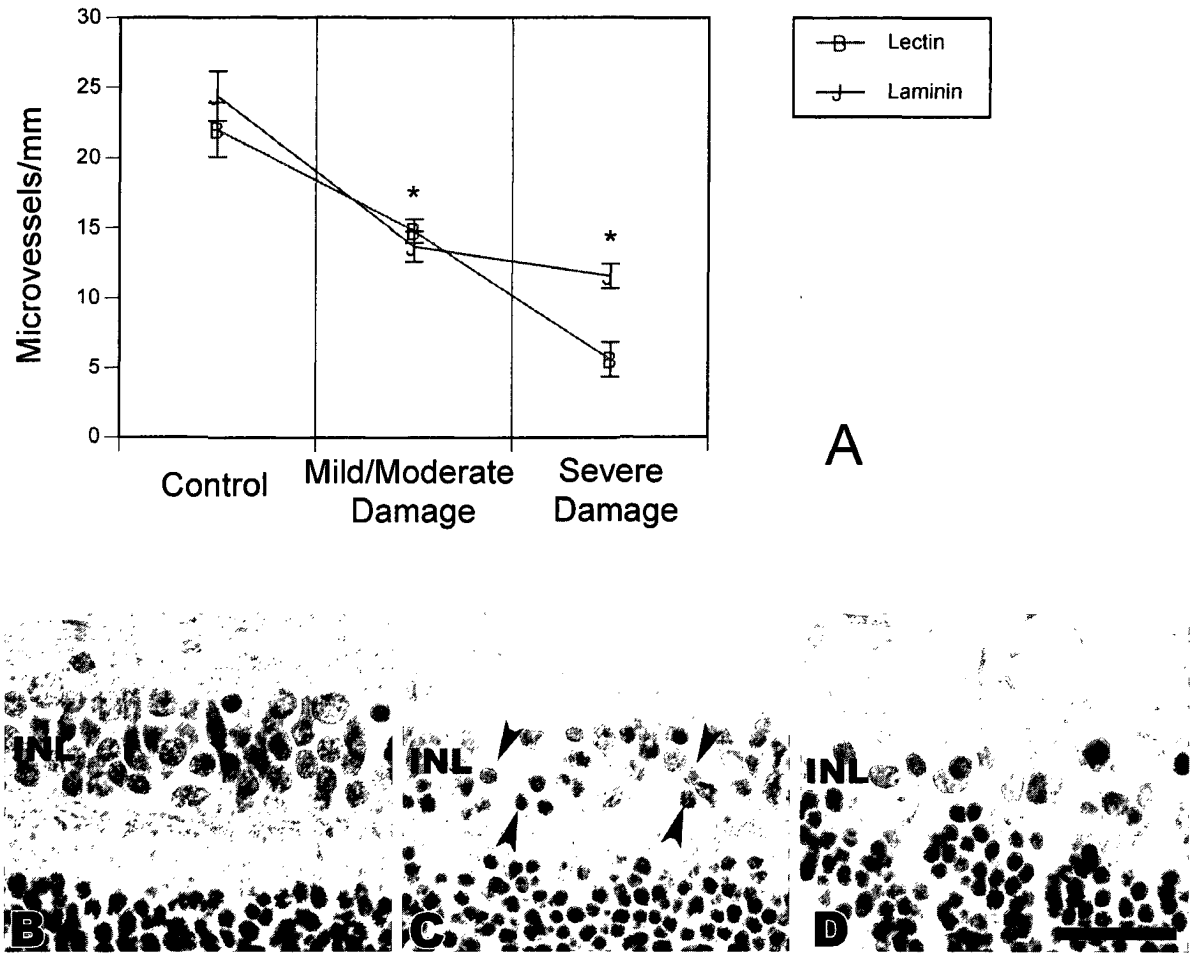

Fig. 2.7 A. Microvessel densities were decreased in regions with increased severity of damage when either lectin staining or laminin immunohistochemistry were used to identify blood vessels. Microvessels were counted in 250 μm regions of retina with different severities of damage in the INL. Bars = SEM. * $p < 0.05$ for both lectin and laminin compared to control (Tukey's multiple comparison test). B. Control retina showing lack of damage to the INL. C. Moderately damaged retina showing damaged INL cells (arrows). D. Severely damaged retina with reduced INL thickness. B-D Hematoxylin and eosin staining. All images are shown with the same orientation and magnification. Bar = 25 μm.

Larger vessels were damaged but not lost in PG.

In contrast to microvessels, the density of larger vessels (lumen > 10 μm) was not significantly reduced in PG (Fig. 2.8A). However, the larger vessels showed signs of damage,

including thickened vessel walls (Fig. 2.8B), albumin leakage (Fig. 2.8C&D) and cuffing by leukocytes (Fig. 2.8E). The finding of albumin immunoreactivity outside the lumen of larger vessels in PG suggests a breakdown of the blood-retinal barrier (see Discussion).

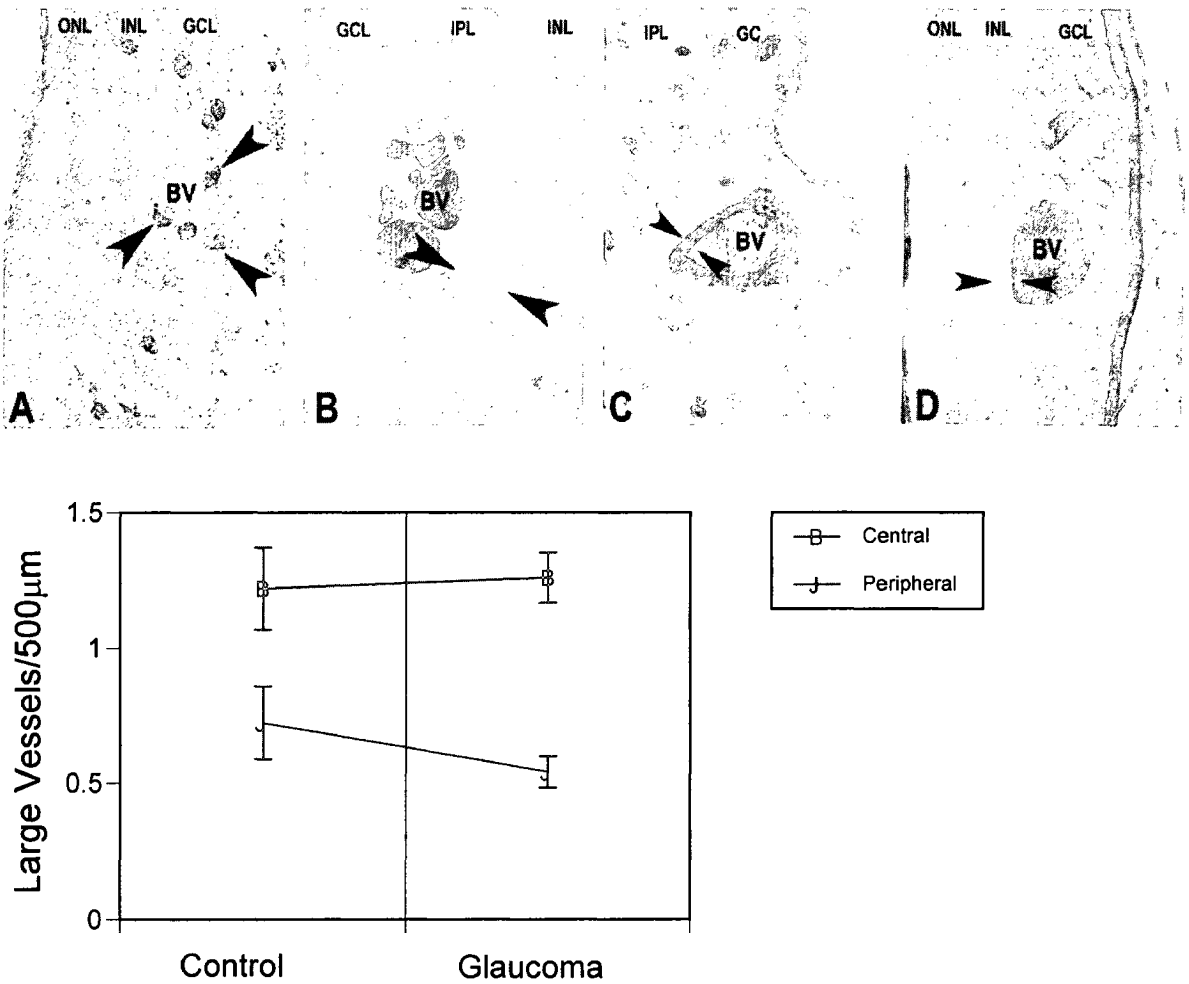

Fig. 2.8 Larger vessels showed signs of inflammation and damage in PG retinas. A. Immunohistochemical staining for CD3 revealed vascular cuffing with T lymphocytes around some vessels (arrowheads) of PG retinas. BV indicates a blood vessel. B. Larger vessel walls were often thickened in PG. Arrowheads indicates the thickened wall of a blood vessel. Plastic section stained with toluidine blue. C. Albumin was often found outside the lumen of blood vessels in PG. Immunohistochemical staining for albumin was especially prominent in the walls of blood vessels (arrowheads). D. Albumin was normally found only in the lumen of vessels in control retinas immunohistochemically stained for albumin. Arrowheads indicate the unlabeled

wall of a blood vessel. E. No significant loss of larger vessels was apparent in PG. Bars indicate SEM.

Microvessel obliteration in PG does not require the loss of photoreceptors.

Microvessel obliteration occurs in several retinal diseases, including those where hyperoxia is induced by a loss of photoreceptors (see Discussion). To determine whether photoreceptor loss was necessary to induce microvessel obliteration, we measured the thickness of the ONL in the central region of chronic PG retinas where microvessel loss occurs (Fig. 2.6). No decrease in ONL thickness was seen in chronic PG retinas compared to control retinas. The central ONL thickness was 33 μm ± 3.6 in control retinas and 43.8 μm ± 4.4 in chronic PG ($p > 0.05$). This suggests that thinning of the outer retina with a subsequent hyperoxia is not necessary to induce microvessel obliteration.

2.5 Discussion

In previous studies of PG in dogs we reported that alterations in glutamate distribution occurred in regions with more neuronal damage. This glutamate redistribution was consistent with an ischemia-induced glutamate release that we hypothesized may have contributed to the damage (McIlnay et al, 2004; Madl et al, 2005). In other studies, vascular abnormalities have been reported in canine glaucoma (Brooks et al, 1989, Gelatt et al, 2003) including PG (Smedes and Dubielzig, 1994). In the current study we tested the hypothesis that vascular damage may lead to microvessel obliteration and focal ischemia. We compared the microvessel densities of retinal regions with differing degrees of damage and glutamate redistribution to determine if microvessel loss may contribute to glutamate redistribution and retinal damage in PG. We also examined the types of damage seen in larger vessels of PG retinas to better understand the pathogenesis of the disease and to determine if leakage of glutamate from vessels might

contribute to the pathologic glutamate redistribution previously reported in PG PG (McIlnay et al, 2004; Madl et al, 2005).

A loss of microvessels and damage to larger vessels may occur in PG retinas.

In this study we found that the densities of microvessels in PG eyes were significantly reduced compared to control retinas. This finding was consistent in all three of the different methods of identifying blood vessels (Figs. 2.4 & 2.7). In contrast to the microvessels, the densities of larger vessels in both the central and peripheral regions of PG retinas were not significantly reduced (Fig. 2.8). This suggests that a selective loss of microvessels occurs as PG progresses. This loss could be similar to diseases such as microscopic polyangitis in which small vessels but not larger vessels develop vasculitis (Sorokin et al, 1992).

The loss of microvessels appears greatest in the most severely damaged retinal regions. Neuronal damage in PG is characterized by swelling of cell bodies and nuclear changes in the INL. This is especially prominent in acute PG (McIlnay et al, 2004). In some regions of the retina the INL and ONL may be thinned (Whiteman et al, 2002; McIlnay et al, 2004), as a result of neuronal loss that presumably follows the neuronal damage. This study supported the idea that decreases in microvessel numbers are dependent on the severity of INL damage, which suggests that the loss of microvessels may increase as retinal damage progresses.

In a concurrent study we found vascular changes in the larger blood vessels of retinas of glaucomatous dog eyes that were consistent with inflammation. These changes include an infiltration of leukocytes around some larger vessels, thickening of vessel walls, and increased

permeability of the blood vessels to albumin (Fig. 2.8) and possibly to other smaller molecules such as glutamate.

Glutamate leakage from damaged vessels into the extracellular fluid of the retina potentially contributes to ongoing retinal damage. It is well established that high extracellular levels of glutamate are toxic to retinal neurons (Kwong et al. 2000; Valencia et al, 2002). Plasma concentrations of glutamate are variable but have typically been reported to be about 50 μM (Valencia et al, 2002). The extracellular fluid of the central nervous system, including the normal retina, is believed to contain only very low levels of glutamate, perhaps only a few μM as seen in normal vitreous of dogs (Brooks et al, 1989), which suggests that glutamate will leak from the blood into the retina down a concentration gradient. Although the initial exposure of the retina to higher levels of glutamate may not cause neuronal damage due to the very robust uptake systems for glutamate present on glial cells, it is likely that in regions where the glial cells may be low on energy, glutamate uptake and conversion to glutamine will be reduced. Both the uptake of glutamate and formation of glutamine are energy-requiring processes and may be reduced in ischemic regions, perhaps including regions of microvessel loss.

Glutamate redistribution may occur in mildly damaged regions and is associated with a loss of microvessels.

The relationship of glutamate redistribution to microvessel loss and neuronal damage was examined in plastic-embedded eyes. In those sections, glutamate redistribution could be detected even in some mildly damaged regions of INL (Fig. 2.2). The regions with glutamate redistribution also had significantly lower microvessel densities (Fig. 2.4B). This is consistent with the idea that vascular changes initiate early glutamate redistribution and PG damage.

However, it should be noted that both damage and glutamate redistribution were observed in cells very close to remaining microvessels. This indicates that ischemia induced by microvessel loss is not the sole factor involved in inducing glutamate redistribution or neuronal damage.

Mechanisms that may induce microvessel loss.

In some retinal diseases such as retinopathy of prematurity (Ishida et al, 2003), retinal degeneration (Blanks et al, 1986) and retinitis pigmentosa (Padnick-Silver et al, 2006), microvessel loss is believed to occur in response to hyperoxia. The hyperoxia may be due to decreased oxygen demand induced by a previous loss of retinal cells. For example, in retinal degenerations in which photoreceptors are lost, a microvessel obliteration has been induced in the retina that is believed to be secondary to increased oxygen availability from the choroid vasculature (Padnick-Silver et al, 2006).

To determine if photoreceptor loss might account for the microvessel loss in PG, we measured the thickness of the ONL in the central portion of chronic PG retinas where microvessel obliteration occurred. No thinning of the ONL was seen in these regions of microvessel obliteration, suggesting that photoreceptor loss, decreased oxygen demand, and a subsequent hyperoxia was not the mechanism leading to microvessel obliteration in PG. However, in PG there is a greater loss of microvessels in regions of severe damage where thinning of the INL has occurred. This suggests that loss of neurons of the inner retina may lead to decreased oxygen demand, and a subsequent hyperoxia that may induce a subsequent pruning of microvessels. However, the observation that some of the microvessel loss occurs in mildly damaged INL prior to sunstantial thinning of the INL argues that hyperoxia due to thinning of the retina does not initiate microvessel loss in PG.

Implications for future studies and treatment.

Losses of microvessels and glutamate redistribution may occur even in mildly damaged regions in PG retinas. If these processes contribute to early PG damage, glutamate antagonists may prove effective in reducing or preventing early excitotoxic damage to neurons. However, the mechanism(s) that induce microvessel loss and damage to larger blood vessels remain to be determined. Without effective treatments for the vascular changes, these vascular changes may continue to contribute to the progressive retinal damage seen in PG.

CHAPTER THREE:
LOSS OF GLUTAMINE SYNTHETASE IMMUNOREACTIVITY FROM THE RETINA IN CANINE PRIMARY GLAUCOMA

Chu-Te Chen, Khaleel Alyahya, Juliet R. Gionfriddo, Richard R. Dubielzig, and James E. Madl

Acknowledgment

My roles in the study described in chapter 3 were helping conducting the immunohistochemical studies under the supervision and direction of Dr James Madl. Also, I was involved in interpreting the results of the study and I was a co-author of the manuscript describing this study. The manuscript describing this study has been published in Veterinary Ophthalmology volume 11, 2008.

This study was to examine the immunohistochemical distribution of GS in the retinas of dogs with PG to determine if decreases in the amount of GS occur in PG and if the decreases are associated with glutamate redistribution and neuronal damage.

3.1 Abstract

Purpose: Changes in retinal glutamate distribution occur in primary glaucoma (PG) in dogs. Although the redistribution resembles that induced by ischemia, decreases in glutamine synthetase (GS) activity may also induce similar glutamate redistribution. We examined the distribution of GS, glutamate, and glial fibrillary acidic protein (GFAP), a marker for reactive glia, in PG retinas by immunohistochemistry to determine if decreases in GS and formation of reactive glia are associated with glutamate redistribution and neuronal damage. Animals: Sections from 14 control dog eyes and 22 eyes from dogs with PG. Methods. Sections from 14 control and 22 glaucomatous globes were immunohistochemically stained for GS, glial fibrillary

acidic protein or glutamate. Results: In semiquantitative immunogold studies, decreases in GS staining density were highly correlated with glutamate redistribution and neuronal damage. In less quantitative immunoperoxidase staining of acute ($\leq$ 5 days after clinical signs) and chronic PG retinas, GS immunoreactivity was decreased in focal regions of some acute PG retinas, and there were widespread decreases in chronic PG retinas. GFAP immunoreactivity was increased in Müller cells primarily in severely damaged regions of chronic PG retinas. Conclusions: Decreases in GS immunoreactivity were associated with glutamate redistribution. These decreases in GS occurred even in mildly damaged regions of retina before retinal thinning. Reactive Müller cells were seen primarily in chronic PG in severely damaged regions. Decreases in GS may potentiate ischemia-induced early glutamate redistribution and neuronal damage in canine PG.

3.2 Introduction

Glaucoma is characterized by a progressive loss of retinal ganglion cells that is often associated with increased intraocular pressure (Miller et al, 1995; Gelatt et al, 1999) and altered blood flow (Gelatt et al, 2003). PG in dogs is a very severe retinal disease that often damages all layers of the neuroretina (Whiteman et al, 2002; McIlnay et al, 2004). We have previously found focal regions with redistributions of glutamate in canine PG that are consistent with ischemia (McIlnay et al, 2004; Madl et al, 2005). This redistribution includes increased concentrations of glutamate in Müller cells and decreased concentrations in neurons. We have recently found that microvessel losses are associated with glutamate redistribution and neuronal damage in PG (Alyahya et al, 2007). These results are consistent with microvessel losses leading to local ischemia, glutamate release, and neuronal damage. However, glutamate redistribution and

neuronal damage were seen near the remaining microvessels in PG, suggesting that microvessel loss was not the only factor leading to glutamate redistribution and neuronal damage.

Another way in which glutamate may redistribute in retinal cells is by altered glutamate metabolism. GS is a major enzyme involved in the metabolism of glutamate in glial cells. GS catalyzes the amidation of glutamate to glutamine, which is an essential part the cycling of the transmitter pool of glutamate between neurons and glia. Decreased GS activity will lead to increased levels of glutamate in glial cells and decreased levels of glutamate in neurons in a manner similar to the redistribution of glutamate seen in PG in dogs. Decreased GS activity has been seen in glaucoma in rats (Moreno et al, 2005). Decreased GS activity has also been reported after hypoxia in the brain (Krajnk et al, 1996) and some of the glutamate redistribution seen in ischemia has been attributed to decreased GS activity (Torp et al, 1996). GS requires ATP to synthesize glutamine from glutamate, and ischemia-induced ATP depletion inhibits GS activity. In retinal detachment with presumptive hypoxia, the redistribution of glutamate and other amino acids is suggestive of decreased GS activity (Marc et al, 1998). In addition to loss of GS enzymatic activity in hypoxia/ischemia, loss of GS immunoreactivity has also been reported after ischemia in the retina (Nishiyama et al, 2000).

Decreased GS activity may contribute to higher extracellular glutamate levels and subsequent neuronal damage. Decreased GS activity may lead to an accumulation of glutamate in glial cells. Models of glutamate transport by GLAST, the main glutamate transporter in the retina (Rauen et al, 1998), suggest an increase in the intracellular level of glutamate in glial cells may lead to a proportionate increase in the minimum extracellular level of glutamate (see Discussion). (Attwell, 1993; Bouvier et al, 1992).

Reactive Müller cells are induced in several different types of retinal diseases, including some types of glaucoma (Scheuttauf et al, 2004; Low et al, 2006). The reactive glial cells alter their cytoskeleton, thus allow their detection by immunohistochemical staining for glial fibrillary acidic protein (GFAP) and other cytoskeletal components. Other changes that occur in reactive glia include altered expression of enzymes. Thus one possible mechanism leading to changes in the expression of GS would be reactive changes in the glial cells.

3.3 Methods

Acquisition and processing of eyes

Retinal samples were of two types: 1) plastic-embedded retinas which were acquired for immunohistochemical studies of glutamate distribution and 2) archived, paraffin-embedded retinas (acquired by RRD) which were used for studies of the effects of chronicity of glaucoma and retinal position on GS and GFAP immunoreactivity. The retinas that were plastic-embedded were from dogs with PG undergoing enucleation as part of treatment. Control plastic-embedded retinas were obtained from dogs euthanized at a local Humane Society. A complete ophthalmic examination (slit-lamp biomicroscopy, binocular indirect ophthalmoscopy, and applanation tonometry) was performed prior to euthanasia and found to be normal in each control dog. Eyes were obtained with adherence to the Association for Research in Vision and Ophthalmology Statement for the Use of Animals in Ophthalmic and Vision Research with approval from the Animal Care and Use Committee of Colorado State University.

The 10 plastic-embedded glaucomatous retinas were acquired from several veterinary ophthalmologists and from the Colorado State University Veterinary Medical Center. In the plastic-embedded eyes, no more than two globes were obtained from any single breed. The 23

paraffin embedded glaucomatous samples were obtained from 19 Cocker Spaniels, 3 Basset Hounds, and 1 Dachshund. The duration between presentation of the dogs to ophthalmologists for clinical signs and subsequent enucleation was known for the archived specimens. Retinas acquired $\leq$ 5days after onset of clinical signs were considered acute, while retinas acquired > 5 days after onset of signs were considered chronic.

Fixation and sectioning

Plastic embedded specimens were fixed as previously described (McIlnay et al, 2004). Eyes were rapidly dissected and the dorsotemporal quadrant of the globe was then placed in 0.3 % glutaraldehyde-4% paraformaldehyde in 0.05 M phosphate buffered saline (PBS). Quarters were then processed and embedded in epon as previously described. Paraffin embedded retinas were fixed by immersion in either 4% buffered formalin or Bouin's fixative/ethanol, without penetration of the globe. The samples were embedded in paraffin and sagittally sectioned at 5 μm thickness.

Staining of paraffin sections

Paraffin sections from PG and control dog eyes were stained for GS using an avidin-biotin method. In brief, sections were dewaxed in xylene and graded ethanol. Sections underwent antigen retrieval by autoclaving for 15 min in a 0.1 M citrate buffer, PH 6.0. After endogenous peroxidase was inactivated in 3% peroxide for 15 min, sections were incubated in primary mouse monoclonal antibody to GS (1:100 in PBS) from Chemicon International (Temecula, CA) overnight. A Vectastain elite kit for rabbit antisera (Vector Laboratories, Burlingame, CA) was then used to visualize the primary antibody using peroxidase with diaminobenzidine as

chromogen. All slides were dehydrated through graded ethanol, cleared in xylene, and coverslipped. Controls for specificity included omission of the primary antibody.

Staining of plastic-embedded eyes

Post-embedment immunogold and toluidine blue staining were performed on adjacent, 0.5 μm sections using the same methods we have previously employed(Mad et all, 2005; Alyahya et al, 2007). Serial semi-thin sections (0.5μm) of retinas embedded in Epon were made using an ultramicrotome. Some sections were stained for 20 min at 60° C with 1% toluidine blue in 1% sodium borate buffer. Other, near-adjacent sections were etched and immunogold stained for glutamate or GS using a method for silver-intensified immunogold labeling. Sections mounted on gel coated slides were etched with sodium ethoxide diluted 1:5 in ethanol for 20 min, rinsed in ethanol and water, and blocked with 5% normal goat serum diluted in 0.05 M, PBS. Sections were rinsed in PBS and incubated overnight in 1:400 dilutions of rabbit antisera to glutamate (Sigma-Aldrich, St. Louis, MO) or 1:100 dilutions of mouse antibody to GS (Chemicon International, Temecula, CA) in PBS. After rinsing in PBS, sections were incubated for 4 h in secondary gold-labeled (ultrasmall particles) anti-rabbit or anti-mouse antisera (Electron Microscopy Sciences, Hatfield, PA) diluted in PBS (1:20). Sections were rinsed for 30 min in PBS and then two rapid changes of water. Staining was silver enhanced for 6 min, rinsed in water, and the slides coverslipped for image capture. Controls for specificity included

Image capture and analysis

Digital images were captured using a Zeis Axioplan 2 microscope with Axiovision 3.1 software (Carl Zeiss MicroImaging, Inc.,Thornwood, NY). For measurements of staining density, images were analyzed using ImageJ 1.34 (National Institutes of Health, Bethesda, MD).

After inversion, background densites of immunostaining of blank plastic or paraffin were subtracted from each image.

For measurements of glutamate immunogold densities in INL regions, the average densities in regions 15 μm X 15 μm in the INL of plastic sections were quantified. Three INL regions were measured in each image. For measurements of glutamate immunostaining densities in Müller cells, the densities in three putative Müller cells per region were measured. In similar manner measurements of GS immunogold densities in plastic sections were made in three putative Müller cell bodies in each region.

For measurement of GS staining densities in paraffin sections, average densities were measured in 60 μm X 60 μm boxes in the inner retina. For measurements of GFAP staining densities, densities were measured in 80 μm lengths of retina from the outer limiting membrane through the INL. Three regions from central and peripheral areas of each eye were measured in each captured image for both GS and GFAP.

Assessment of damage

Regions of INL in glaucomatous retinas were classified as mildly damaged or severely damaged by the estimated percentage of damaged cells and the thickness of the INL in the region in plastic sections. Plastic sections were stained with toluidine blue to evaluate damage. Mildly damaged regions contained $\leq$ 10% damaged INL cells and an INL thickness of $\geq$ 2 cells. Severely damaged regions showed thinning of the INL to < 2 cells in thickness. Damaged INL cells were defined as those with a dark, condensed nucleus and/or swollen, pale cytoplasm. Regions with highly variable thickness of INL or variable percentages of damaged cells were not included in the study unless at least 70% of the region fit one of the categories.

Statistical analysis

Immunohistochemical staining densities obtained from sections were analyzed for statistical significance using ANOVA followed by Tukey's multiple comparison tests using GraphPad Instat 3 software (GraphPad Software, San Diego, CA).

3.4 Results

GS immunoreactivity was decreased in regions with neuronal damage and glutamate redistribution.

We have previously found that a redistribution of glutamate occurs in PG, characterized by a loss of glutamate from neurons and an accumulation of glutamate in glial cells (McIlnay et al, Madl et al, 2005; Alyahya et al, 2007). The average level of glutamate immunostaining in the INL decreases as the severity of damage increases (Alyahya et al, 2007) due to loss of glutamate from many of the INL neurons.

Regions of PG retinas with different degrees of damage and glutamate redistribution were evaluated for GS immunostaining in plastic sections. Damage to INL cells in PG may progress from mild damage, where a normal number of cells are still present but some ($\leq$ 10%) have clumping of chromatin and pale, swollen cytoplasm, to severe damage where the loss of cells results in thinning of the INL. To determine if the severity of damage affected the levels of GS immunoreactivity, damage to INL regions was classified as mild or severe (see description in Methods). Cells were classified as damaged if they had dark nuclei with condensed chromatin or pale, swollen cytoplasm.

Immunogold staining for GS and glutamate were performed on adjacent 0.5 μm plastic sections of control and PG retinas. Control retinas had high levels of GS immunoreactivity in

Müller cells and their processes, with low levels of glutamate in the same Müller cells and processes (Fig. 3.1A & E). Mildly damaged regions that maintained high levels of glutamate had slightly reduced levels of GS (Fig. 3.1B & F), while mildly damaged regions showing glutamate redistribution had low levels of GS immunoreactivity (Fig. 3.1C & G). In regions with severe damage, little GS immunoreactivity remained in Müller cells while almost all INL neurons had low levels of glutamate (Fig. 3.1D & H).

The density of GS immunostaining was measured in Müller cells in regions with different degrees of damage (Fig. 3.2). In mildly damaged regions of retina where glutamate immunoreactivity was not reduced in 15 μm X 15 μm regions of INL (mild, high glutamate), the immunostaining for GS was significantly reduced. In neighboring areas where INL neurons contained significantly lower levels of glutamate immunoreactivity (mild, low glutamate), GS immunoreactivity showed a further reduction. The density of GS immunostaining decreased as the severity of damage increased and glutamate decreased in INL neurons (Fig. 3.2).

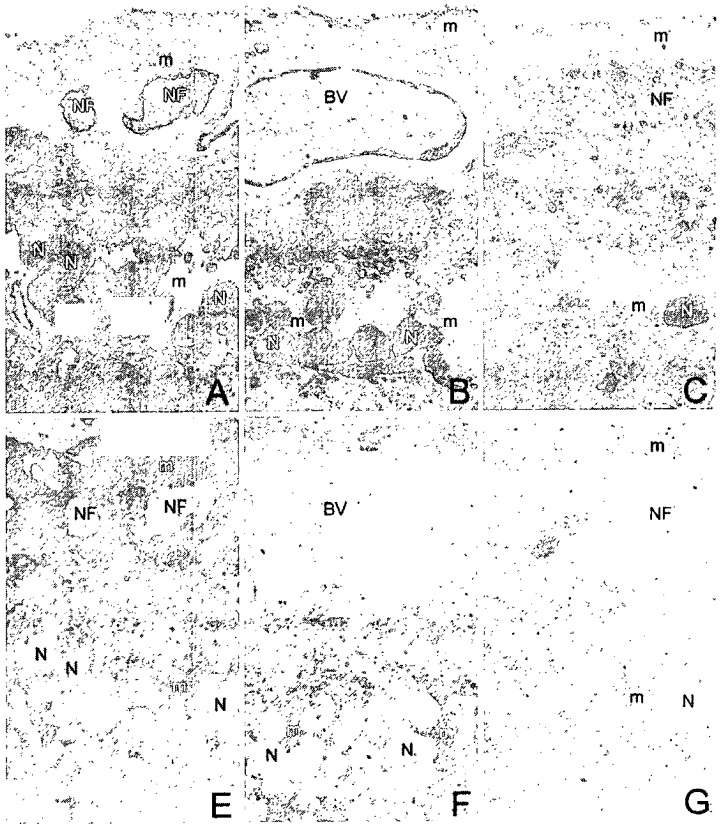

Fig. 3.1 Immunogold localization of glutamate and GS in plastic sections of control and PG retinas. A-D Immunostaining for glutamate in 0.5 μm sections of regions with different severities of damage. E-F. Immunostaining for GS in sections adjacent to A-D. A. Control glutamate staining. Note the low levels of glutamate in Müller cells and their processes (m). High levels of glutamate were found in many neurons (N) of the INL. Nerve fiber bundles (NF) also contained high levels of glutamate. B. A region with mild damage and high glutamate levels. Müller cells contained low levels of glutamate. C. A region with mild damage and low glutamate levels in neurons. One neuron retained a high level of glutamate. D. A region with severe damage. Note thinning of the INL (between arrowheads). E. In a control section adjacent to A, GS immunoreactivity was high in Muller cell bodies and their processes (m). F. In a mildly damaged region with high glutamate levels adjacent to B, GS immunoreactivity was reduced in Muller cells and their processes (m). G. In a mildly damaged region with low glutamate adjacent to C, GS immunoreactivity was further reduced in Muller cells. H. In severely damaged regions of PG retinas where INL thickness was reduced, GS immunoreactivity was reduced to low levels. All images are in the same orientation and magnification. Scale bar = μm.

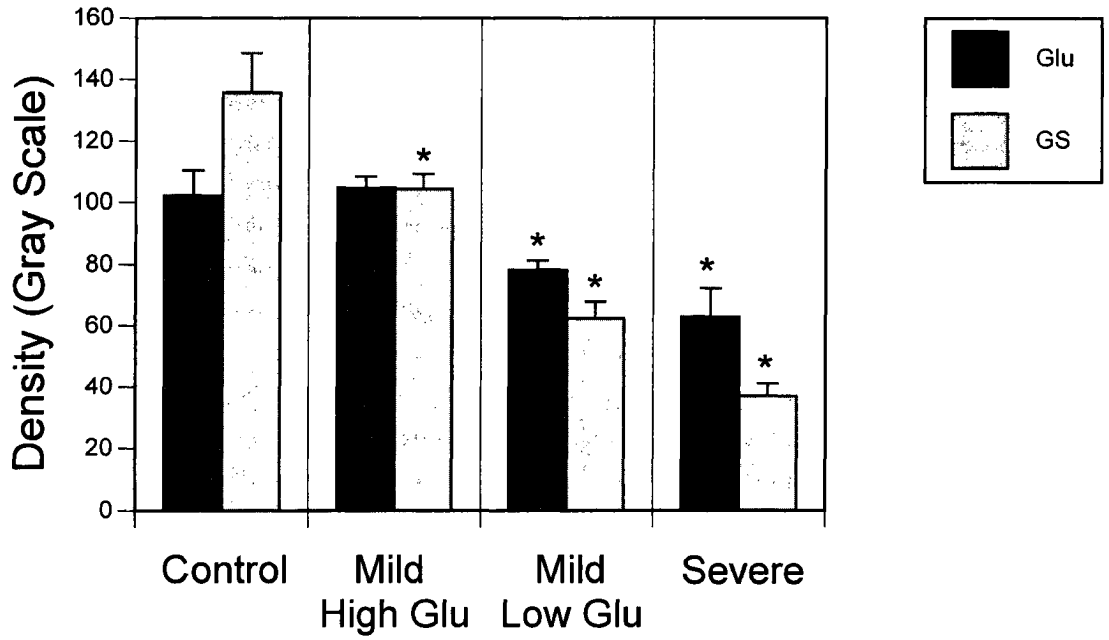

Fig. 3.2 GS and neuronal glutamate immunostaining densities were dependent on the severity of damage. GS staining densities in Müller cells and average glutamate staining densities in the INL (primarily neurons) were measured in regions with different severities of damage. In mildly damaged regions, staining densities were measured in areas with high levels of glutamate immunostaining (Mild, High Glu) and areas with low levels of glutamate immunstaining (Mild, Low Glu). Significant decreases in GS immunostaining densities compared to controls were seen in mildly damaged regions and in severely damaged regions ($p < 0.05$ by Tukey's multiple comparison test). Bars = SEM. $N \geq 18$ for all PG values and $N = 6$ for control values.

To further examine the relationship between glutamate and GS immunoreactivity, we plotted the average densities of glutamate immunostaining in the INL (predominantly neurons) against the densities of GS immunostaining in Müller cells. There was a loss of glutamate immunoreactivity in the neurons of the INL as GS immunoreactivity decreased in damaged regions. As shown in Figure 3.3A, the average density of glutamate immunostaining was highly correlated with the density of GS immunostaining ($R^2 = 0.88$, linear fit).

In contrast to neurons, the levels of glutamate immunoreactivity increased in glial cells as GS decreased in damaged regions (Fig. 3.3B; R2 = -0.82, linear fit). In severely damaged

regions, Müller cells had very low levels of immunoreactivity for glutamate and GS (Fig. 3.1D & H) and were difficult to distinguish from neurons, so average values for the region were used as estimates of staining density in Müller cells in these regions.

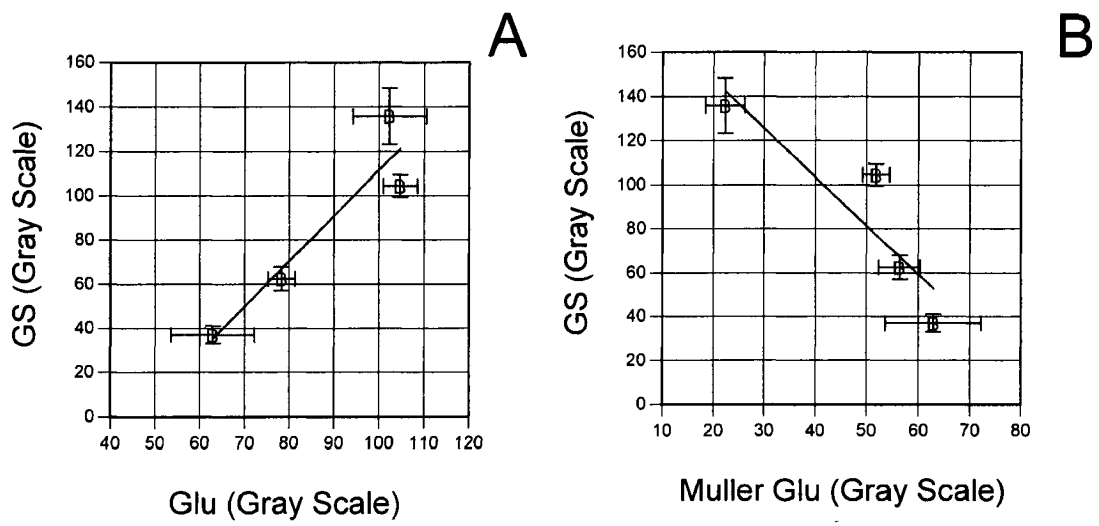

Fig. 3.3 GS immunostaining density was highly correlated with glutamate immunostaining densities in neurons and Müller cells. A. The average immunostaining densities for glutamate in the INL were plotted against GS immunostaining densities (data from Fig. 3.2). There was a strong correlation (R^2 = 0.88) between decreases in GS immunoreactivity and decreases in glutamate immunoreactivity in INL regions. The decreases in the average INL levels of glutamate reflect primarily the glutamate loss that occurs in neurons in PG. B. Glutamate immunostaining in Müller cells increased as GS immunostaining decreased. There was a strong correlation (R^2 = -0.82) between decreases in GS immunoreactivity and increases in glutamate immunoreactivity in Müller cell bodies. Bars = SEM. N $\geq$ 18 for all PG values and N = 6 for control values.

Effects of chronicity of glaucoma and location within the retina on GS immunoreactivity.

Sagittal sections of archived, paraffin-embedded eyes were immunohistochemically stained for GS using a less quantitative avidin-biotin immunoperoxidase method to allow evaluation of the effects of position within the retina and chronicity of glaucoma on GS

immunoreactivity. Control retinas had substantial GS immunoreactivity in Müller cells and astrocytes (Fig. 3.4). No control retinas had regions with markedly decreased immunostaining for GS except in areas with obvious sectioning or staining artifacts. Two of 6 acute ($\leq$ 5 days since clinical detection) PG retinas showed distinct patches of retina with decreased GS immunoreactivity (Fig. 3.4B). Five of 6 chronic PG retinas (> 5 days since clinical detection) appeared to have relatively homogeneous lighter immunostaining for GS than control retinas (Fig. 3.4C).

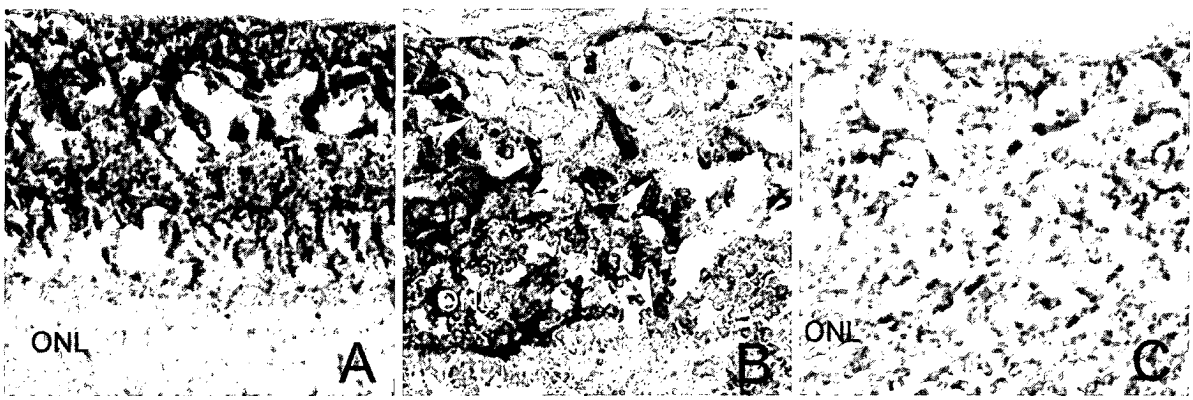

Fig. 3.4 Immunostaining for GS in paraffin sections of archived eyes was similar to plastic sections. A. Avidin-biotin peroxidase immunostaining of control sections revealed strong GS immunoreactivity in Müller cells and astrocytes homogeneously distributed throughout the length of the retinas. B. Some acute ($\leq$ 5 days from clinical detection) PG retinas had focal regions with reduced immunostaining for GS. The edge of a region of reduced staining is indicated by arrowheads. C. Chronic PG retinas had reduced immunostaining for GS distributed in a more homogeneous manner. All images are in the same orientation and magnification. Scale bar = 30μm.

Although the avidin-biotin peroxidase method of immunohistochemical staining is generally considered less quantitative than the immunogold method of immunohistochemical staining, measurements of GS staining density were performed to confirm our visual

impressions. Central and peripheral regions of control retinas did not have significant differences in GS staining density. Mean staining density in peripheral regions was 76.2 $\pm$ 8.4 and in central regions the mean staining density was 78.8 $\pm$ 7.8 ($n = 18$; $p > 0.4$ by t test). The lack of variation in GS staining intensity in these different locations in control retinas suggests that the focal decreases in immunoreactivity seen in acute PG retinas were unlikely to be due to normal regional differences in GS levels within the retina.

Chronic PG retinas had significantly less GS immunoreactivity than control retinas in central regions (Fig. 3.5A; $p < 0.01$). Acute retinas did not have significantly less GS immunoreactivity in central regions than control retinas ($p > 0.05$), but distinct patches of central retina containing low levels of GS immunoreactivity were evident in 2 of 6 acute PG retinas (Fig. 3.4B). Regions of acute PG retina that appeared to be less intensely stained on visual inspection did indeed have significantly lower levels of GS immunoreactivity (Fig. 3.5B), while adjacent regions were found to have control levels of GS immunoreactivity.

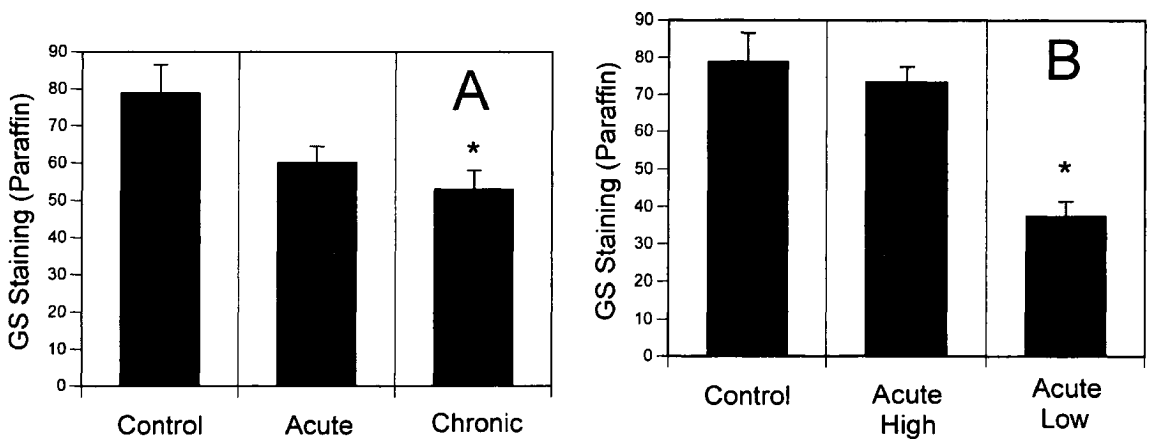

Fig. 3.5 In paraffin sections, GS immunostaining was reduced in chronic PG retinas and in small regions of some acute retinas. A. GS immunostaining densities (Gray scale) were reduced in the central regions of chronic PG retinas. B. In focal regions of some acute retinas, decreases in GS immunostaining densities were observed. Bars = SEM. $N \geq 12$ for each column.

Reactive Müller cells may occur in PG.

GFAP was expressed in Müller cells of PG retinas. Müller cells did not normally have detectable GFAP immunoreactivity in control sections (Fig. 3.6A). GFAP immunoreactivity was normally seen in presumptive astrocytes of dog retina, found primarily in the inner layers of control retinas. The expression of GFAP by Müller cells has been used as an indicator of reactivity. GFAP was detectable in Müller cell bodies and processes in the outer nuclear layer primarily in chronic PG (> 5 days from clinical detection). Six of 6 chronic PG retinas from paraffin embedded eyes had substantial GFAP immunoreactivity in a radial pattern consistent with Müller cells in a large portion of the retinas. In general the GFAP immunoreactivity was seen in most regions of the chronic PG retinas, but varied somewhat in intensity and seemed more intense in thinned regions of retina. In contrast, 2 of 6 acute PG retinas ($\leq$ 5 days from clinical detection) had substantial GFAP in Müller cells, but only in a limited number of regions. High levels of GFAP were usually limited to regions where the inner nuclear layer (INL) was thinned (< 2 cells thick). Measurement of GFAP staining density in 80μm lengths of retina from INL through the outer limiting membrane confirmed that average GFAP immunoreactivity was increased in the central regions of chronic PG retinas ($p < 0.001$) but not in the central regions of acute PG retinas (Fig. 3.6D). No significant differences were seen between GFAP densities in central and peripheral regions of control retinas ($p > 0.3$; data not shown) confirming that there were no substantial regional differences in GFAP in normal retinas.

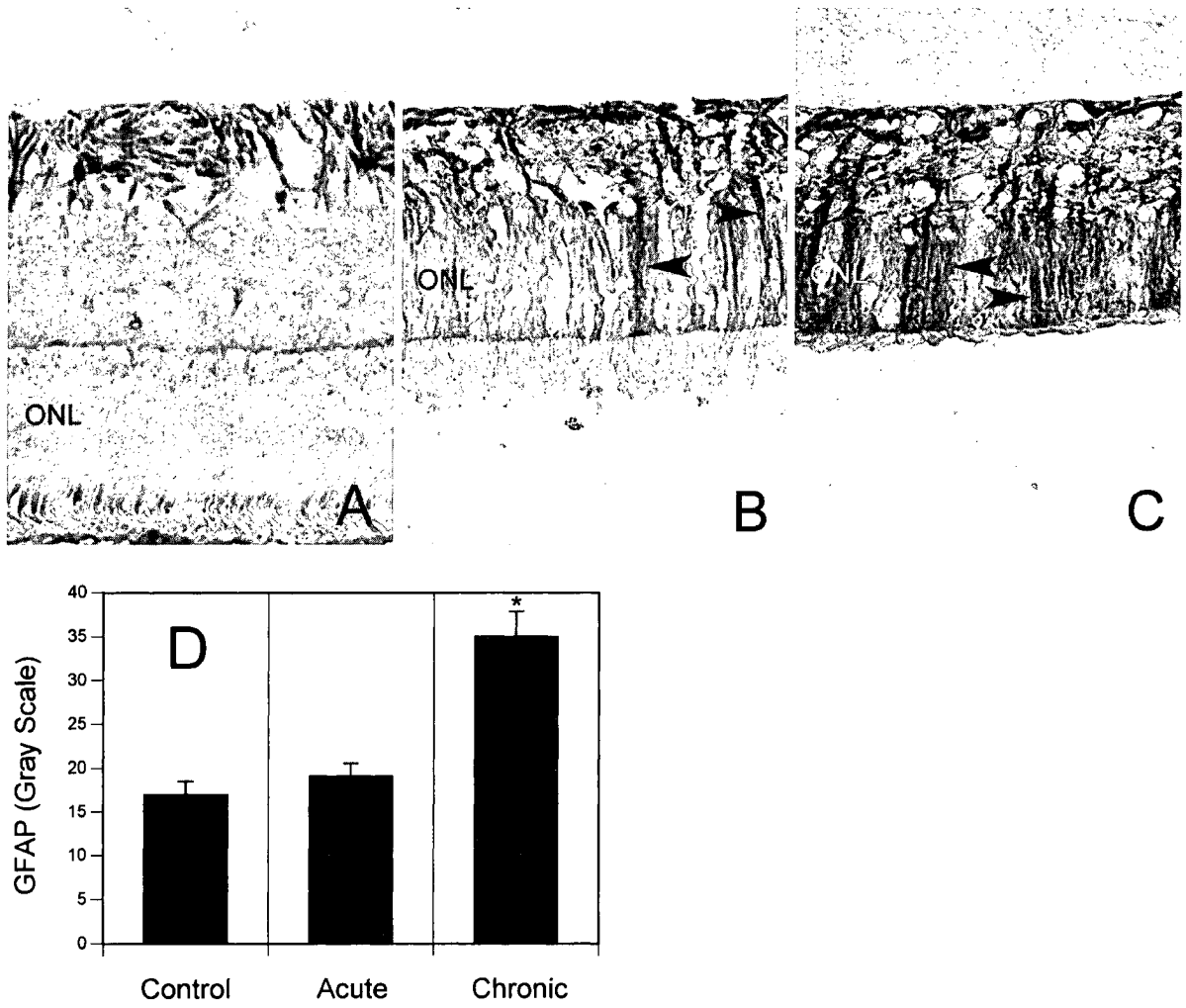

Fig. 3.6 GFAP may be induced in reactive Müller cells in PG. A. Paraffin section of control retina showing lack of GFAP immunostaining in Müller cell processes in the ONL. Note the immunostaining of putative astrocytes in the inner layers of the retina. B. Paraffin section of an acute PG retina showing GFAP immunostaining of Müller cell processes (arrowheads). Such regions with GFAP immunostaining in the ONL were infrequent seen. C. Paraffin section of a chronic PG retina showing strong GFAP immunostaining in many regions of the retina. All micrographs are in the same orientation and magnification. Scale bar = 30μm. D. Average GFAP immunostaining density was increased in chronic PG. Bars = SEM. N = 18 for each column.

3.5 Discussion

GS may be decreased in glial cells beginning in early PG.

GS immunoreactivity was decreased in PG retinas (Figs. 3.2, 3.3). We speculate that the decrease in immunoreactivity may reflect a decreased quantity of functional GS in these regions, resulting in decreased GS enzymatic activity. The decrease in GS immunoreactivity may be due to decreased synthesis or increased degradation/modification. The rate of GS synthesis may be altered by exposure to numerous substances or conditions such as high extracellular glutamate (Shen et al, 2004), ischemia (Krajnk et al, 1996), pigment epithelium-derived growth factor (Jablonski et al, 2001), and glucorticoids (Rauen et al, 1998). GS is also very vulnerable to modification by oxidation (Tetzel, 2005) and nitration (Gorg et al, 2007). Modification of GS by these processes may lead to decreased enzymatic activity (Gorg et al, 2007) and perhaps to decreased immunoreactivity. Oxidative stress and nitration by peroxynitrile derived from NO may be expected in PG since these processes are increased in retinal ischemia (Hardy et al, 2005) and in glaucoma (Neufeld, 2003).

The decreases in GS immunoreactivity may begin in the early stages of PG. Decreased levels of GS immunoreactivity were seen in some regions of acute PG retinas in paraffin sections (Fig. 3.5B). In more quantitative immunogold studies, significant decreases in GS immunoreactivity began in mildly damaged regions of INL and further decreases occurred in the more severely damaged regions (Fig. 3.2).

Reductions in GS may contribute to glutamate redistribution.

We have seen a decrease in GS immunoreactivity in PG that is highly correlated with a redistribution of glutamate in the same regions (Fig. 3.3). We speculate that this decrease in immunoreactivity may reflect a decrease in functional GS in these regions.

GS is a major enzyme involved in the metabolism of glutamate in glial cells. GS catalyzes the amidation of glutamate to glutamine, which is an essential part the cycling of the transmitter pool of glutamate between neurons and glia. Decreased GS activity may then account for at least some of the increased levels of glutamate in glial cells and decreased levels of glutamate in neurons seen in PG in dogs.

Reductions in GS may contribute to higher extracellular glutamate levels and neuronal damage.

Decreased GS immunoreactivity was associated with increased damage in PG retinas (Fig. 3.2). Chronic high intraocular pressure decreases GS activity in a rodent model of glaucoma (Moreno et al, 2005), suggesting that decreased GS activity may also occur in other types of glaucoma. Uptake and metabolism of glutamate by glial cells is the main mechanism by which extracellular glutamate is kept low in the retina, thereby preventing toxicity to neurons. *In vitro* studies suggest that if GS activity is not maintained at a high level, neurons are more vulnerable to glutamate toxicity and hypoxia (Heidinger et al, 1999).

Reductions in GS may lead to neuronal damage by allowing extracellular glutamate to accumulate. Microdialysis studies suggest that the extracellular level of glutamate in the central nervous system may be approximately 1 μM (Cavalier et al, 2005). Studies of glutamate levels in

the vitreous body of normal dogs suggest similar levels of about 5 □M (Brooks, 1997). Models of glutamate transport suggest that the minimum levels of extracellular glutamate will increase proportionately to any increases in the intracellular level of glutamate (Bouvier et al, 1992; Owe et al, 2006) if no other factors driving transport are altered. These other factors affecting transport include membrane potential and the membrane gradients of Na^+, K^+, and H^+ (Owe et al, 2006). We have previously estimated the levels of glutamate may be increased about four-fold in Müller cells in PG (McIlnay et al, 2004). This suggests extracellular glutamate may increase to approximately 4 □M in mildly damaged regions if there is no ischemia-induced ATP depletion and subsequent changes in ion gradients (see Hansen). Although this concentration of glutamate is not rapidly toxic to neurons in culture, high levels of glutamate are believed to potentiate other pathologic processes such as hypoxic neuronal damage (Peirera et al, 1998).

Müller cells may become reactive in PG.

GFAP immunoreactivity is often used as a marker for reactive glia (Lewis and Fisher, 2003; Davidson et al, 1990). Müller cells do not normally express GFAP (Davidson et al, 1990). In many regions of chronic PG retinas, putative Müller cells contained substantial amounts of GFAP immunoreactivity (Fig. 3.6), indicating that these glia are reactive. However, it should be noted that astrocytes normally contain GFAP (Fig. 3.6A) and the increased GFAP in thinned retinas may be at least partially due to retention of astrocytes in these severely damaged regions.

In contrast to chronic PG, fewer GFAP-containing Müller cells were seen in acute PG. In those regions of acute PG retinas where GFAP immunoreactivity was substantial, severe damage was generally seen in the INL. This suggests that Müller cells show signs of classic reactive glia in the later stages of the pathogenesis of glaucoma after many of the INL neurons have been lost.

Loss of GS and ischemia may act in a cooperative manner to increase extracellular glutamate levels and neuronal damage.

In the current studies we observed decreased GS immunoreactivity in PG retinas that may reflect decreased GS function. We have also reported microvessel losses and vascular damage that may lead to ischemia in canine PG (Alyahya et al, 2007). These two processes may act cooperatively to allow glutamate to accumulate in the extracellular fluid. Decreases in functional GS protein may result in glutamate accumulation in glial cells. These increases in glial glutamate will raise the minimum extracellular level of glutamate reached by transporters (Attwell et al, 1993). Ischemia reduces cellular ATP levels. This reduction in ATP will have several effects on glial cells, including a further reduction in GS activity and also decreases in the ion gradients that drive glutamate transporters. If severe enough, the ATP depletion-induced changes in ion gradients will then reverse the glutamate transporters and release glutamate into the extracellular fluid (Madl et al, 2005; Owe et al, 2006), leading to excitotoxic damage to neurons.

CHAPTER FOUR:
RETINAL PIGMENT EPITHELIUM DAMAGE, BREAKDOWN OF BLOOD-RETINAL BARRIER, AND RETINAL INFLAMMATION IN DOGS WITH PRIMARY GLAUCOMA

Brendan G. Mangan, Khaleel Al-Yahya, Chu-Te Chen, Juliet R. Gionfriddo, Cynthia C. Powell, Richard R. Dubielzig, Eugene J. Ehrhart and James E. Madl

Acknowledgment

My roles in the study described in chapter 4 were helping conducting the immunohistochemical studies under the supervision and direction of Dr James Madl. Also, I was involved in interpreting the results of the study and I was a co-author of the manuscript describing this study. The manuscript describing this study has been published in Veterinary Ophthalmology volume 10, 2008.

4.1 Abstract

Objective: This paper aims to determine if abnormalities of the retinal pigment epithelium (RPE) and retinal inflammation occur in primary glaucoma. *Procedure:* Twenty-three canine globes with primary glaucoma, goniodysgenesis, and elevated intraocular pressure were evaluated. Sections from 6 control and 23 glaucomatous canine globes were stained with hematoxylin and eosin, *Griffonia simplicifolia* isolectin B4, or immunohistochemically stained for CD3 or albumin. The retinal sections were evaluated with light microscopy for morphological and immunohistochemical evidence of pigmentary changes and inflammation. *Results:* Abnormal pigmented cells including displaced RPE cells and macrophages (identified by lectin binding) were found in the neuroretinas and vitreous bodies of glaucomatous eyes. Other abnormalities

included hypertrophy of RPE cells and loss of RPE continuity. Regions of neuroretina with more displaced pigment had fewer remaining neurons. Signs of retinal inflammation found in glaucomatous eyes included infiltration with leukocytes, retinal swelling, and albumin leakage from vessels. Accumulation of perivascular CD3-positive T lymphocytes also occurred in glaucomatous retinas. Chronic glaucomatous retinas had increased pigmentary changes, fewer neutrophils, and less swelling than acute glaucomatous retinas. *Conclusions:* Disruption of the RPE, increased permeability of the vascular endothelium,accumulation of inflammatory cells, and retinal swelling or thinning occur in canine primary glaucoma. The displacement of pigment and accumulation of inflammatory cells in the neuroretina suggests that inflammation may be an important contributor to retinal damage.

4.2 Introduction

Glaucoma is characterized by a progressive loss of retinal ganglion cells, and is often associated with damage to the anterior segment and increased intraocular pressure (Gelatt et al, 2003; Miller et al, 1995). Primary glaucoma (PG) in dogs is a neurodegenerative disease that can involve all layers of the neuroretina and not just the retinal ganglion cells (McIlnay et al, 2004; Whiteman et al, 2002). Pigment dispersion and inflammation in the anterior segment have been reported in a form of canine primary angle-closure glaucoma (PACG) and in the DBA/2J murine model of pigmentary glaucoma (Anderson et al, 2002; John et al, 1998; Zhou et al, 2005).

Uveitis occurs in association with some types of canine PACG (Brooks et al, 1990; Gelatt et al, 1991; Wyman et al, 1976), and it is an important cause of secondary glaucoma in cats (Blocker et al, 2001; Glaze et al, 1999; Wilcock et al, 1990) and horses (Miller et al, 1995;

Pickett et al, 1993; Wilcock et al, 1991; Cullen et al, 2000). In both canine PACG (Reilly et al, 2005) and DBA/2J mouse glaucoma, inflammation and pigment dispersion occur in the anterior segment. Inflammation of the anterior uveal tract in canine PACG and DBA/2J glaucoma (Zhou et al, 2005) may contribute to iridocorneal angle and trabecular meshwork alterations, and a subsequent increase in intraocular pressure (John et al, 1998; Reilly et al, 2005). Pigmentary uveitis in Golden Retrievers is associated with pigment dispersion in the anterior chamber, and in one study a 46% incidence of glaucoma was reported (Sapienza et al, 2003). Another glaucoma syndrome has been associated with ocular pigment deposition and the accumulation of putative melanophages in the canine choroid and retina (Van de Sandt et al, 2003).

It is possible that abnormalities of pigment epithelium and pigment dispersion contribute to inflammatory responses in the anterior and posterior segment. Loss of pigment epithelium from the posterior iris, pigment epithelial clumping, accumulation of pigmented cells in the anterior and posterior chambers and dependent regions of the iridocorneal angle, and anterior uveitis have been described in association with pigment dispersion in canine PACG (Reilly et al, 2005). Disruption of pigment epithelial cells presumably results in a loss of cellular tight junctions and breakdown of the blood–aqueous barrier. Breakdown of the blood–retinal barrier occurs when tight junctions between retinal vascular endothelial cells or retinal pigment epithelium (RPE) cells are compromised (Cioffi et al, 2003). In an experimental model of posterior uveitis, intraocular accumulation of albumin occurred in association with retinal vascular damage and increased permeability (Howes et al, 1978). It is possible that further inflammation and retinal damage may occur as naïve intraocular tissues are exposed to cells of the immune system.

The anterior chamber, vitreous body, and retina are immune privileged sites, and breakdown of the blood–ocular barriers can be associated with an autoimmune response. A number of proteins have been isolated from the retina (Bora et al, 2004; Bora, 1997; Broekhuyse et al, 1991) that acts as auto-antigens in rodents (Bora et al, 1997; Deeg et al, 2006; Donoso et al, 1988; Caspi et al, 1988) and horses (Deeg et al, 2006; Deeg et al, 2006; Deeg et al, 2002; Deeg et al, 2001) when exposed to the immune system. For example, an eye-specific glycosylated type I collagen isolated with melanin from RPE induces an autoimmune anterior uveitis in rodents. Other type I collagens with different forms of glycosylation are not able to generate this inflammatory response (Bora et al, 2004).

No studies have specifically examined whether disruption of the RPE and inflammation of the retina occur in dogs with PG. In one study, hypertrophy of the RPE not associated with retinal detachment was identified in dogs with PG (Smedes and Dubielzig, 1994). These canine retinas also contained inflammatory cells including polymorphonuclear cells and macrophages (Smedes and Dubielzig, 1994). We hypothesize that pigmentary changes and inflammation are important factors associated with retinal degeneration in canine PG.

4.3 Methods

The archived, paraffin-embedded canine globes used in this study were obtained from one of the investigators (R.R.D.), and were from 6 control dogs, 11 dogs with acute glaucoma (acquired within 5 days after the onset of clinical signs), and 12 dogs with chronic glaucoma (acquired not earlier than 5 days after the onset of clinical signs). Dogs in the control group included a 2-year-old Golden Retriever, a 6-year-old Samoyed, a 1.7-year-old Sheltie (both

eyes), a 12-year-old Scottish Terrier, and a 7-year-old Staffordshire Terrier. There were 19 Cocker Spaniels (5–13 years old), 3 Basset Hounds (4–6 years old), and a 10-year-old Dachshund that represented in the glaucoma group, and all had elevated intraocular pressure. All dogs in the glaucoma group were diagnosed with goniodysgenesis and PG.

Treatment of glaucoma was described for six dogs, and no response to treatment was indicated for two dogs; however, treatment was not specified. One dog was treated with transscleral laser cyclophotocoagulation, one dog was treated with latanoprost and pilocarpine, and another dog was treated with latanoprost. The other three dogs were treated with various combinations of mannitol, methazolamide, timolol, and oral and topical steroids.

Saggital, 5 □m sections were obtained from each eye and stained with hematoxylin and eosin (H&E) to evaluate pigment dispersion and structural changes. Other sections from the same blocks were immunohistochemically stained for albumin or CD3 using an avidin-biotin method. The sections were dewaxed in xylene and graded ethanol. Sections were then autoclaved for 15 min in a pH 6.0 citrate buffer for antigen retrieval. After endogenous peroxidase was inactivated in 3% peroxide for 15 min, sections were incubated in primary rabbit antisera to albumin (1 : 400 in phosphatebuffered saline) or CD3 (1 : 100 in phosphate-buffered saline; Dako, Carpinteria, CA, USA) overnight. A Vectastain elite kit for rabbit antisera (Vector Laboratories, Burlingame, CA, USA) was then used to visualize the primary antibody using peroxidase and diaminobenzidine as chromogen. A negative control for specificity of the antibodies was performed by eliminating the primary antibodies, which resulted in greatly reduced staining. As an additional negative control for albumin immunostaining, the primary antibody was preincubated with bovine serum albumin (1 mg/mL in phosphate-buffered saline; Sigma-Aldrich, St. Louis, MO, USA), which resulted in decreased staining. All retinas were

examined to ensure that the antibodies were indeed labeling known positive structures. This included labeling of the lumens of blood vessels by albumin immunostaining in both control and glaucomatous retinas, and labeling of putative T lymphocytes within the lumens of blood vessels by CD3 immunostaining.

Other sections were stained with biotinylated *Griffonia simplicifolia* isolectin B4 (GSL) (Vector Laboratories). Sections were processed as described for albumin mmunohistochemistry with biotinylated lectin diluted 1 : 100 substituting for the primary antibody. The biotinylated lectin was visualized with the ABC component of the Vectastain kit with metalenhanced diaminobenzidine (Sigma-Aldrich) as chromogen. All slides were dehydrated through graded ethanol, cleared in xylene, and coverslipped. A negative control for lectin staining was performed by eliminating the lectin, which resulted in greatly reduced staining. A positive control to ensure that the lectin was indeed labeling known positive structures was the strong labeling of blood vessels in all retinas, including control retinas that did not have macrophage infiltrates.

Chronic glaucomatous retinas were evaluated for thinning by comparing regions with abnormal pigmentary changes to adjacent regions within 1000 □m that lacked Pigmentary changes. The retinas were considered thinned if the inner nuclear and outer nuclear layers were < 67% of the thickness of adjacent regions that lacked pigmentary changes. Retinal thickness was evaluated in the tapetal regions of chronic glaucomatous retinas for comparison to nontapetal regions with increased pigmentary changes and thinning.

Acute glaucomatous retinas were evaluated for swelling by comparing regions with significant neutrophilic infiltrates to adjacent regions within 1000 □m that contained few or no neutrophils. Control retinas were also evaluated for average thickness (137 ± 12.4 microns).

Photomicrographs (Zeis Axioplan/2Axiovision, Carl Zeis Microimaging, Thornwood, NY, USA) were obtained, and measurements from the outer limiting membrane to the inner limiting membrane were acquired using an image analysis program (ImageJ 1.37, National Institutes of Health, Bethesda, MD, USA). Comparison of retinal thickness was evaluated with statistical software (GraphPad InStat 3.06, San Diego, CA, USA) by applying values of swollen and not swollen adjacent regions in a paired *t* -test. The values were expressed as a percentage of the mean ± SEM, and significance was designated as values of *P* less than or equal to 0.05.

4.4 Results

Abnormalities of RPE and pigment distribution may occur in PG

The nontapetal RPE displayed focal to multifocal abnormalities in most glaucomatous eyes. Hypertrophy and rounding of RPE cells with separation from the neuroretina consistent with retinal detachments were identified in two eyes. In 9 of 23 (39%) glaucomatous eyes, some of the RPE cells were hypertrophied and had a rounded appearance without retinal detachment (Fig. 4.1b). In 12 of 23 (52%) acute and chronic glaucomatous eyes there were isolated RPE cells in the outer layers of the neuroretina (Fig. 4.1c), and 6 of 23 (26%) eyes showed apparent large disruptions in the RPE in areas where there were no obvious sectioning artifacts. Changes were more severe and common in chronic glaucoma. In sections from six control eyes stained with H&E, no disruption or invasion of RPE cells into the underlying neuroretina was observed.

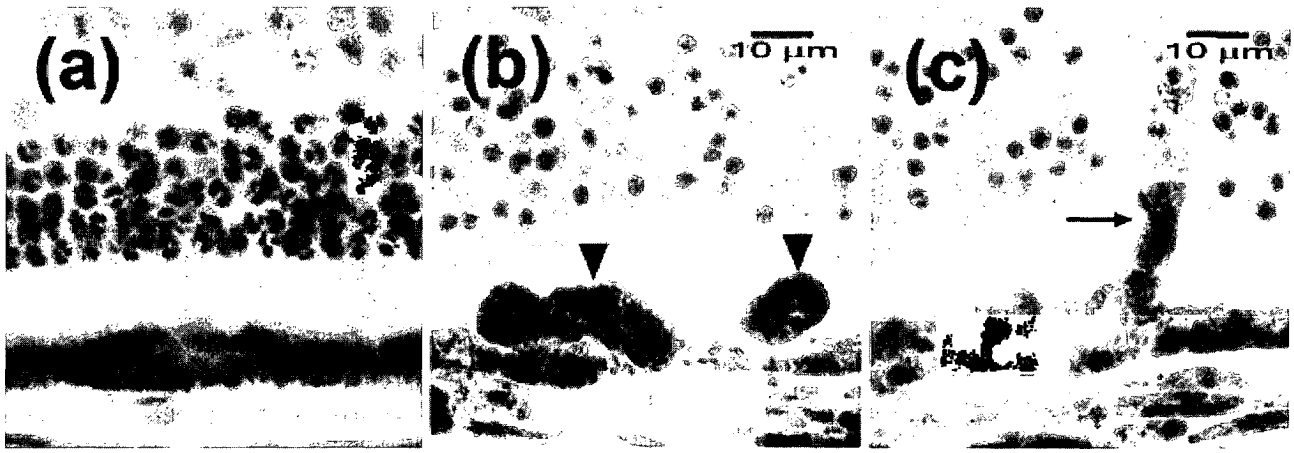

Fig. 4.1 The retinal pigment epithelium (RPE) was abnormal in glaucomatous eyes. (a) Control RPE (H&E stain). (b) Hypertrophied and disrupted RPE (arrowheads) with a rounded appearance in primary glaucoma (PG) retina (H&E stain). (c) Putative RPE cells (arrow) displaced into the neuroretina in PG (H&E stain).

Abnormal distribution of pigment granules and pigmented cells was also seen in the neuroretinas of glaucomatous eyes. In contrast to control eyes, 20 of 23 glaucomatous eyes were found to have free pigment granules and/or pigmented cells in the neuroretinas greater than 1.0 mm from the ora ciliaris retinae. Pigmented cells in glaucomatous neuroretinas greater than 1.0 mm from the ora ciliaris retinae included both putative macrophages (Fig. 4.2a) and putative displaced RPE cells in H&E-stained sections. To confirm that some of these pigmented cells were macrophages, staining with GSL was performed. Lectin staining of adjacent sections confirmed the presence of macrophages in these regions (Fig. 4.2b), and indicated that many of the pigmented cells were most likely macrophages. Numerous lanceolate pigment granules that did not appear to be contained within cells were also seen in glaucomatous neuroretinas (Fig. 4.2a). There were four pigment-containing cells (one cell in two different retinas, and two cells in one retina) in the periphery of control neuroretinas, and in more central regions they were absent. No associated inflammation or retinal damage was identified.

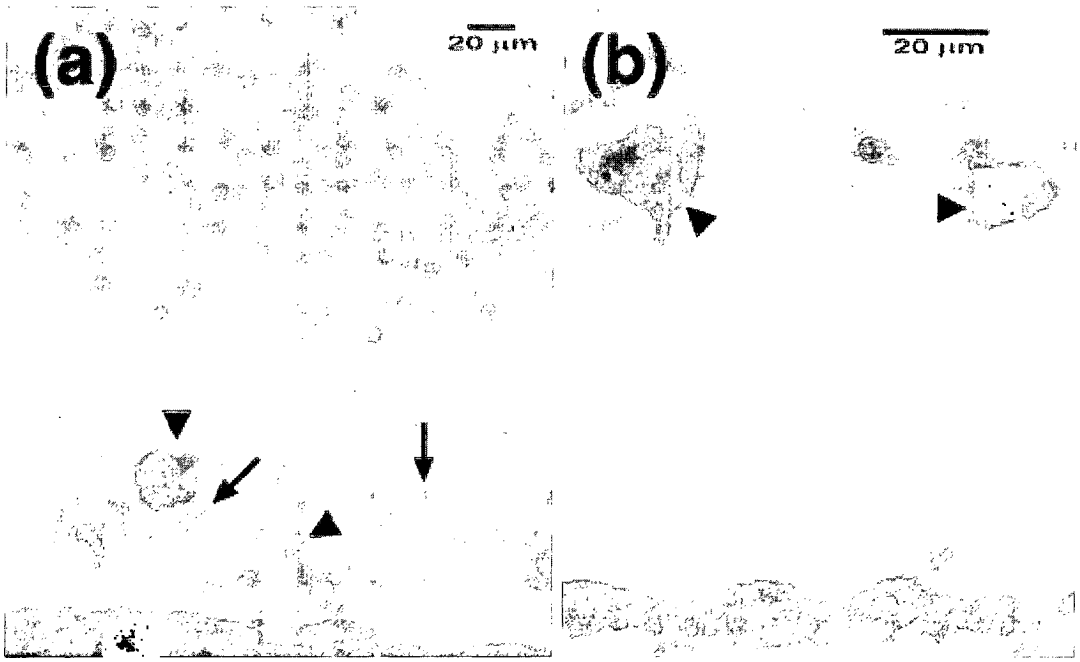

Fig. 4.2 Putative macrophage/microglia and pigment granules accumulate in the neuroretina of glaucomatous eyes. (a) Putative macrophages (arrowheads) containing pigment granules and free pigment granules (arrows) in the neuroretina in primary glaucoma (PG) (H&E stain). (b) Lectin-labeled macrophages (arrowheads) in the neuroretina in PG (GSL stain).

Increased numbers of pigmented cells and free pigment granules were observed in the vitreous bodies of glaucomatous eyes compared to controls. The pigment granules were round (Fig. 4.3a), and possibly associated with pigment loss from the peripheral retina or pigment epithelium of the anterior segment. Pigmented cells were found in the vitreous bodies within 0.5 mm of the inner limiting membrane in 19 of 23 glaucomatous eyes. These pigment changes occurred more frequently and to a greater extent in chronic glaucoma as compared to acute glaucoma. Most of these cells had the morphologic characteristics of macrophages that had phagocytized pigment granules (Fig. 4.3a). Of the nucleated cells in the vitreous body, almost all stained with GSL (Fig. 4.3b), confirming that many of the cells containing pigment were macrophages. Other pigmented cells in the vitreous body included putative pigment epithelial

cells from the anterior segment. These cells were larger than macrophages, usually contained a very high density of pigment granules, and did not stain with lectin. A small number of free pigment granules and only two pigmented cells were seen in the vitreous bodies within 0.5 mm of the retinas in the control eyes.

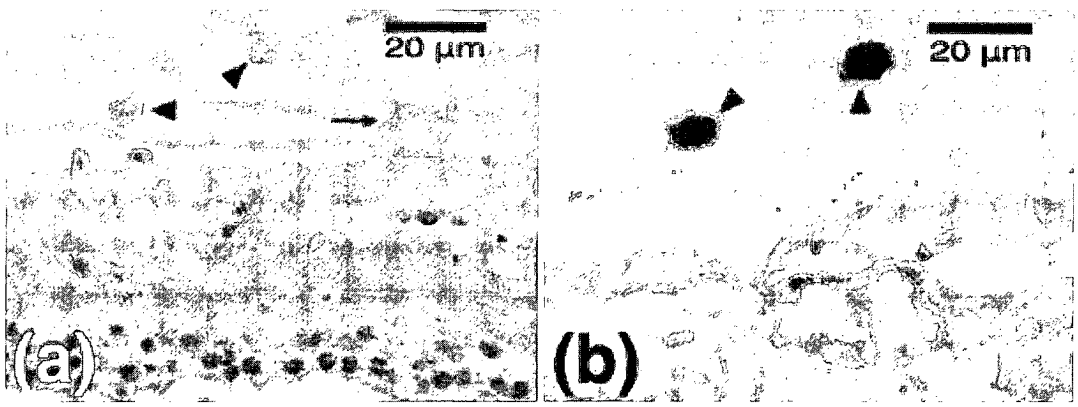

Fig. 4.3 Pigmented cells and pigment granules accumulated in the vitreous body of glaucomatous eyes. (a) Pigment-containing cells with the typical appearance of macrophages (arrowheads) and free pigment granules (arrow) found in the vitreous body of an eye with primary glaucoma (PG) (H&E stain). (b) Lectin-positive cells (arrowheads) in the vitreous consistent with macrophages (GSL stain).

Regions of retina with more pigment showed a more severe thinning of the inner and outer nuclear layers

Regions of glaucomatous retinas that contained pigmented cells or free pigment granules were examined for signs of neuronal damage and death. There was less retinal swelling in chronic glaucoma, and damaged regions with obvious neuronal loss and thinning of the nuclear and plexiform layers were identified. In the tapetal regions there were fewer pathologic pigmentary changes and disruptions of the RPE (Fig. 4.4a). Neuronal damage was generally less

severe in the nonpigmented tapetal regions than in the pigmented nontapetal regions of the same retinas. Thinning of the neuroretina occurred in 14 of 23 heavily pigmented regions (Fig. 4.4c).

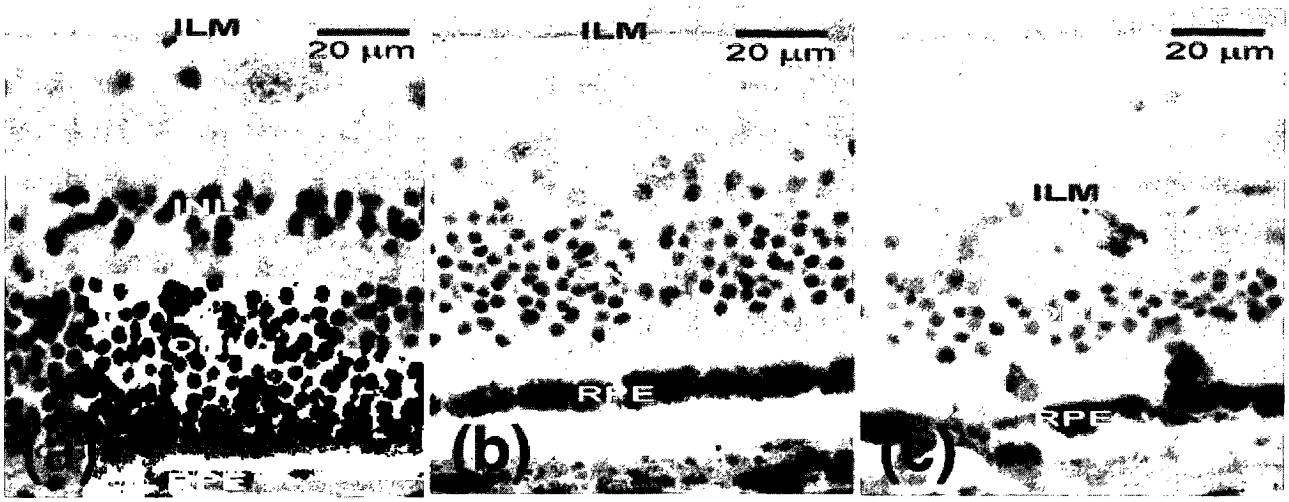

Fig. 4.4 Regions of neuroretina with pigment accumulations were more severely damaged than other regions. (a) Tapetal region showing no thinning or abnormal pigmentation (H&E stain). (b) Nontapetal region without pigmentary changes (H&E stain). (c) Loss of the inner nuclear layer (INL) and attenuation of the outer nuclear layer (ONL) in a region with an accumulation of pigmented cells and pigment granules (H&E stain). ILM, internal limiting membrane; RPE, retinal pigment epithelium.

Inflammatory changes were seen in glaucomatous retinas

The magnitude of inflammatory cell infiltrates and alterations in retinal thickness appeared to be associated with the duration of glaucoma in most cases. Neutrophilic inflammation and retinal thickening were associated more commonly with acute glaucoma. Chronic glaucoma tended to have a greater association with retinal thinning, and more significant pigment accumulation. Lymphoplasmacytic inflammation was less specific in terms of duration of glaucoma, but CD3-positive T lymphocytes were identified in the vitreous and perivascularly in the neuroretinas of dogs with PG. In addition, the observation of albumin leakage from blood vessels indicated breakdown of the blood–retinal barrier.

Neutrophilic inflammation was seen in the vitreous and retinas of eyes with acute glaucoma. Large numbers of cells with morphologic characteristics consistent with neutrophils were seen in the neuroretinas of all acute glaucoma eyes (Fig. 4.5b,c). The distribution of neutrophils varied from focal to multifocal, and in one eye retinal detachment appeared to be associated with the accumulation of neutrophils and macrophages in the subretinal space. In the central retinal regions containing many neutrophils, retinal thickness from the outer limiting membrane to the inner limiting membrane was increased to 122 ± 13.8% ($P < 0.004$) of adjacent nonswollen regions. Neutrophils were not observed in the neuroretinas of control dogs. The mean thickness in control retinas was 137 ± 12.4 μm, and there was no significant difference when compared to nonswollen regions ($P = 0.7$).

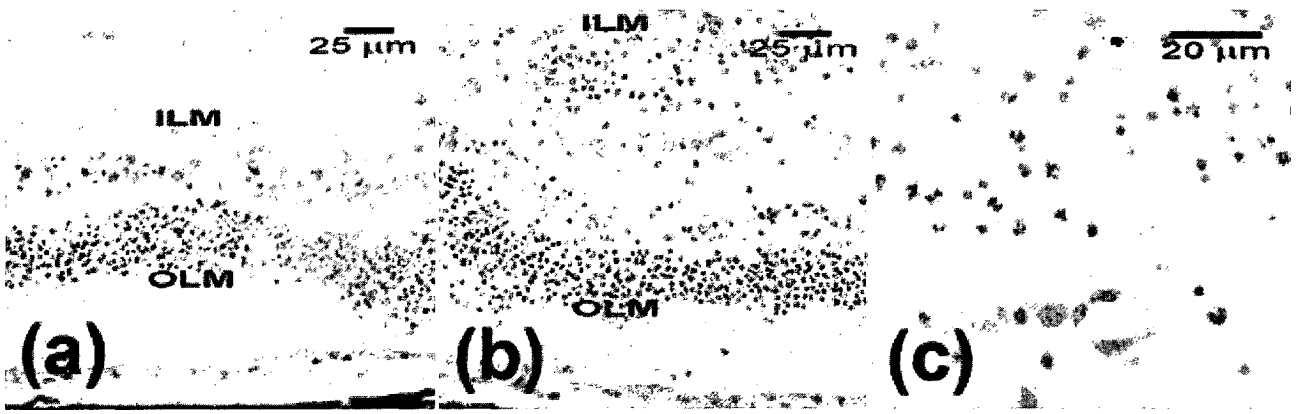

Fig. 4.5 Adjacent regions of nonswollen and swollen regions exhibiting neutrophilic inflammation in acute PG. (a) Nonswollen region (H&E stain). (b) Neutrophilic inflammation in the inner layers of the retina (H&E stain). (c) Neutrophils in the neuroretina (H&E stain).

Cells consistent with lymphoplasmacytic inflammation were seen in the vitreous bodies and neuroretinas of glaucomatous eyes, but not in control eyes. Perivascular inflammatory cells were observed in the inner layers of the neuroretina (Fig. 5.6a). Presumptive T lymphocytes with

CD3 immunoreactivity were found in both acute and chronic glaucomatous retinas. Furthermore, many of the inflammatory cells observed in the perivascular regions of H&E-stained sections were CD3-positive T lymphocytes (Fig. 4.6b). Control retinas contained a population of cell bodies confined to the inner nuclear layer that were labeled by immunohistochemical staining for CD3 (Fig. 4.6c). These presumptive amacrine cells often had visible processes projecting into the inner plexiform layer, and did not appear to have any association with blood vessels. In contrast to control retinas, very few cells of the inner nuclear layer of glaucomatous retinas were labeled by immunohistochemical staining for CD3.

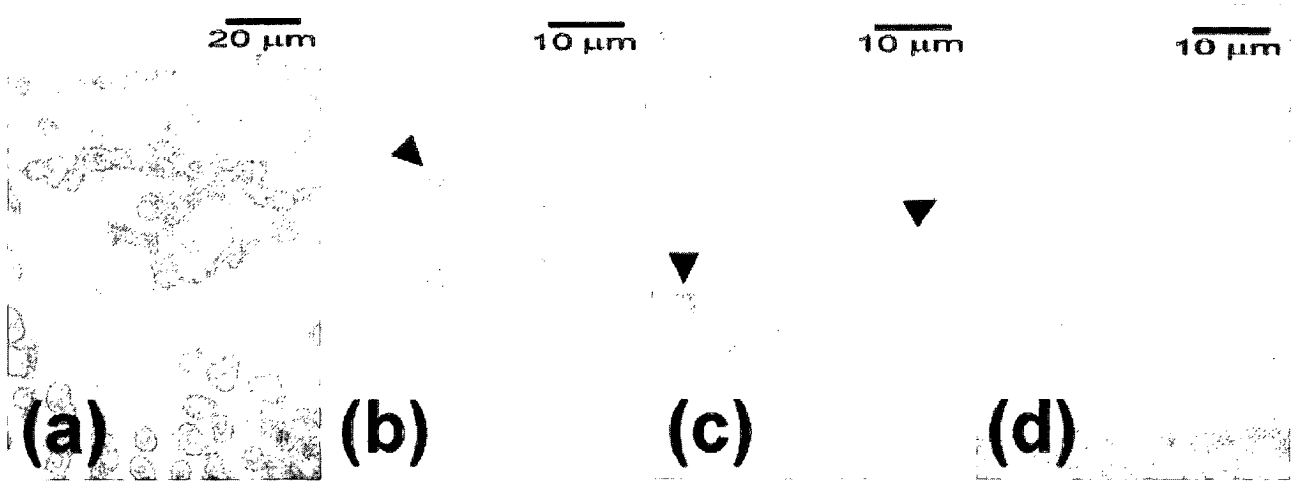

Fig. 4.6 Perivascular inflammation in the neuroretinas of glaucomatous eyes. (a) Perivascular inflammatory cells in the neuroretina in PG (H&E stain). (b) CD3 positive cells (arrowhead) associated with a retinal blood vessel in PG (Immunohistochemical CD3 stain). (c) Presumptive amacrine cells with cross-reactivity to CD3 in the inner retina of a control eye (Immunohistochemical CD3 stain). (d) A negative control showing absence of staining when the primary antibody is not applied (Immunohistochemical CD3 stain).

Other signs of inflammation, including breakdown of the blood–retinal barrier occurred in glaucomatous retinas. Following immunohistochemical staining, albumin accumulation was observed around retinal blood vessels, which indicated an abnormal increase in vascular

permeability. Detection of albumin outside the vessel lumina was seen in 15 of 23 glaucomatous neuroretinas, but not in control retinas (Fig. 4.7a,b).

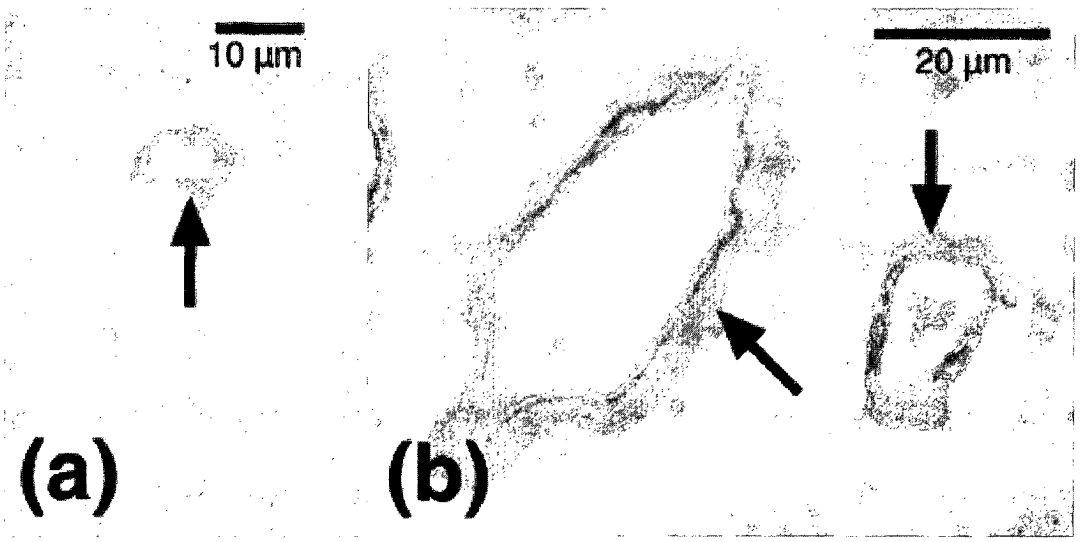

Fig. 4.7 Albumin leakage from retinal blood vessels. (a) Control retina showing albumin within the blood vessel lumen (arrow) (Immunohistochemical albumin stain). (b) Albumin leakage (arrows) from a vessel in the outer layers of the retina in primary glaucoma (immunohistochemical albumin stain).

4.5 Discussion

In a form of canine PACG, pigment dispersion and inflammatory changes were found in the anterior segment (Reilly et al, 2005). The accumulation of pigment-containing macrophages in the retina has also been associated with glaucoma and ocular pigment deposition in dogs (Van de Sandt et al, 2003). In the present study, we determined if abnormalities of the RPE and abnormal pigment distribution were associated with inflammatory changes in the retinas of dogs with PACG.

Morphologic changes in the RPE and abnormal pigment distribution in the neuroretina and vitreous body occur in PG (Van de Sandt et al, 2003; Smedes and Dubielzig, 1994). In contrast to control retinas, hypertrophy of the RPE occurred in many regions of glaucomatous

retinas. Extensive RPE hypertrophy without retinal detachment, which was repeatedly observed in numerous glaucomatous eyes, appears to be associated with inflammation. In regions of two eyes, RPE hypertrophy with separation of the neuroretina consistent with retinal detachemnt was seen. However, it should be noted that these changes may have been due to artifacts associated with the processing of severely damaged retinas. In addition, substantial numbers of pigmented cells and free pigment granules were found in the neuroretinas and vitreous bodies of glaucomatous eyes, but not in control eyes. The majority of these pigmented cells were macrophages identified by their appearance with H&E and confirmed with GSL staining. Retinal necrosis occurs in glaucoma (McIlnay et al, 2004; Whiteman et al, 2002; Smedes and Dubielzig, 1994), and the presence of macrophages would be consistent with the phagocytic role of these cells in damaged and inflamed tissues. Melanophages have been described in the uveal tract and retina in association with pigment dispersion (Reilly et al, 2005; Van de Sandt et al, 2003). The infiltration of the neuroretina by clumps of cells contiguous with the RPE also suggests that many of the infiltrating pigmented cells may be from the RPE. Pigment granules contained within pigmented cells or free in the neuroretina were lanceolate, which is typical of pigment granules contained within the RPE of dogs (Samuelson, 1999). In a process termed phagocytic metaplasia, RPE may transform into acrophages in response to an inflammatory episode (Peiffer et al, 1999). This could explain the observation of migration of RPE cells and the presence of macrophages in the neuroretina.

Pigment in the neuroretina may be associated with more severe damage. In most areas of the neuroretina where pigmented cells and free pigment accumulated, retinal damage was more severe. Pigmentary changes appeared to be more prominent in the chronic cases; hence, some of the neuronal loss in these regions may be due simply to a longer duration of the disease. To

eliminate differences in time of onset, neighboring regions of the same retina were compared. Retinal thinning was more severe in regions with Pigmentary changes within the same retina, which is consistent with these regions being associated with more local damage. In contrast to nontapetal regions, tapetal regions had fewer pigmentary changes and there were no significant changes in retinal thickness. Other studies have reported that the tapetal regions of neuroretinas tend to have less severe damage than the nontapetal regions (Whiteman et al, 2002; Smedes and Dubielzig, 1994). Inflammatory cells, including neutrophils, lymphocytes, and plasma cells, have been reported in the anterior segment of dogs with PACG (Reilly et al, 2005). The presence of inflammatory cells has also been reported in the neuroretinas of dogs with PG (Smedes and Dubielzig, 1994). In this study macrophages were present in the neuroretinas and vitreous bodies of dogs with both acute and chronic glaucoma. Neutrophilic infiltrates were seen primarily in acute glaucoma and were associated with retinal swelling. Cells with the morphologic characteristics of lymphocytes and plasma cells were also found in the neuroretinas of dogs with acute and chronic glaucoma. Immunohistochemical staining for CD3 indicated that T lymphocytes accumulated around some blood vessels of the inner layers of the retina. To our knowledge, there is no precedent for the observation of CD3-positive cells in the inner nuclear layer of normal controls or for the absence of these cells in glaucomatous neuroretinas. Based on location and morphology, it is possible the CD3-positive cells in control eyes were amacrine cells, which expressed reactivity to the CD3 immunohistochemical stain. Furthermore, these cells were negative for CD3 immunoreactivity when the primary antibody was withheld (Fig. 4.6d). The lack of CD3- positive cells in the inner nuclear layer in laucomatous eyes may reflect damage to these cells; however, the significance of this staining profile is unknown. The

presence of Perivascular CD3-positive cells in neuroretinas of glaucomatous eyes, but not in control eyes, provides evidence of an inflammatory disease process.

Both disruption of the RPE and increased vascular permeability may lead to exposure of retinal auto-antigens to the immune system, perhaps initiating or contributing to neuronal damage. The observations of perivascular inflammatory cells and albumin leakage from retinal blood vessels indicate inflammation and a breakdown of the blood–retinal barrier, respectively. In rodents (Bora et al, 1997; Deeg et al, 2006; Donoso et al, 1988; Caspi et al, 1988) and horses (Deeg et al, 2006; Deeg et al, 2006; Deeg et al, 2002; Deeg et al, 2001) purified or synthesized antigens from the RPE have been used to induce both uveitis and uveoretinitis. The histopathologic changes seen in some types of uveoretinitis have several similarities to those seen in PG in the dog. These changes include eventual loss of most types of retinal neurons including photoreceptors, damage to the RPE, vasculitis, accumulation of pigment in macrophages, and regional differences in the severity of damage (McIlnay et al, 2004; Whiteman et al, 2002; Van de Sandt et al, 2003; Smedes and Dubielzig, 1994). Thus, the inflammation associated with PG could lead to a cascade of events resulting in further neuronal damage.

It remains unclear if the retinal inflammation and RPE abnormalities observed this study are initiating factors in certain forms of PG or just a response to other causes of retinal damage and necrosis. The pigmentary changes, and association between duration of glaucoma and inflammatory cell morphology, parallel changes seen in the anterior segment in dogs with PACG (Reilly et al, 2005). As stated in the study by Reilly et al (2005), a cause-and-effect relationship cannot be discerned through histopathology, and there are inherent limitations to classifying and comparing samples based on a resumptive chronology of the disease process (Reilly et al, 2005). Other factors, including previous medical or surgical intervention, may also affect

histopathologic analysis. One dog in this series was treated with laser cyclophotocoagulation, which could have contributed to more severe inflammation and pigmentary changes. Latanoprost and/or pilocarpine were used in two dogs, and these procedures can cause anterior uveitis. In humans, latanoprost has been associated with macular edema and increased pigmentation of the iris (Albert et al, 2004; Cracknell et al, 2007; Miyake et al, 2002; Schumer et al, 2002). The pigmentary changes and inflammation, however, did not appear to be more severe when compared to cases that did not list treatments in the history. Similarly, we cannot make any conclusions about the effects topical or oral steroids may have had on slowing the progression of retinal damage in several cases. It should also be noted that these results represent a small sample size, and are limited to one form of canine PG. The results do, however, warrant a retrospective and prospective assessment for signs of pigmentary and inflammatory changes in the neuroretinas of dogs with various forms of PG.

The findings of RPE abnormalities and inflammation in the neuroretina in canine PG may have implications for further studies of pathogenesis and treatment. Damage to the RPE and leakage of albumin from blood vessels indicates a disruption of the blood–retinal barrier. We speculate that disruption of the blood–retinal barrier could make these eyes more susceptible to immune-mediated processes, which could cause further retinal degeneration. However, it is also possible that the pigmentary changes and inflammation are simply a response to severe retinal damage caused by other factors, such as elevated intraocular pressure and/or vascular damage. Regardless of whether or not pigmentary changes and inflammation are key risk factors in canine PG, they may contribute substantially to its progression. If true, anti-inflammatory treatment may prove effective in slowing the progression of neurodegeneration in canine PG.

CHAPTER FIVE:
DISCUSSION

Glaucoma may result in blindness in both humans and dogs. In our investigations, we have previously found that changes in glutamate distribution occur selectively in damaged areas of retinas of dogs with PG (Chen et al, 2008; Alyahya et al, 2007; McIlnay et al, 2004). This glutamate redistribution is consistent with high levels of extracellular glutamate (↑GluE) contributing to excitotoxic damage to neurons. We have tested three mechanisms by which this glutamate redistribution may occur (Chapters 2, 3 and 4).

5.1 Initial Hypothesis

In our laboratory, we have tested three mechanisms by which glutamate redistribution may occur in glaucoma. The rationale for choosing these hypotheses was discussed earlier in the introduction of this dissertation.

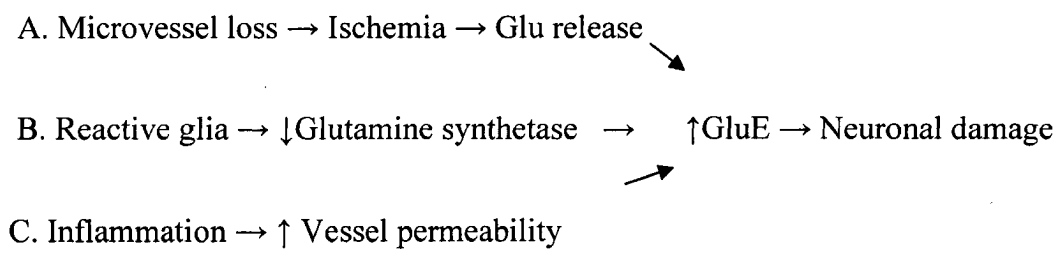

Fig. 5.1 Initial hypothesized mechanisms of neuronal damage in canine PG. We have found changes in glutamate (Glu) distribution in damaged regions of PG retinas. We hypothesized three mechanisms which may induce an increase in extracellular glutamate (↑GluE). In A, microvessel obliteration may lead to focal ischemia that releases Glu from cells. In B, reactive glia may reduce their levels of glutamine synthetase, leading to decreased glial metabolism of Glu, decreased levels of Glu in neurons, and perhaps decreased clearance of Glu from the extracellular fluid. In C, inflammation increases leakage of Glu from blood vessels.

5.1.1 Conclusions from the Test of Hypothesis A

First, we compared the densities of microvessels in damaged and less damaged regions of retinas (Chapter 2). In these studies we found significantly lower microvessel density in regions of INL thinning and in regions with mild neuronal damage but no obvious loss of neurons. Since regions with mild neuronal damage have not yet lost large numbers of neurons, we claimed that microvessels are obliterated in the mildest stages of PG we could detect. However, we have also seen large changes in glutamate distribution very close to the remaining microvessels. This suggests that it is not necessary to lose the microvessels in a region for glutamate to redistribute. Thus, we reject the hypothesis that microvessel loss is the only factor leading to glutamate redistribution and neuronal damage.

5.1.2 Conclusions from the Test of Hypothesis B

The following is a summary of the results of the test of hypothesis B (Chapter 3). To test hypothesis B that reactive changes in Muller cells are induced in damaged regions and that these changes include reduced glutamine synthetase levels, we determined if Muller cells in damaged regions express GFAP, a marker for reactive Muller cells, and have decreased levels of glutamine synthetase. In the studies, we have found significantly decreased amounts of glutamine synthetase in areas with neuronal damage and glutamate redistribution. We have also found that glutamine synthetase decreases in many glia cells that are not reactive and have not expressed GFAP. Thus, we have rejected this hypothesis that reactive glia cause decreases in glutamine synthetase that then leads to glutamate redistribution and neuronal damage. However, we have found that decreased glutamine synthetase levels were associated with even the mildest

damage we could detect in PG, suggesting that a loss of glutamine synthetase may mediate the initial stages of damage.

5.1.3 Conclusions from the Test of Hypothesis C

To test hypothesis C that inflammation leads to increased vascular permeability, leakage of glutamate into the extracellular fluid, and neuronal damage (Chapter 4), we have determined first if there is albumin leakage from blood vessels in damaged regions and second if these damaged regions have another indicator of inflammation, inflammatory cell infiltrates. We have found from our studies that there is albumin leakage from blood vessels in damaged regions with other inflammatory indicators in those areas. Albumin is a large molecule of approximately 68,000 Daltons molecular weight, while glutamate is much smaller with a weight of 147 Daltons. The smaller size of glutamate suggests that it should also diffuse out of blood into the extracellular fluid of the retina even more readily than albumin. Therefore, we cannot reject this hypothesis that inflammation contributes to increase extracellular Glu and neuronal damage.

5.2 Retained Parts of Initial Hypothesis

Neuronal damage and redistribution of glutamate in the INL occurs even in the presence of microvessels, although a statistically significant decrease of microvessels occurs even in mildly damaged regions. Thus, we have rejected the hypothesis A that microvessel loss is necessary for glutamate redistribution and neuronal damage but have not rejected the concept that microvessel loss may contribute to the damage. A recent study has confirmed that hypoxia may occur in canine PG (Savagian et al, 2008). This study found an increase of hypoxia inducible factor 1-alpha suggesting that parts of retina may be hypoxic-ischemic. We speculate

that this might occur through lack of blood flow in damaged vessels even though the vessels may still be present. This possible ischemia due to occlusion could explain the presence of blood vessels in regions where glutamate has redistributed.

We speculate that other factors induced by ischemia may also play a role in the glutamate redistribution and neuronal damage. Oxidative stress is one of those factors that are initiated by decreased blood flow (Doyle et al, 2008) that we believe may contribute to the glutamate redistribution and damage.

From hypothesis B, we have retained the concept that decreases in glutamine synthetase may also contributed to glutamate redistribution and neuronal death. However, glutamine synthetase reduction occurs in glial cells that are often not reactive. Thus, we reject the hypothesis B that reactivity in glia causes the decrease of glutamine synthetase and leads to neuronal death. Meanwhile, the decrease of glutamine synthetase could be caused by the oxidative stress (Gorg et al, 2006; Butterfield, 2002), resulting in an increase in extracellular glutamate and neuronal death.

From hypothesis C, we have retained the concept that inflammation may contribute to retinal damage. Albumin leakage from blood vessels and inflammation occurs in PG, and leakage of glutamate or other neurotoxic molecules across the blood-retinal barrier may contribute to neuronal damage. However, inflammation also could initiate oxidative stress and increase the extracellular glutamate by decreasing glutamine synthetase.

5.3 Revised Hypothesis / Future Investigation

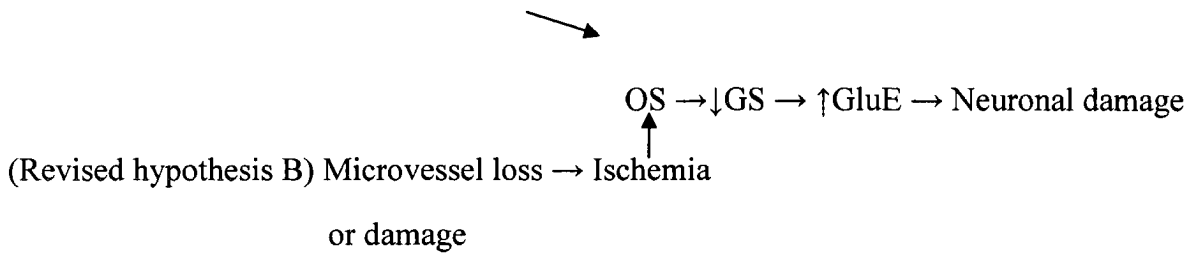

Fig. 5.2 Revised hypothesized mechanisms of neuronal damage in canine PG. We have found changes in glutamate distribution in damaged regions of PG retinas. We revised the mechanisms of the original three hypotheses (Fig. 5.1) to a new mechanism, which may induce an increase in extracellular glutamate (↑GluE). In A, inflammation may lead to oxidative stress (OS) that decreases glutamine synthetase (↓GS). In B, ischemia may play a role in decreasing glutamine synthetase through oxidative stress leading to Glu redistribution and neuronal damage.

There is a growing body of evidence supporting the role of oxidative stress in the pathophysiology of a number of neurodegenerative diseases such as Parkinson's disease and Alzheimer's disease (Facheris et al., 2004 ; Gorg et al, 2007). Recent studies suggest that oxidative stress may be a factor linking the retained parts of initial hypotheses with glutamate redistribution. Decreases in glutamine synthetase may be caused by oxidative stress (Gorg et al, 2007; Poon et al., 2006). Other studies have also shown that inflammation may increase oxidative stress by inflammatory cells that produce reactive free radicals. Ischemia has also been shown to cause oxidative stress and play a role in glutamate redistribution (Doyle, 2008; Liang et al., 2008).

5.4 Possible Tests of Revised Hypothesis

We could use similar methods in our previous studies (Chapters 2, 3, and 4) to test the revised hypothesis (Fig. 5.2).

To test specifically if oxidative stress may lead to loss of glutamine synthetase, we could perform immunohistochemical measurements similar to those in Chapter 3, figure 2. We would measure levels of markers for oxidative stress in the regions with different severities of damage and different levels of glutamine synthetase. If oxidative stress is not increased in regions with decreased glutamine synthetase, we would reject the hypothesis. We have chosen to propose the use of a marker of increased oxidative stress, malondialdehyde, a marker of nitrative stress, nitrotyrosine and the loss of glutathione as indicators of oxidative stress. Each of these immunohistochemical markers has been used successfully in our laboratory and should allow us to test the revised hypothesis.

Nitrotyrosine is an indicator of cell damage and oxidative stress as well as of the production of nitric oxide. It has been shown that nitrotyrosine functions as a marker for damage caused by oxidative stress in the cell (Sajdel-Sulkowska et al, 2008; Viappiani and Schulz, 2006). Increased nitrotyrosine formation suggests a high level of oxidative stress that could decrease glutamine synthetase and enhance neuronal cell damage. Nitrotyrosine is a specific marker of oxidative damage mediated by peroxynitrite, which is formed by the reaction of superoxide with nitric oxide (NO) on tyrosine residues in proteins (Beckman and Koppenol, 1996) or by reaction of nitrite and hydrogen peroxide (Sampson et al, 1998). Inactivation of glutamine synthetase by nitration and formation of nitrotyrosine has been shown to occur in oxidative stress (Gorg et al, 2006). Oxidative inactivation and loss of glutamine synthetase has

been proposed to contribute to other neurodegerative diseases such as Alzheimer's disease (Butterfield et al, 2002).

As we described in Chapter 3, the density of immunohistochemical staining for glutamine synthetase was measured in Müller cell bodies in regions with different degrees of damage, i.e. mildly to severely damaged regions of retina. If the revised hypothesis is correct, we would expect the expression and activity of oxidative stress to increase as glutamine synthetase decreases in those Müller cell. If normal levels of glutamine synthetase are present in regions with high density of nitrotyrosine, we will reject the hypothesis that oxidative stress causes the decrease of glutamine synthetase and neuronal damage.

Malondialdehyde is one of the most frequently used biomarkers providing an indication of the overall lipid peroxidation level (Nielsen et al, 1997). Non-dividing cells, such as neurons, are particularly vulnerable to cumulative oxidative damage because they survive for decades. The generation of oxidants leads to damage to proteins, lipids and nucleotides, which may contribute significantly to neuron dysfunction and degeneration associated with aging and neurodegenerative diseases (Liu and Mori, 1999).

Similar to the technique of testing for increased nitrotyrosine as an indicator for oxidative stress, we could also test for increases in the marker malondialdehyde to measure the level of oxidative stress in regions with low level of glutamate synthetase in glial cells. Increased immunohistochemical staining for malondialdehyde would indicate the high level of oxidative stress in the regions. If increased malondialdehyde occurs in regions that maintain normal level of glutamine synthetase, we will also reject the revised hypothesis which oxidative stress initiate the decrease of glutamine synthetase and lead to redistribution of glutamate and neuronal death.

Another way to test for oxidative stress might be the depletion of antioxidants. It has been found that the antioxidant glutathione may be depleted during oxidative stress in the CNS (Arakowa M, 2007). Normal levels of glutathione are essential for normal retinal function and depletion of glutathione leads retinal neuronal death (Roh et al., 2007). We hypothesized that this cell death may be mediated, at least in part, by the mechanism described in revised hypothesis. In the revised hypothesis, we speculate that glutamine synthetase is especially vulnerable to oxidative stress as shown by (Gorg et al, 2007; Kosenko et al, 2003; Minana et al, 1997). This loss of glutamine synthetase may then lead to extracellular accumulation of glutamate and neuronal death.

Glutathione is a small molecule made up of three amino acids (cysteine, glutamate, and glycine), which exists in almost every cell of the body (Dringen, 2000; Roh et al, 2007). Glutathione is an important intracellular antioxidant that protects against a variety of different antioxidant species (Hall et al, 1999; Roh et al, 2007). The presence of glutathione is required to maintain the normal functions of cells. For example, it is known to play a critical role in the multiplication of lymphocytes which occurs in the development of an effective immune response (Hall et al, 1999).

To test the hypothesis that oxidative stress may lead to decreased glutamine synthetase, we propose measuring the level of glutathione in regions with high level of oxidative stress using established immunohistochemical methods. We speculate that in regions where the antioxidant glutathione is depleted, oxidative stress will increase, resulting in a decrease in glutamine synthetase and neuronal death.

5.4.1 The Test of Revised Hypothesis A

Inflammation may lead to oxidative stress. The presence of reactive inflammatory cells including macrophages/microglia and neutrophils strongly suggests that inflammation may play a major role for the cell death in PG (Mangan et al, 2007; Whiteman et al, 2002).

Reactive oxygen and nitrate species produced by inflammatory cells seen in PG are toxic to the neurons (Jeohn et al, 1998). Microglia are considered the resident immune cells of the central nervous system and during physiologic conditions they serve a role in immune surveillance and host defense (Liu and Hong, 2003). These cells have been implicated in the pathogenesis of a number of neurodegenerative diseases such as multiple sclerosis (Hofman et al, 1989), Alzheimer's disease (Rogers et al, 1988; Combs et al, 2001) and Parkinson's disease (McGeer et al, 1989). They are particularly sensitive to changes in the surrounding environment and readily become activated in response to infection or injury in the brain (Kreutzberg, 1996). Reactive microglia can produce oxidizing species such as nitric oxide, superoxide ions and peroxynitrite (Boje and Arora, 1992; Chao et al, 1992; McGuire et al, 2001). In a similar manner, neutrophils produce an oxidative burst of nitric oxide, superoxide ions and peroxynitrite when stimulated (Cowburn et al, 2008).

If the level of glutamine synthetase decreases in regions with inflammatory cells infiltrates, we will not reject the revised hypothesis that inflammation may contribute to neuronal death through oxidative stress-induced decreases in glutamine synthetase.

5.4.2 The Test of Revised Hypothesis B

There is an evidence to support the concept that the oxidative stress is initiated by tissue with hypoxia or ischemia (Doyle et al, 2008). Experimental elevation of IOP induces oxidative

stress in the retina. Oxidative stress is generated in the retina not only in retinal ischemia models induced by acute IOP elevation (Bonne et al., 1998; Muller et al., 1998), but also in experimental models induced by moderate and chronic elevation of IOP. To test the revised hypothesis, we may use similar method described in chapter 2 to measure the number of blood vessels in areas with oxidative stress to determine the involvement of ischemia in leading the elevation of oxidative stress and decreasing the glutamine synthetase.

We could detect the number of microvessels vessels in different damaged regions with oxidative stress. We speculate we will see a decreased number of microvessels in those regions with oxidative stress as we hypothesized that ischemia may initiate oxidative stress and cause glutamate redistribution by decreasing glutamine synthetase. Thus, if there are fewer microvessels in regions with increased oxidative stress, we will not reject this revised hypothesis that ischemia could lead to oxidative stress and enhance the neuronal damage.

REFERENCES

Adachi K, Kashii S, Masai H et al. Mechanism of the pathogenesis of glutamate neurotoxicity in retinal ischemia. Graefe's Archive for Clinical and Experimental Ophthalmology 1998; 236: 766–774.

Albert DM, Gangnon RE, Zimbric ML *et al.* A study of iridectomy histopathologic features of latanoprost- and non-latanoprost-treated patients. *Archives of Ophthalmology* 2004; 122: 1680–1685.

Alyahya K, Chen C., Mangan, B., Gionfriddo, J., Legare, M., Dubielzig, R. and Madl. Microvessel loss, vascular damage and glutamate redistribution in the retinas of dogs with primary glaucoma. *Veterinary Ophthalmology*, 10(1), 70-77.

Anderson M., Smith R., Hawes N. Zabaleta, A., Chang, B., Wiggs' J. and John' S. (2001). Mutations in genes encoding melanosomal proteins cause pigmentary glaucoma in DBA/2J mice. *Nature Genetics,* 30, 81–85.

Arakawa, M., Ishimura, A., Arai, Y., Kawabe, K., Suzuki, S., Ishige, K. and Ito, Y. (2007). N-Acetylcysteine and ebselen but not nifedipine protected cerebellar granule neurons against 4-hydroxynonenal-induced neuronal death. *Neuroscience Research*, 57(2), 220-229.

Attwell D, Barbour B, Szatkowski M. Nonvesicular release of neurotransmitter. *Neuron* 1993; 11: 401–407.

Bentley E, Miller PE, Murphy CJ, et al. Combined cycloablation and gonioimplantation for treatment of glaucoma in dogs: 18 cases (1992–1998). *J Am Vet Med Assoc* 1999;215:1469–1472.

Beckman, J. and Koppenol, W. (1996). Nitric oxide, superoxide and peroxynitrite the good, the bad and the ugly. *American Journal Physiology*, 271, 1424-1437.

BlanksJC, JohnsonLV. Vascular atrophy of the retinal degenerative rd mouse. *Journal of Comparative Neurology* 1986; 254: 543–553.

Blocker T, Van Der Woerdt A. The feline glaucomas: 82 cases (1995–1999). *Veterinary Ophthalmology* 2001; 4: 81–85.

Bonne, C., Muller, A. and Villain, M. (1998). Free radicals in retinal ischemia. *Gen. Pharmacology*, 30, 275–280.

Boje, K. and Arora, P. (1992). Microglial-produced nitric oxide and reactive nitrogen oxides mediate neuronal cell death. *Brain Research*, 587, 250–256.

Bora NS, Sohn JH, Kang SG *et al.* Type I collagen is the autoantigen in experimental autoimmune anterior uveitis. *Journal of Immunology* 2004; 172: 7086–7094.

Bora NS, Woon MD, Tandhasetti MT *et al.* Induction of experimental autoimmune anterior uveitis by a self-antigen: melanin complex without adjuvant. *Investigative Ophthalmology & Visual Science* 1997; 38: 2171–2175.

Bouvier M, Szatkowski M, Amato A *et al.* The glial cell glutamate uptake carrier countertransports pH-changing anions. *Nature* 1992; 360: 471–474.

Brand-SchieberE, LowerySL, WernerP. Select ionotropic glutamate AMPA/kainate receptors are expressed at the astrocyte–vessel interface. *Brain Research* 2004; 1007: 178–182.

Bresnick GH, Segal P, Mattson D (1983) Fluorescein angiographic findings in diabetic retinopathy. In: Little HL, Jack RL, Patz A, Forsham PH (eds) Diabetic retinopathy. Thieme-Stratton, New York, pp 37–51

Broekhuyse RM, Kuhlmann ED, Winkens HJ *et al.* Experimental autoimmune anterior uveitis (EAAU), a new form of experimental uveitis. I. Induction by a detergent-insoluble, intrinsic protein fraction of the retinal pigment epithelium. *Experimental Eye Research* 1991; 52: 465–474.

Brooks DE. Glaucoma in the dog and cat. *Veterinary Clinics of North America. Small Animal Practice* 1990; 20 (3): 775–797.

Brooks DE, Garcia GA, Dreyer EB *et al.* Vitreous body glutamate concentration in dogs with glaucoma. *American Journal of Veterinary Research* 1997; 58: 864–867.

BrooksDE, SamuelsonDA, GelattKN. Ultrastructural changes in laminar optic nerve capillaries of beagles with primary open-angle glaucoma. *American Journal of Veterinary Research* 1989; 50: 929–935.

Butterfield D. (2002). Amyloid beta-peptide (1-42)-induced oxidative stress and neurotoxicity: implications for neurodegeneration in Alzheimer's disease brain. *Free Radical Research*, 36(12), 1307-1313.

Caspi RR, Roberge FG, Chan CC *et al.* A new model of autoimmune disease. Experimental autoimmune uveoretinitis induced in mice with two different retinal antigens. *Journal of Immunology* 1988; 140: 1490–1495.

Cavelier P, Hamann M, Rossi D *et al.* Tonic excitation and inhibition of neurons: ambient transmitter sources and computational consequences. *Progress in Biophysics and Molecular Biology* 2005; 87: 3–16.

Chao, C., Hu, S., Molitor, T., Shaskan, E., and Peterson, P. (1992). Activated microglia mediate neuronal cell 92 Shavali, Combs, and Ebadiinjury via a nitric oxide mechanism. *J. Immuno.*, 149, 2736–2741.

Chen, C., Alyahya, K., Gionfriddo, J., Dubielzig, R. and Madl, J. (2008). Loss of glutamine synthetase immunoreactivity from the retina in canine primary glaucoma. *Veterinary Ophthalmology*, 11(3), 150-157.

Chen, N., Chiu, P. and Ko, K. (2008). Schisandrin B enhances cerebral mitochondrial antioxidant status and structural integrity, and protects against cerebral ischemia/reperfusion injury in rats. *Biological & Pharmaceutical Bulletin*, 31(7), 1387-91.

ChengCY, LiuCJ, ChiouHJ *et al.* Color Doppler imaging study of retrobulbar hemodynamics in chronic angle-closure glaucoma. *Ophthalmology* 2001; 108: 1445–1451.

ChungHS, HarrisA, EvansDW *et al.* Vascular aspects in the pathophysiology of glaucomatous optic neuropathy. *Survey of Ophthalmology* 1999; 43 (Suppl. 1): S43–S50.

CioffiGA. Three common assumptions about ocular blood flow and glaucoma. *Survey of Ophthalmology* 2001; 45 (Suppl. 3): S325–S331.

Cioffi GA, Granstam E, Alm A. Ocular circulation. In: *Adler's Physiology of the Eye*, 10th edn. (eds Kaufman PL, Alm A) Mosby, St. Louis, MO, 2003; 747–784.

Combs, C., Karlo, J., Kao, S., and Landreth, G. (2001). Amyloid stimulation of microglia and monocytes results in TNF-dependent expression of inducible nitric oxide synthase and neuronal apoptosis. *Journal of Neuroscience*, 21, 1179–1188.

Cowburn, A., Condliffe, A., Farahi, F., Summers, C., and Chilvers, E. (2008). Advances in neutrophil biology. *Translating Basic Research Into Clinical Practice*, 134(3), 606-612.

Cracknell KP, Grierson I, Hogg P. Morphometric effects of long-term exposure to latanoprost. *Ophthalmology* 2007; 114: 938–948.

Cullen CL, Grahn BH. Equine glaucoma: a retrospective study of 13 cases presented at the Western College of Veterinary Medicine from 1992 to 1999. *Canadian Veterinary Journal* 2000; 41: 470–480.

Davidson M, Nasisse M, Kornegay J. Intermediate filament complement of the normal and gliotic canine retina. *Journal of Comparative Pathology* 1990; 103: 125–134.

Deeg CA, Amann B, Raith AJ *et al.* Inter- and intramolecular epitope spreading in equine recurrent uveitis. *Investigative Ophthalmology & Visual Science* 2006; 47: 652–656.

Deeg CA, Ehrenhofer M, Thurau SR *et al.* Immunopathology of recurrent uveitis in spontaneously diseased horses. *Experimental Eye Research* 2002; 75: 127–133.

Deeg CA, Kaspers B, Gerhards H *et al.* Immune responses to retinal autoantigens and peptides in equine recurrent uveitis. *Investigative Ophthalmology & Visual Science* 2001; 42 (2): 393–398.

Deeg CA, Pompetzki D, Raith AJ *et al.* Identification and functional validation of novel autoantigens in equine uveitis. *Molecular & Cellular Proteomics* 2006; 5: 1462–1470.

Donoso LA, Merryman CF, Sery TW *et al.* Human IRBP: characterization of uveitopathogenic sites. *Current Eye Research* 1988; 7: 1087–1095.

Doyle, P., Simon, R., and Stenzel-Poore, M. (2008). Mechanisms of ischemic brain damage. Elsevier, 55, 310-318.

Dringen, R. (2000). Glutathione metabolism and oxidative stress in neurodegeneration, *Eur. J. Biochemistry,* 267, 4903.

Facheris, M., Beretta, S. and Ferrarese, C. (2004). Peripheral markers of oxidative stress and excitotoxicity in neurodegenerative disorders: tools for diagnosis and therapy? *Journal of Alzheimer's Disease*, 6(2), 177-84.

Farrar SM. Shields MB. Current concepts in pigmentary glaucoma. [Review] [173 refs] [Journal Article. Review] Survey of Ophthalmology. 37(4):233-52, 1993 Jan-Feb.

Gelatt, K., Miyabayashi, T., Gelatt-Nicholson, K. and MacKay, E. (2005). Progressive changes in ophthalmic blood velocities in Beagles with primary open angle glaucoma. *Veterinary Ophthalmology,* 6(1), 77–84.

Gelatt KN. The canine glaucomas. In: *Veterinary Ophthalmology*, 2nd edn. (ed. Gelatt KN) Lea & Febiger, Philadelphia, 1991; 396–428.

Glaze MB, Gelatt KN. Feline ophthalmology. In: *Veterinary Ophthalmology*, 3rd edn. (ed. Gelatt KN) Lippincott Williams & Wilkins, Philadelphia, 1999; 997–1052.

Gorg B., Qvartskhava N., Voss P., Grune T., Haussinger D., Schliess F. (2007). Reversible inhibition of mammalian glutamine synthetase by tyrosine nitration. *FEBS*, 581(1), 84-90.

Gorg B., Qvartskhava N., Voss P., Grune T., Haussinger D., Schliess F. (2007). Reversible inhibition of mammalian glutamine synthetase by tyrosine nitration. *FEBS*, 581(1), 84-90.

Hall, A. (1999). Review: the role of glutathione in the regulation of apoptosis, *Eur. J. Clin. Invest.*, 29, 238–245

Hansen AJ. Effects of anoxia on ion distribution in the brain. *Physiological Reviews* 1985; 65: 101–148

Hardy P, Beauchamp M, Sennlaub F *et al.* New insights into the retinal circulation: inflammatory lipid mediators in ischemic retinopathy. *Prostaglandins, Leukotrienes and Essential Fatty Acids* 2005; 72: 301–325

Hare, W., WoldeMussie, E., Lai, R., Ton, H., Ruiz, G., Feldman, B., Wijono, M., Chun, T., Wheeler, L. (2001). Efficacy and safety of memantine, an NMDA-type open-channel blocker, for reduction of retinal injury associated with experimental glaucoma in rat and monkey. *Surv. Ophthalmology*, 3, 284–289

Harris, A., Jonescu-Cuypers, C., Martin, B., Kagemann, L., Zalish, M. and Garzozi, H. (2001).Simultaneous management of blood flow and IOP in glaucoma. Acta Ophthalmology Scand,79, 336–341

Heidinger V, Hicks D, Sahel J *et al.* Ability of retinal Müller glial cells to protect neurons against excitotoxicity in vitro depends upon maturation and neuron–glial interactions. *Glia* 1999; 25: 229–239.

Hofman, F., Hinton, D., Johnson, K., and Merrill, J. (1989). Tumor necrosis factor identified in multiple sclerosis brain. *J. Exp. Med.*, 170, 607–612.

Howes EL Jr, Cruse VK. The structural basis of altered vascular permeability following intraocular inflammation. *Archives of Ophthalmology* 1978; 96: 1668–1676.

HughesS, Chang-LingT. Roles of endothelial cell migration and apoptosis in vascular remodeling during development of the central nervous system. *Microcirculation* 2002; 7: 317–333.

IshidaS, YamashiroK, UsuiT *et al.* Leukocytes mediate retinal vascular remodeling during development and vaso-obliteration in disease. *Nature Medicine* 2003; 9: 781–788.

Jablonski MM, Tombran-Tink J, Mrazek DA *et al.* Pigment epithelium-derived factor supports normal Müller cell development and glutamine synthetase expression after removal of the retinal pigment epithelium. *Glia* 2001; 35: 14–25.

Jeohn, G., Kong, L., Wilson, B., Hudson, P., and Hong, J. (1998). Synergistic neurotoxic effects of combined treatments with cytokines in murine primary mixed neuron/glia cultures. *J. Neuroimmunol*, 85:1–10.

John, S., Smith, R., Savinova, O., Hawes, N., Change, B., Turnbull, D., Davisson, M., Roderick, T. and Heckenlively, J. (1998). Essential iris atrophy, pigment dispersion, and glaucoma in DBA/2J mice. *Investigative Ophthalmology & Visual Science,* 39(6), 951–962.

JoussenAM, PoulakiV, MitsiadesN *et al.* Suppression of Fas-FasL-induced endothelial cell apoptosis prevents diabetic blood–retinal barrier breakdown in a model of streptozotocin-induced diabetes. *FASEB Journal* 2003; 17: 76–78.

L.M. Katz, C.W. Callaway, V.E. Kagan, P.M. Kochanek, Electron spin resonance measure of brain antioxidant activity during ischemia/reperfusion, NeuroReport 9 (1998) 1587– 1593.

Katz, L., Younga, A., Franka, J., Wanga, Y. and Parkb. K. (2004). Regulated hypothermia reduces brain oxidative stress after hypoxic-ischemia. *Brain Research,* 1017, 85–91

Komara, J., N.R. Nayini, H.A. Bialick, R.J. Indrieri, A.T. Evans, A.M. Garritano, T.J. Hoehner, W.A. Jacobs, R.R. Huang, G.S. Krause, et al., Brain iron delocalization and lipid peroxidation following cardiac arrest, Ann. Emerg. Med. 15 (1986) 384– 389.

Kosenko, E., Lansola, M., Montoliu, C., Monfort, P., Rodrigo, R., Hernandez-Viadel, M., Erceg, S., Sanchez-Perez, A.M. and Felipo, V. (2003) Glutamine synthetase activity and glutamine content in brain: modulation by NMDA receptors and nitric oxide. *Neurochemistry Int.*, 43, 493–499.

Krajnc D, Neff NH, Hadjiconstantinou M. Glutamate, glutamine and glutamine synthetase in the neonatal rat brain following hypoxia. *Brain Research* 1996; 707: 134–137.

Kreutzberg, G. (1996). Microglia: a sensor for pathological events in the CNS. *Trends Neuroscience*, 19, 312–318.

KwongJM, LamTT. N-methyl-D-aspartate (NMDA) induced apoptosis in adult rabbit retinas. *Experimental Eye Research* 2000; 71: 437–444.

Lewis GP, Fisher SK. Up-regulation of glial fibrillary acidic protein in response to retinal injury: its potential role in glial remodeling and a comparison to vimentin expression. *International Review of Cytology* 2003; 230: 263–290.

Liang, H., Qiu, S., Shen J., Sun, L., Wang, J., Bruce, I. and Xia Q. (2008). Genistein attenuates oxidative stress and neuronal damage following transient global cerebral ischemia in rat hippocampus. *Neuroscience Letters*, 438(1), 116-120.

Liu, B. and Hong, J. (2003). Role of microglia in inflammation-mediated neurodegenerative diseases: Mechanisms and strategies for therapeutic intervention. *J. Pharmacol Exp. Ther.*, 304, 1–7.

Liu, J. and Mori, A. (1999). Stress, Aging, and Brain Oxidative Damage. *Neurochemical Research*, 24(11), 1479-1497.

LowHC, GionfriddoJR, MadlJE. Assessment of glutamate loss from the ganglion cell layer of young DBA/2J mice with glaucoma. *American Journal of Veterinary Research* 2006; 67: 302–309.

LucasDR, NewhouseJP. The toxic effects of sodium 1-glutamate on the inner layers of the retina. *Archives of Ophthalmology* 1957; 58: 193–201.

Madl JE, McIlnay TR, Powell CC, Gionfriddo JR. Depletion of taurine and glutamate from damaged photoreceptors in the retinas of dogs with primary glaucoma. *American Journal of Veterinary Research* 2005; 66: 791–799.

Mangan, B., Alyahya K, Chen C., Gionfriddo, J., Powell, C., Dubielzig, R. Ehrhart, E., and Madl, J. (2007). Retinal pigment epithelial damage, breakdown of the blood–retinal barrier, and retinal inflammation in dogs with primary glaucoma. *Veterinary Ophthalmology*, 10(1), 70-77, 117-124,

Marc RE, Murry RF, Fisher SK *et al.* Amino acid signatures in the detached cat retina. *Investigative Ophthalmology and Visual Science* 1998; 39: 1694–1702.

McGeer, P., Itagaki, S., Boyes, B., and McGeer, E. (1988). Reactive microglia are positive for HLA-DR in the substantia nigra of Parkinson's and Alzheimer's disease brains. *Neurology*, 38, 1285–1291.

McGuire, S., Ling, Z., Lipton, J., Sortwell, C., Collier, T., and Carvey, P. (2001). Tumor necrosis factor alpha is toxic to embryonic mesencephalic dopamine neurons. *Exp. Neurol.*, 169, 219–230.

McIlnay, T., Gionfriddo, J., Dubielzig, R., Powell, C., and Madl, J. (2004). Evaluation of glutamate loss from damaged retinal cells of dogs with primary glaucoma. *American Journal of Veterinary Research*, 65(6), 776–786.

Migliazzo CV. Shaffer RN. Nykin R. Magee S. Long-term analysis of pigmentary dispersion syndrome and pigmentary glaucoma. [Comparative Study. Journal Article] Ophthalmology. 93(12):1528-36, 1986 Dec. UI: 3808615

MiharaM, HayasakaS, WatanabeK *et al.* Ocular manifestations in patients with microscopic polyangiitis. *European Journal of Ophthalmology* 2005; 15: 138–142.

Miller P. (1995). Glaucoma. In: *Current Veterinary Therapy XII.* (eds Bonagura JD, Kirk RW) W.B. Saunders, Philadelphia, 1265–1272.

Miller TR, Brooks DE, Gelatt KN *et al.* Equine glaucoma: clinical findings and response to treatment in 14 horses. *Veterinary and Comparative Ophthalmology* 1995; 5 : 170–182.

Minana, M., Kosenko, E., Marcaida, G., Hermenegildo, C., Montoliu, C., Grisolia, S. and Felipo, (1997). Modulation of glutamine synthesis in cultured astrocytes by nitric oxide. Cell. *Mol. Neurobiology*, 17, 433–445.

Miyake K, Ibaraki N. Prostaglandins and cystoid macular edema. *Survey of Ophthalmology* 2002; 47 (Suppl. 1): S203–S218.

Moreno M., Sande P., Marcos H., Zavalia N., Sarmiento, K., Rosenstein R. (2005). Effect of glaucoma on the retinal glutamate/glutamine cycle activity. *FASEB Journal*, 19(9):1161-1162

MoritaT, MizutaniY, SawadaM *et al.* Immunohistochemical and ultrastructural findings related to the blood–brain barrier in the blood vessels of the cerebral white matter in aged dogs. *Journal of Comparative Pathology* 2005; 133: 14–22.

Muller, A., Maurin, L. and Bonne, C. (1998). Free radicals and glutamate uptake in the retina. *Gen. Pharmacology*, 30, 315–318.

Neufeld AH, Liu B. Glaucomatous optic neuropathy: when glia misbehave. *Neuroscientist* 2003; 9: 485–495.

Nielsen, F., Mikkelsen, B., Nielsen, J., Andersen, H., and Grandjean, P. (1997). Plasma malondialdehyde as biomarker for oxidative stress: reference interval and effects of life-style factors. *Clinical Chemistry*, 43(7), 1209–1214.

Nickells, R. (2007). Ganglion cell death in glaucoma: from mice to men. Veterinary Ophthalmology, 10, 88–94.

Nishiyama T, Nishukawa S, Hiroshi B *et al.* Müller cells in the preconditioned retinal ischemic injury rat. *The Tohoku Journal of Experimental Medicine* 2000; 191: 221–232.

Owe SG, Marcaggi P, Attwell D. The ionic stoichiometry of the GLAST glutamate transporter in salamander retinal glia. *Journal of Physiology* 2006; 577: 591–599.

Padnick-SilverL, DerwentJJ, GiulianoE *et al.* Retinal oxygenation and oxygen metabolism in Abyssinian cats with a hereditary retinal degeneration. *Investigative Ophthalmology and Visual Science* 2006; 47: 3683–2689.

Peiffer RL, Wilcock BP, Dubielzig RR *et al.* Fundamentals of veterinary ophthalmic pathology. In: *Veterinary Ophthalmology*, 3rd edn. (ed. Gelatt KN) Lippincott Williams & Wilkins, Philadelphia, 1999; 355–425.

Pereira C, Santos MS, Oliveira C. Metabolic inhibition increases glutamate susceptibility on a PC12 cell line. *Journal of Neuroscience Research* 1998; 51: 360–370.

Pickett JP, Ryan J. Equine glaucoma: a retrospective study of 11 cases from 1988 to 1993. *Veterinary Medicine* 1993; 88: 756–763.

Poon H., Vaishnav R., Getchell T., Getchell M., Butterfield D. (2006). Quantitative proteomics analysis of differential protein expression and oxidative modification of specific proteins in the brains of old mice. *Neurobiology of Aging*, 27(7),1010-9.

Rauen T, Taylor WR, Kuhlbrodt K *et al.* High-affinity glutamate transporters in the rat retina: a major role of the glial glutamate transporter GLAST-1 in transmitter clearance. *Cell and Tissue Research* 1998; 291: 19–31.

Rauen T, Wiessner M. Fine tuning of glutamate uptake and degradation in glial cells: common transcriptional regulation of GLAST1 and GS. *Neurochemistry International* 2000; 37: 179–189.

Reichenbach, A. *et al.* (1989) *Anat. Embryol. 180, 71-79*

Reilly CM, Morris R, Dubielzig RR. Canine goniodysgenesis-related glaucoma: a morphologic review of 100 cases looking at inflammation and pigment dispersion. *Veterinary Ophthalmology* 2005; 8: 253–258.

Ritch R. Pigment dispersion syndrome.[comment]. [Review] [37 refs] [Comment. Editorial. Review] American Journal of Ophthalmology. 126(3):442-5, 1998 Sep.

Ritch R. Chaiwat T. Harbin TS Jr. Asymmetric pigmentary glaucoma resulting from cataract formation. [Case Reports. Journal Article. Research Support, Non-U.S. Gov't] American Journal of Ophthalmology. 114(4):484-8, 1992 Oct 15. UI: 1415461

Rogers, J., Luber-Nardo, J., Styren, S., and Civin, W. (1988). Expression of immune system associated antigens by cells of the central nervous system: relationship to the pathology of Alzheimer's disease. *Neurobiology Aging*, 9, 339–349.

Roh, Y., Moon, C., Kim, S., Park, M., Bae, Y., Chun, M. and Moon, J. (2007). Glutathione depletion induces differential apoptosis n cells of mouse retina, in vivo. *Elsevier*, 417, 266–270.

Sajdel-Sulkowska, E., Lipinski, B., Windom, B., Audhya, T. and McGinnis, W. (2008). Oxidative Stress in Autism: Elevated Cerebellar 3-nitrotyrosine Levels. *American Journal of Biochemistry and Biotechnology*, 4(2): 73-84.

Sampson, J., Ye, Y., Rosen, H. and Beckman, J. (1998). Myeloperoxidase and horseradish peroxidase catalyze tyrosine nitration in proteins from nitrite and hydrogen peroxide. *Arch. Biochem. Biophys.*, 356, 207-213.

Samuelson DA. Ophthalmic anatomy. In: *Veterinary Ophthalmology*, 3rd edn. (ed. Gelatt KN) Lippincott Williams & Wilkins, Philadelphia, 1999; 30–150.

Sapienza JS, Simo FJ, Prades-Sapienza A. Golden Retriever uveitis: 75 cases (1994–1999). *Veterinary Ophthalmology* 2000; 3: 241–246.

Smedes SL, Dubielzig RR. Early degenerative changes associated with spontaneous glaucoma in dogs. *Journal of Veterinary Diagnostic Investigation* 1994; 6 (2): 259–263.

Savagian, C., and Dubielzig, R., and Nork, M. (2008). Comparison of the distribution of glial fibrillary acidic protein, heat shock protein 60, and hypoxia-inducible factor-1α in retinas from glaucomatous and normal canine eyes. *American Journal of Veterinary Research*, 69(2), 265-272.

Siegel, G. J., Agranoff, B. W., Albers, R. W., & Molinoff, P. B. (1993). Basic Neurochemistry. 5th Ed. Raven Press: New York, NY.

Shen F, Chen B, Danias J *et al.* Glutamate-induced glutamine synthetase expression in retinal Müller cells after short-term ocular hypertension in the rat. *Investigative Ophthalmology and Visual Science* 2004; 45: 3107–3112.

Schuettauf F, Rejdak R, Walski M *et al.* Retinal neurodegeneration in the DBA/2J mouse – a model for ocular hypertension. *Acta Neuropathologica* 2004; 107: 352–358.

Schumer RA, Camras CB, Mandahl AK. Putative side effects of prostaglandin analogs. *Survey of Ophthalmology* 2002; 47 (Suppl. 1): S219.

SmedesSL, DubielzigRR. Early degenerative changes associated with spontaneous glaucoma in dogs. *Journal of Veterinary Diagnostic Investigation* 1994; 6: 259.

SorokinSP, HoytRFJr, BluntDG *et al.* Macrophage development. II. Early ontogeny of macrophage populations in brain, liver, and lungs of rat embryos as revealed by a lectin marker. *Anatomical Record* 1992; 232: 527–550.

Stewart, WC., Feldman, R., and Mychaskiw, MA. Ocular blood flow in glaucoma: the need for further clinical evidence and patient outcomes research. *British Journal of Ophthalmology* 2007; 91:1263-1264

Suzuki, Y., Tanaka, M., Sohmiya, M., Ichinose, S., Omori, A., and Okamoto, K. (2005). Identification of nitrated proteins in the normal rat brain using a proteomics approach. *Neurol. Research*, 27, 630-633.

Tezel G, Yang X, Cai J. Proteomic identification of oxidatively modified retinal proteins in a chronic pressure-induced rat model of glaucoma. *Investigative Ophthalmology and Visual Science* 2005; 46: 3177–3187.

Torp R, Arvin B, Le Peillet E *et al.* Effect of ischaemia and reperfusion on the extra- and intracellular distribution of glutamate, glutamine, aspartate and GABA in the rat hippocampus, with a note on the effect on the sodium channel blocker BW1003C87. *Experimental Brain Research* 1993; 96: 365–376.

Traystman, R., J.R. Kirsch, R.C. Koehler, Oxygen radical mechanisms of brain injury following ischemia and reperfusion, J. Appl. Physiol. 71 (1991) 1185–1195

Uga, S. and Smelser, G. (1973). Comparative study of the fine structure of retinal Miiller cells in various vertebrates. *Investigative Ophthalmology,* 12(6), 434-448.

Van de Sandt RR, Boeve MH, Stades FC *et al.* Abnormal ocular pigment deposition and glaucoma in the dog. *Veterinary Ophthalmology* 2003; 6: 273–278.

Viappiani, S. and Schulz, R. (2006). Detection of specific nitrotyrosine-modified proteins as a marker of oxidative stress in cardiovascular disease. *Physiol Heart. Circ. Physiology*, 290, 2167–2168.

Whiteman, A., Klauss, G., Miller, P., Dubielzig, R. (2002). Morphologic features of degeneration and cell death in the neurosensory retina in dogs with primary angle-closure glaucoma. *American Journal of Veterinary Research*, 63(2), 257–261.

Wilcock BP, Brooks DE, Latimer CA. Glaucoma in horses. *Veterinary Pathology* 1991; 28: 74–78.

Wilcock BP, Peiffer RL Jr, Davidson MG. The causes of glaucoma in cats. *Veterinary Pathology* 1990; 27 (1): 35–40.

Wyman M, Ketring K. Congenital glaucoma in the basset hound: a biologic model. *Transactions. Section on Ophthalmology. American Academy of Ophthalmology and Otolaryngology* 1976; 81: OP645–652.

Yang, C., P.J. Tsai, N.N. Lin, J.S. Kuo, Elevated extracellular glutamate concentrations increased malondialdehyde production in anesthetized rat brain cortex, Neurosci. Lett. 243 (1998) 33– 36

Zhou, X., Li, F., Kong, L., Tomita, H., Li, C. and Cao, W. (2005). Involvement of inflammation, degradation, and apoptosis in a mouse model of glaucoma. *Journal of Biological Chemistry*, 280, 31240–31248.